CIRCULATION OF NORTH AMERICAN EPICONTINENTAL SEAS DURING THE CARBONIFEROUS USING STABLE ISOTOPE AND TRACE ELEMENT ANALYSES OF BRACHIOPOD SHELLS

A Thesis

by

RYAN CHRISTOPHER FLAKE

Submitted to the Office of Graduate Studies of
Texas A&M University
in partial fulfillment of the requirements for the degree of

MASTER OF SCIENCE

May 2011

Major Subject: Geology

Circulation of North American Epicontinental Seas during the Carboniferous Using

Stable Isotope and Trace Element Analyses of Brachiopod Shells

CIRCULATION OF NORTH AMERICAN EPICONTINENTAL SEAS DURING THE CARBONIFEROUS USING STABLE ISOTOPE AND TRACE ELEMENT ANALYSES OF BRACHIOPOD SHELLS

A Thesis

by

RYAN CHRISTOPHER FLAKE

Submitted to the Office of Graduate Studies of
Texas A&M University
in partial fulfillment of the requirements for the degree of

MASTER OF SCIENCE

Approved by:

Co-Chairs of Committee,	Ethan L. Grossman
	Thomas E. Yancey
Committee Members,	Debbie J. Thomas
	Thomas D. Olszewski
Head of Department,	Andreas K. Kronenberg

May 2011

Major Subject: Geology

ABSTRACT

Circulation of North American Epicontinental Seas during the Carboniferous Using Stable Isotope and Trace Element Analyses of Brachiopod Shells. (May 2011)

Ryan Christopher Flake, B.S, Washington State University

Co-Chairs of Advisory Committee, Dr. Ethan Grossman
Dr. Thomas Yancey

Previous studies have identified $\delta^{13}C$ events in the Carboniferous that imply major shifts in the carbon cycle. However, inherent in this interpretation is the assumption that epicontinental seas are chemically representative of the global ocean. Our study uses stable isotope and trace element analyses of brachiopod shells to examine changes in climate and circulation of the North American epeiric sea. Formations were selected for study to provide shallow marine environments with geographic coverage of North America. These units include the Grove Church and Mattoon Formations (Illinois Basin), Glenshaw Formation (Appalachian Basin), Bird Spring Formation (Bird Spring Basin), and Oread Formation (US midcontinent). In all, 98 brachiopod shells were found to be well preserved based on screening with plane light and cathodoluminescence microscopy of thin-sections, and trace element analyses.

Upper Chesterian Grove Church (Illinois Basin) samples have $\delta^{13}C$ and $\delta^{18}O$ averages of 1.1‰ and -3.1‰ respectively. These low values are interpreted as a local or regional effect caused by terrestrial runoff. Terrestrial influences are also suggested by the depositional environment: nearshore marine. Chesterian samples from the Bird

Spring Formation at Arrow Canyon, Nevada average 3.7‰ and -1.4‰ for $\delta^{13}C$ and $\delta^{18}O$ respectively. The higher $\delta^{13}C$ and $\delta^{18}O$ values, compared with samples from the time equivalent Grove Church, likely reflect the freer exchange with the Panthalassa Ocean at this most western edge of North America, and best represent open-ocean conditions. Samples from the Virgilian Ames-Shumway-Plattsmouth cyclothem show a progression of $\delta^{13}C$ and $\delta^{18}O$ enrichment moving west from near the Appalachians (1.9‰ and -3.8‰) to the Illinois Basin (3.2‰ and -2.4‰) and finally to the US midcontinent (4.2‰ and -1.5‰). This is interpreted as the transition from nearshore, terrestrial influence with enhanced organic matter oxidation and lower salinity to well-mixed conditions with normal salinities and potential for seafloor ventilation and upwelling. This is supported by published sediment $\Sigma Nd_{(t)}$ values from the Appalachian Basin ($\Sigma Nd_{(t)} = -9$) that increase further westward ($\Sigma Nd_{(t)} = -6$) due to higher influence from the eastern Panthalassa Ocean. Mass balance calculations based on the $\delta^{18}O$ of the brachiopod shells suggest salinities of 25 and 31 psu for the Appalachian and Illinois Basins, respectively, assuming salinities of 34.5 psu for the US midcontinent.

Trace element analyses do not show a systematic east-west trend similar to stable isotopes. In both time slices, spiriferids from the intermediately-located Illinois Basin are enriched in Mg/Ca and Sr/Ca relative to those in other basins. This Mg and Sr enrichment in Illinois Basin brachiopods suggests delivery of Sr-rich fresh waters and restricted circulation in that basin.

DEDICATION

To my parents for their unwavering support

ACKNOWLEDGEMENTS

First, I would like to thank my advisor Dr. Ethan Grossman for his support and guidance of this thesis. Thanks also to Dr. Yancey for his help with identification of brachiopod samples and characterization. Thanks to Dr. Thomas Olszewski for accompanying me during the field collection of samples. Finally, thanks to Dr. Debbie Thomas for being the primary investigator of this project and her oceanographic insight which was very much appreciated.

I would also like to thank three individuals who helped with sample collection in the field: Dr. Joe Lebold in West Virginia and Joe Devera and Scott Elrick in Illinois. Also, thanks go to Art Kasson, Luz Romero, Dr. Guillemette and Dr. Marcantonio for their invaluable assistance with the instrumentation and analyses during this study.

I would also like to thank the National Science Foundation (Grant EAR-0643309) for without which, this project would not have occurred.

TABLE OF CONTENTS

Page

LIST OF FIGURES

Page

LIST OF TABLES

Page

1. INTRODUCTION

1.1 Carboniferous Epicontinental Seas

The Carboniferous was a period of great global change. Beginning in the Chesterian around 327 Ma, the late Paleozoic ice age continued through the Pennsylvanian and into the Early Permian (Smith and Read, 2000; Fielding et al., 2008; Rygel et al., 2008; Elrick and Scott, 2010). As a result of changing ice volumes, sea level fluctuated as much as 95 m in the Mississippian (Smith and Read, 2000) and greater than 120 m during the Pennsylvanian (Soreghan and Giles, 1999; Joachimski et al., 2006). During the Upper Pennsylvanian, waxing and waning of Gondwanan glaciation produced sea level fluctuations and created cyclic deposits. As sea levels rose, ocean waters covered low land surfaces on the continents until regrowth of the glaciers resulted in falling sea-levels and regression. Within continental interior basins on the craton, many cyclothem units accumulated as a result of repeated fluctuations in sea-level. During a maximum transgression, water circulation driven by wind could have caused upwelling of deep waters and eventually anoxia (Heckel, 1977) in these basins. More recently, Algeo and Heckel (2008) have proposed that anoxia occurred through a combination of several factors: contact with the global ocean through small capacity deep water channels, shallow bathymetry, elevated runoff, and a raised oxygen-minimum zone within channels connecting the basins to the Panthalassa Ocean. During the Carboniferous, the increasing abundance of vascular plants aided in deposition of large amounts of organic carbon and the drawdown of CO_2 (Berner, 1997).

This thesis follows the style of Geology.

Prior to the collision of Gondwana and Laurussia, the Rheic Ocean connected the Panthalassa and Paleo-Tethys Oceans, potentially allowing waters to circulate freely resulting in more homogeneous water chemistries in the world ocean (Mii et al., 2001). After the Rheic Ocean's closure, global circulation shifted and caused chemical heterogeneity as revealed by carbon isotopes. Popp et al. (1986a) identified a +3‰ $\delta^{13}C$ shift during the late Chesterian which they attributed to global burial of organic carbon. Mii et al. (1999) accounted for the $\delta^{13}C$ shift in terms of the equal influence of carbon burial and changes in ocean circulation. The $\delta^{13}C$ enrichment has also been tied to the Variscan (Alleghenian) Orogeny during the mid-Carboniferous coupled with the expansion of glaciation indicating the possibility of climate shifts as a result of tectonism (Bruckschen et al., 1999). According to Mii et al. (2001), increased upwelling in the epeiric North American midcontinent accounted for 1.5‰ of the $\delta^{13}C$ shift and carbon burial accounted for 1.5‰ (Figure 1C,D).

An assumption of these carbon isotope studies is that epicontinental seas are chemically representative of the global ocean. However, restriction in modern shallow epeiric seas can cause a $\delta^{13}C$ lightening of -4‰ relative to the open ocean (Lloyd, 1964; Patterson and Walter, 1994). Neighboring epeiric seas of North America during the Ordovician can show a $\delta^{13}C$ divergence of up to 4‰ depending on localized carbon inputs and circulation (Holmden et al., 1998; Panchuk et al., 2006). Sea level or atmospheric CO_2 changes have been hypothesized to alter ocean-atmosphere exchange rates and thus also influence $\delta^{13}C$ shifts (Panchuk et al., 2005).

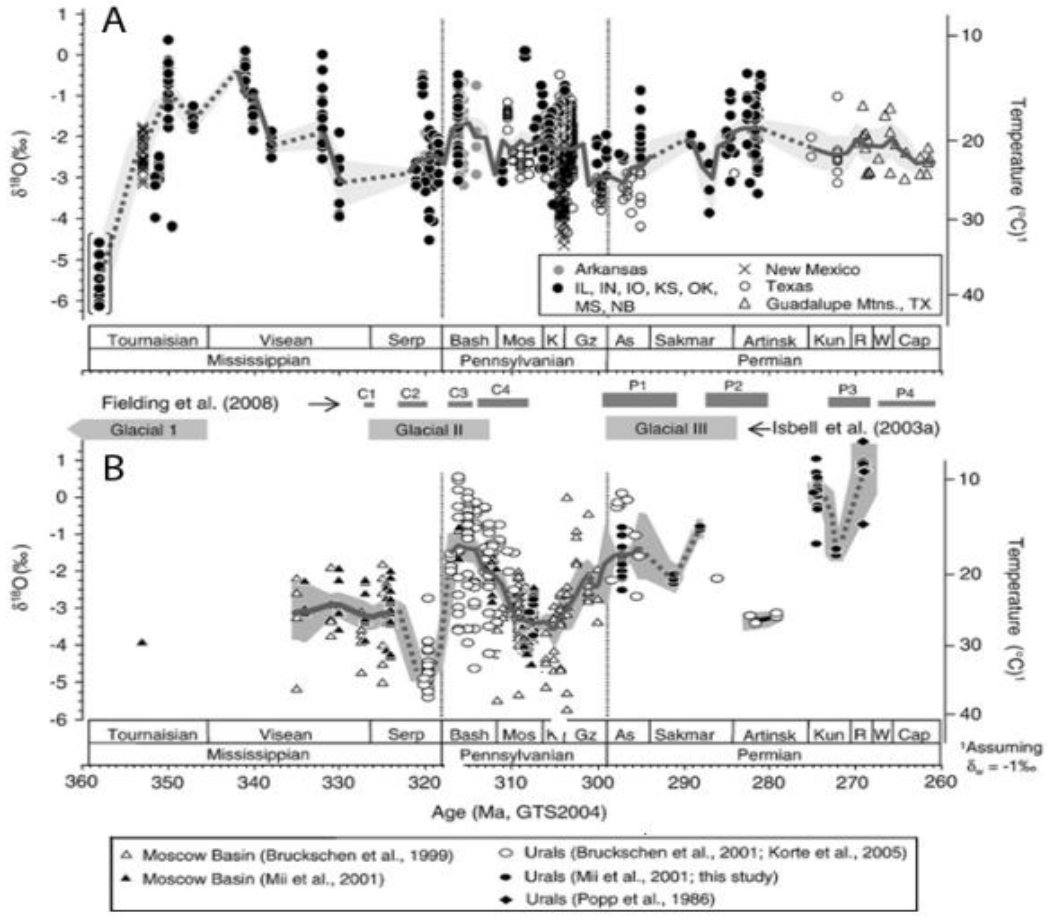

Figure 1. $\delta^{18}O$ and δ13C stratigraphies for the Carboniferous and Permian based upon brachiopod shells (Grossman et al., 2008). Oxygen and carbon isotopic data from the US midcontinent (A and C) are from Grossman et al. (1991, 1993, 2008), Mii et al. (1999), and Korte et al. (2005). Russian Platform data (B and D) are from Popp et al. (1986a), Bruckschen et al. (1999, 2001), Mii et al. (2001), and Korte et al. (2005). Figure 1 continued on next page.

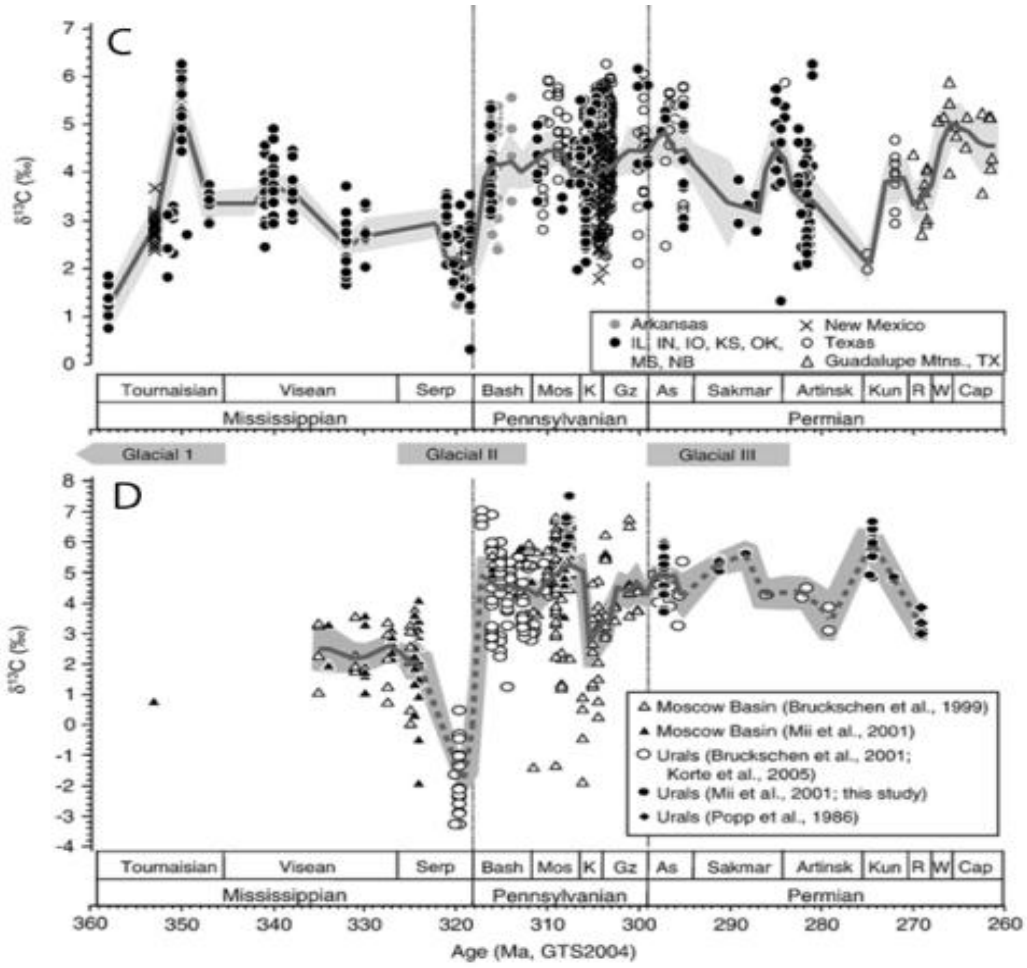

Figure 1, Continued

This study uses isotope and trace element analyses of brachiopod shells to examine changes in gradients of North American seawater during the Carboniferous as a result of the Rheic Ocean's closure. In conjunction with this study, other research is examining the neodymium isotopic composition of seawater, using conodonts from the same deposits (Woodard et al., 2010). Because of Nd's short residence time in the ocean of approximately 1000 years, its isotopic composition can be used to investigate paleocirculation (Broecker and Peng, 1982). The specific objectives are to (1) test for isotopic and trace element differences between epeiric sea basins during Chesterian and Virgilian time slices that would be evidence for restricted circulation and (2) test the hypothesis that waters of the North American basins become more restricted and more influenced by freshwaters, from west to east, due to discharge from the young Appalachian Mountains as indicated by decreasing $\delta^{13}C$ and $\delta^{18}O$.

1.2 Stable Isotopes and Trace Elements in Brachiopod Shells

Brachiopod shells are chosen for isotopic and trace element studies for several reasons. Modern brachiopods precipitate the major portion of their shells in oxygen isotope equilibrium with ambient water (Lowenstam, 1961; Carpenter and Lohmann, 1995). Brachiopods are found throughout the Paleozoic and are widespread geographically. The shells are composed of low magnesium calcite, which is resistant to diagenesis (Lowenstam, 1961). The prismatic and fibrous shell structure is also beneficial in protecting against alteration by minimizing space between the crystals (Compston, 1960). Brachiopod shells are also large enough to sample without risk of incorporating matrix or cement.

Trace element studies of brachiopod shells provide useful paleo-environmental information that can supplement the more conventional stable isotope studies. An example is the application of Mg/Ca ratios in determining original seawater chemistry (Powell et al., 2009). Seawater Mg/Ca ratios are believed to have fluctuated greatly throughout the Phanerozoic (e.g., Hardie, 1996; Lowenstein et al., 2001). Mg/Ca ratios in the shells are dependent on seawater Mg/Ca; as seawater Mg/Ca ratio increases, so does shell Mg/Ca. According to Hardie (1996), seawater Mg/Ca ratios shifted from 1.5 in the Mississippian to 2.5 by the late Pennsylvanian. Mg/Ca in mollusk shells can also vary as a function of temperature (Klein et al., 1996). Unlike oxygen isotopes, ice volume changes and freshwater influx will likely not influence the Mg/Ca ratio (Klein et al., 1996). As yet, no study has demonstrated a consistent relationship between Mg/Ca and temperature for brachiopod calcite. Furthermore, when temperature equations derived from modern mollusks (vander Putten et al., 2000) are applied to Paleozoic brachiopods, temperatures are underestimated (Powell et al., 2009).

Trace element concentrations can vary within and (or) between brachiopod shells due to water temperature and chemistry, precipitation rate, shell microstructure, organic matrix concentration, and vital effect (Popp et al., 1986a; Mii and Grossman, 1994; Grossman et al., 1996). Different brachiopod taxa from the Pennsylvanian US midcontinent show different trace element concentrations. For example, Mg is low in *Neospirifer* and *Composita* but high in *Crurithyrus* (Grossman et al., 1996). Popp et al. (1986a) showed lower Sr and Mg concentrations in spiriferids relative to productids.

Diagenesis can alter the original $\delta^{18}O$, $\delta^{13}C$, and trace element chemistry of brachiopod shells. This altered material develops a chemical and isotopic composition reflective of the diagenetic environment and is no longer indicative of the original brachiopod habitat. $\delta^{18}O$ typically decreases with diagenesis because the diagenetic fluid, most likely meteoric water, is depleted in ^{18}O relative to seawater (Gross, 1964; Allan and Matthews, 1977). $\delta^{13}C$ will also likely decrease with diagenesis. This is because the $\delta^{13}C$ of dissolved inorganic carbon (DIC) is low in meteoric waters due to the incorporation of respired organic carbon, which is depleted in $\delta^{13}C$ relative to seawater DIC. Prismatic shell is preferred for analysis because it resists diagenesis more so than fibrous shell (Grossman et al., 1993). Trace element concentrations are also impacted by diagenesis. Mn and Fe concentrations increase with diagenesis while Sr, Na, and B concentrations decrease (Brand and Veizer, 1980; Veizer, 1983a,b; Joachimski et al., 2005). Because seawater is naturally depleted in Mn and Fe, significant concentrations found in shells (>2 ppm and >0.5- 2 ppb respectively) (Gies, 1976; Wu and Boyle, 1998) are inferred to be the result of meteoric contamination and an indicator of diagenesis (Popp et al., 1986a). This study uses 250 ppm in Mn and cathodoluminescence as a criterion for diagenetically unaltered shell similar to Popp et al. (1986a) and Bruckschen et al. (1999). In contrast, Sr and Na may decrease with diagenesis because seawater is more enriched in these elements than meteoric water.

Preservation of original calcite can be tested with cathodoluminescence microscopy (Popp et al., 1986a, b). Increasing Mn concentrations (> 10-20 ppm) activates luminescence by an electron beam while increasing Fe concentrations (> 35

ppm) quenches luminescence (Medlin, 1961; Gies, 1976; Machel, 1985). Anoxic meteoric water can have significant concentrations of Mn^{2+} which are incorporated into post-depositional carbonate precipitates.

2. SAMPLE LOCALITIES AND GEOLOGIC SETTING

The Appalachian Basin, Illinois Basin, US midcontinent and the western margin of North America (Arrow Canyon) were selected for study because they are geographically dispersed around North America and have shallow marine sediments (Figure 2). Two time slices are considered, the Chesterian and Virgilian (Figure 3). Chesterian brachiopods collected for this study include specimens from the Grove Church and are supplemented by shells previously collected from the Bird Spring Formation (Jones et al., 2003). Virgilian samples were collected from the Ames Member of the Glenshaw Formation and the Shumway Member of the Mattoon Formation. These are supplemented by samples from the Plattsmouth Limestone (Grossman et al., 1993). Samples from the Illinois Basin (Scheining and Langenheim, 1980) and the Appalachian Basin (Lebold and Kammer, 2006) have thick-shelled brachiopods (*Neospirifer*, *Composita*, and *Crurithyrus*) that have yet to be studied geochemically.

Brachiopods collected from the Grove Church Formation (latest Chesterian) are compared with specimens of similar age from the lower Bird Spring Formation (BS_b). Overlying strata of the Bird Spring Formation (BS_c) extending from the mid-Carboniferous boundary to the early Desmoinesian (Figure 3) were also sampled, but no suitable brachiopod shells were found. Samples from the Sausbee Formation of middle Morrowan age studied by Mii et al. (1999) are used for comparison with Early Pennsylvanian samples of the Bird Spring Formation in western North America. Virgilian strata of the Ames, Shumway, and Plattsmouth Members (Virgilian) provide an

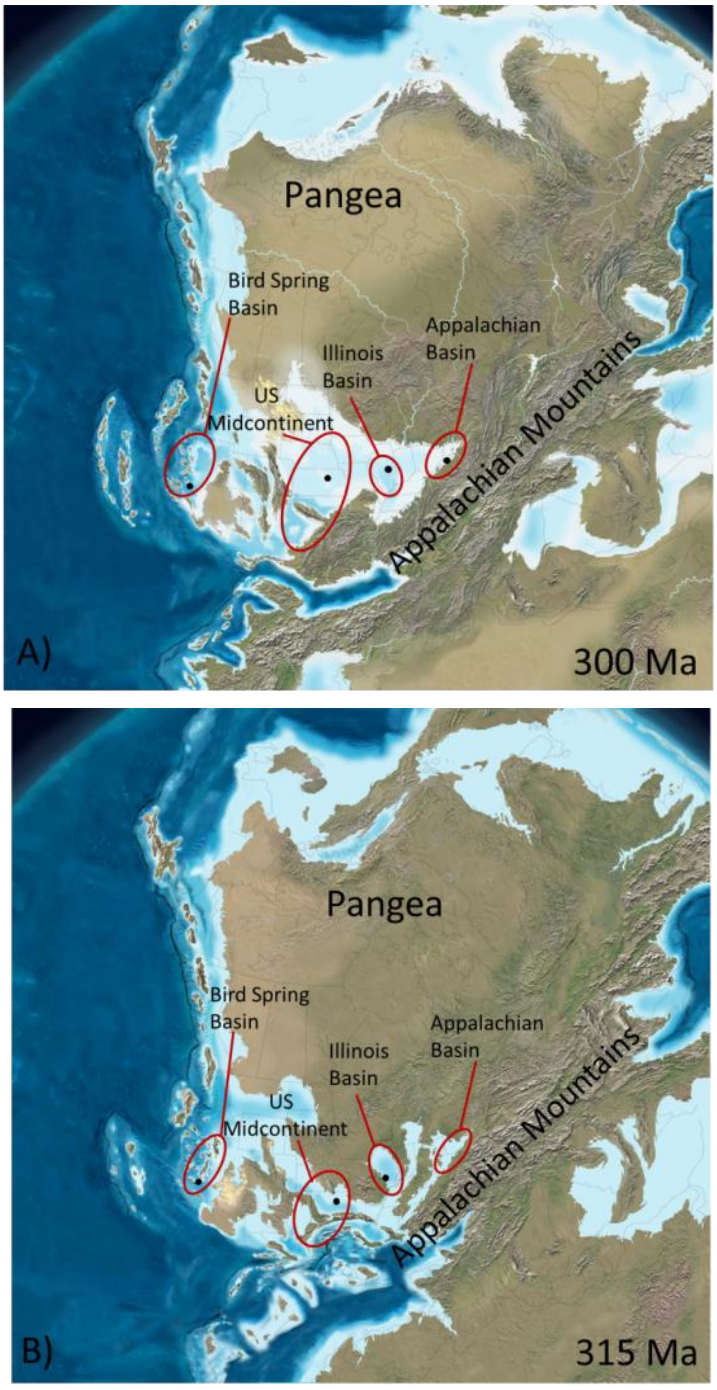

Figure 2. Reconstruction of Carboniferous paleogeography (from Blakey, 2005). Basin locations circled in red and black dots indicate sample location.

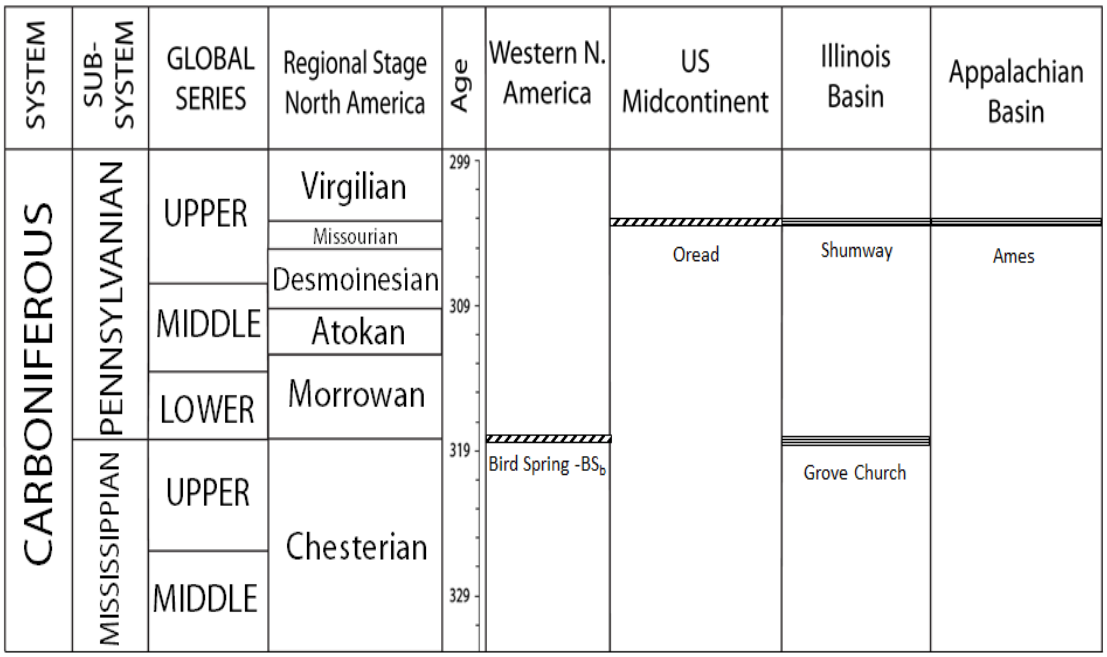

Figure 3. Sample location and units. Bars with horizontal lines represent units sampled directly for this study. Bars with diagonal lines represent units studied by Grossman et al. (1993) and Jones et al. (2003). Stratigraphic limits are the Bird Spring Formation, Grove Church Formation, Plattsmouth Limestone Member of the Oread Cycle, Shumway Member of the Mattoon Formation, and Ames Member of the Glenshaw Formation.

east-west transect within a narrow interval (Figure 3). These cyclic deposits occur along a transect from the Appalachian Basin to the US midcontinent and are correlated based on conodonts (Heckel et al., 1998). The Ames records the last major marine transgression in the Appalachian Basin during the Carboniferous (Lebold and Kammer, 2006).

2.1 Appalachian Basin

2.1.1 *Ames Member of the Glenshaw Formation*

Contained within the Glenshaw Formation of the Conemaugh Group, the lower Virgilian Ames Member is found overlying the Harlin Coal and is the final unit within the Glenshaw Formation of the Appalachian Basin. The lithology varies spatially (Lebold and Kammer, 2006) but is generally a limestone with interbedded shales and sands. Two different stratigraphic intervals were sampled. The first of these was the GRR section in Morgantown, West Virginia from Lebold and Kammer (2006). The fossiliferous unit contained brachiopods (dominantly *Composita, Neochonetes, Neospirifer*, and few *Crurithyris*), gastropods, bryozoans, bivalves, cephalopods, and scaphopods. In ascending order, this section contains gray sparsely fossiliferous shale with micrite concretions and burrows. It grades into a light tan, highly fossiliferous limestone with many species of brachiopods including the thin-shelled *Neochonetes*. Above this is 0.75 m of friable red-brown mudrock. The next layer is 0.45 m of light green fine sandstone which is thin, discontinuous, and bioturbated. Overlying this is 6.65 m of tan mudrock with extensive fossil pavements and thin interbedded sandstone

layers. Overlying the Ames is the Grafton Sandstone. A second section was sampled near the town of Fairmont, West Virginia (FAIR from Lebold and Kammer, 2006) 20 km southwest of the GRR section. At the base is a dark gray shale with few *Neochonetes* which then grades into a 0.30 m thick wackestone bed. Above this is another dark gray shale with abundant preserved mollusks that grades into an interval with numerous *Crurithyris*.

2.2 Illinois Basin

2.2.1 *Grove Church Formation*

The Grove Church Formation is uppermost Chesterian in age and overlays the Goreville Limestone Member of the Kincaid Formation. As defined by Weibel and Norby (1992) the Grove Church Formation is subdivided into four units totaling 7.26 m. The first of these (1.68 m) is a weakly calcareous shale with poorly preserved brachiopod impressions. Unit 2 (3.41 m) is a noncalcareous mudstone. The third unit (0.85 m) is a silty clay shale that is weakly calcareous and is thinly bedded. This was followed by emergence and development of a paleosol on the deposits, indicating an unconformity (Weibel and Norby, 1992). Unit 4 (1.32 m) is the section that was sampled for analyses. The basal portion of the unit is a fossiliferous gray mudrock containing bryozoans, brachiopods, and echinoid spines. The second layer is a thin gray packstone. The third layer is a gray fissile mudrock with brachiopods, bryozoans, and siderite nodules. Above this is a medium gray packstone with crinoid fragments and pyrite crystals. The uppermost layer is poorly exposed medium gray shale. An unconformity exists at the top of the Grove Church as evidenced by a non-planar contact surface,

abrupt shale lithology change within the boundary, and change in lithology across the boundary (Weibel and Norby, 1992).

2.2.2 *Shumway Limestone Member of the Mattoon Formation*

The Shumway Limestone Member is found within the Shumway Cyclothem which is the last unit of the lower Virgilian Mattoon Formation. The exposure studied was the type locality for the unit and is located in Shoal Creek in Effingham County, Illinois**.** The Shumway Cyclothem is composed of 12 different units. In ascending order they are: interbedded siltstone and sandstone; gray shale with plant fragments; gray limestone; underclay; Shumway Coal Bed; fossiliferous calcareous shale; fossiliferous, argillaceous gray limestone; fissile black shale; calcareous gray shale; micritic, gray fossiliferous limestone (Shumway Limestone Member); claystone; and finally a massive sandstone (Sheining and Langenheim, 1980). Fauna found within the Shumway Limestone are brachiopods, bivalves, gastropods, scaphopods, cephalopods, cnidarians, crinoids, trilobites, and bryozoans (Tucker, 1976).

2.3 United States Midcontinent

Oxygen and carbon isotopic data for the midcontinent are available from Grossman et al. (1993) and Mii et al. (1999). Grossman et al. (1993) provide data for the Plattsmouth Limestone Member of the Oread Formation in Kansas There it is well exposed with the Heebner Shale, a 0.25 m thick black fissile shale, exposed at the base and Plattsmouth Limestone Member above. The Plattsmouth Limestone Member is dominantly limestone with thin shale interbeds. Data for the Mid-Morrowan Sausbee Formation in Oklahoma is provided by Mii et al. (1999). The formation is 40.2 m thick

and is dominantly argillaceous limestone with shale interbeds (Sutherland and Henry, 1977).

2.4 Bird Spring Basin (Arrow Canyon)

The Bird Spring Formation in Arrow Canyon, Nevada was deposited from the Late Mississippian to the Early Permian in the Great Basin of the Western United States. The Global Boundary Stratotype Section and Point (GSSP) for the Mid-Carboniferous is located near the base of the formation (Lane et al., 1999). One of the intervals studied is the BS_c unit (Early Pennsylvanian to Late Pennsylvanian) which is roughly 609 m thick. Within the unit, many transgressions and regressions packages are defined by repeating layers of limestone, chert, slightly calcareous shale and sandstone (Langenheim et al., 1962). These repeated packages range in thickness from centimeters to a meter and were a result of glacial cycles on southern Gondwana (Lane et al., 1999).

Below the mid-Carboniferous boundary is the BS_b which comprises the other unit of study and is uppermost Chesterian. This lithologically diverse strata (shales, sandstones, limestone) are 73 m thick but the fossils of interest (productids, *Anthracospirifer*, *Composita*) are contained within the argillaceous limestone.

3. METHODS

3.1 Field Sample Collection

For each outcrop, samples were collected from unweathered surfaces. Care was taken to select samples that appeared free from oxidation. The brachiopods chosen were thicker shelled species relative to others in the rock unit. Multiple locations from the same unit were sampled to increase the true representation of deposition and were recorded by global positioning system (GPS). Samples taken from Arrow Canyon followed the 1.5 m intervals set by the Amoco Petroleum Corporation.

3.2 Laboratory Methods

Samples are immersed in water and cleaned with a brush to remove surface contamination that would hinder identification. They are then dried in an oven overnight at 70^{o} C. Large specimens still embedded in rock matrix are sectioned with a MK 101 tile saw. Potential samples are evaluated based on surface characteristics and are thick shells without punctae, fractures, and surface oxidation. These evaluations were performed under a binocular microscope. In total, 109 shells were selected to be thin-sectioned.

Struers Epoxy Resin and Struers Epoxy Hardener were combined to form the epoxy. A thin layer of epoxy (~2 mm) was poured to create a base. Candidate shells are then identified taxonomically and embedded in preevacuated epoxy and left to harden for three days. After curing, the brachiopod shells are cut longitudinally using an Isomet saw. The thin-section epoxy requires three additional days to cure before being cut to

reduce the likelihood of epoxy flaking off the glass side during polishing. Individual thin sections are examined under a petrographic microscope using a TECHNOSYN Model 8200 MKII cathodoluminescence stage to evaluate for microfractures, crystal translucence, luminescence and microstructure. The operating conditions used for the luminoscope are gun current of 200-300 mA and voltage 10-15 kV. Shells are imaged using a Coolsnap-Pro_{cf} camera attached to a desktop computer. Exposure times are 20 s for more luminescent shells and 60 s for those that need additional time to enhance contrast. Shell images were taken using cathodoluminescence and plane light. The efficacy of cathodoluminescence as a diagenetic indicator can also be impacted by methodology. There are no standard practices for exposure time for image capture, electron beam current or camera type. All these variables can influence the intensity at which the image is rendered and thus the intensity of cathodoluminescence.

Using a gradational scale of cathodoluminescence, the sites are categorized as nonluminescent (NL), slightly luminescent (SL), and cathodoluminescent (CL) or some combination. The six categories are NL, NL/SL, SL/NL, SL/CL, CL/SL, and CL (Figure 4). Shells are sampled from several NL shell areas, or NL/SL areas when NL areas are not available. Shell material permitting, specimens were sampled in a maximum of three locations. Additionally, matrix and cement powders are also collected as diagenetic examples. A dental drill with a 0.5 mm bur is used to bore a round hole which is approximately 0.5 mm in diameter to yield a powder weight of 100-200 µg. The powder is then heated overnight in an oven at 70^{o}C to remove trapped moisture. Phosphoric acid (specific gravity 1.91-1.93) is then reacted with the carbonate powder at 70^{o}C. The

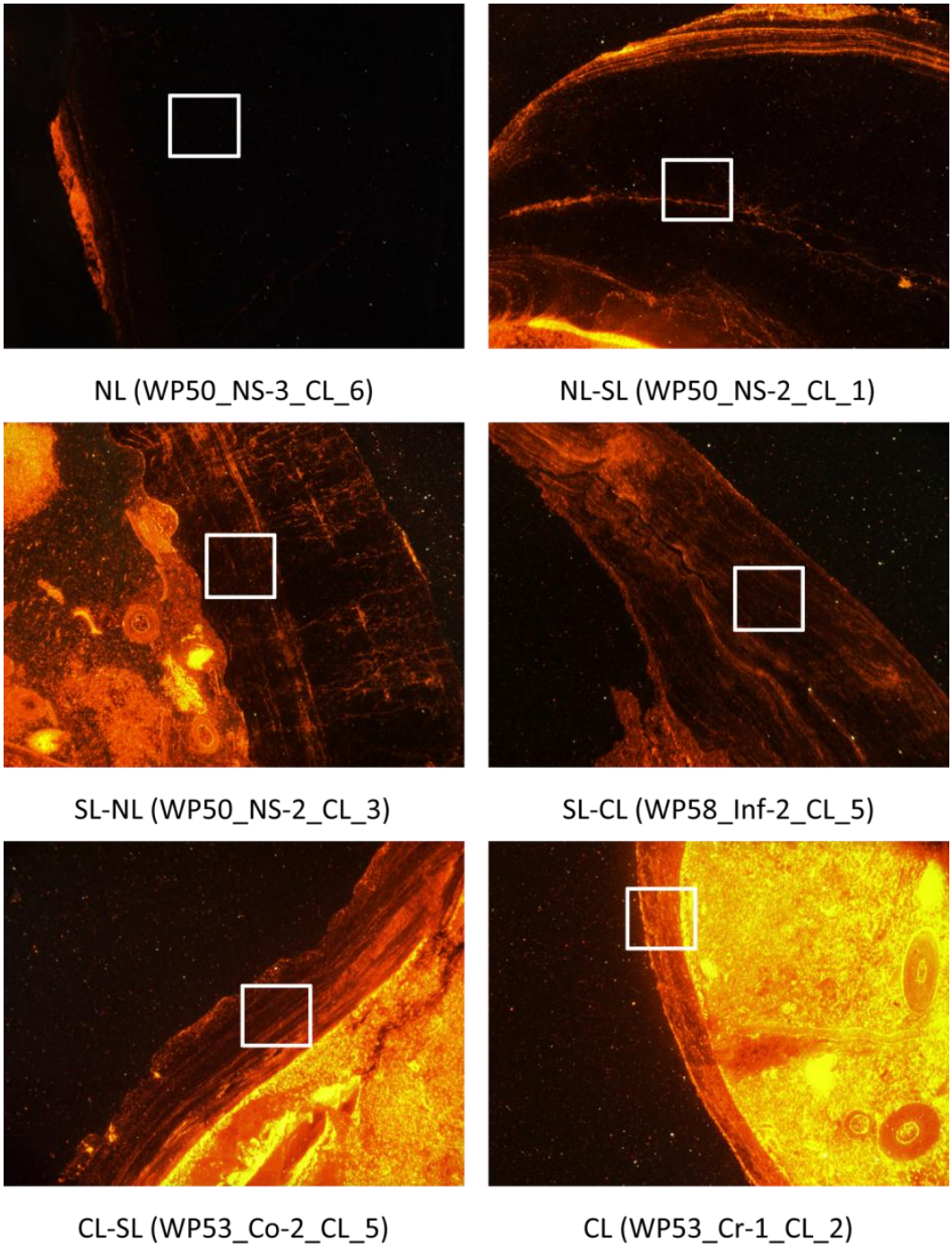

Figure 4. Classification of cathodoluminescence. Alteration is lowest in top left and increases to bottom right. White squares show the relevant areas of the shells.

emitted CO_2 gas is analyzed on a GasBench II via a ThermoFinnigan Delta^{Plus} XL isotope ratio mass spectrometer. The carbonate standard NBS-19 ($\delta^{13}C$ = 1.95‰, $\delta^{18}O$ = -2.20‰) is used to calibrate to Vienna Pee Dee Belemnite (VPDB). The NBS-19 average precision is ±0.1‰ for $\delta^{13}C$ and $\delta^{18}O$.

Shells are analyzed for trace elements using Thermo-Scientific high resolution inductively-coupled plasma mass spectrometer (HR-ICP-MS) and electron microprobe. For HR-ICP-MS analyses, a dental drill with a 0.5 mm bur was used to sample approximately 100 μg of powder from the same sites used for stable isotope analysis. The powder is reacted with 2 ml of 2% HNO_3 for 30 minutes. A standard curve is created by diluting a gravimetrically-prepared stock solution with a suite of elements (Mg, Ca, Mn, Fe, and Sr) to specified concentrations. The elemental ratios in the stock solution are similar to those in the shells analyzed. All concentrations are corrected for machine drift by adding the same amount of indium (internal standard) into each sample and calibration standard solution. To test our technique and the validity of our gravimetric stock solution concentrations, we performed an interlaboratory calibration with gravimetric solutions prepared in the laboratories of Drs. Matthew Schmidt and Yair Rosenthal. Our technique yielded concentration ratios that were within 2% of those determined by Dr. Schmidt's group and within 5% of those determined by Dr. Rosenthal's group. Hence our best estimate of the external reproducibility is less than 5%. Internal run precisions are always significantly better than this.

Additional trace element analyses (Ca, Fe, Mg, Mn, Na, S, and Sr) were performed on shells using a Cameca SX50 electron microprobe and wavelength

dispersive spectrometry (WDS). The beam has an accelerating potential of 15 kV, current of 10 nA, and diameter of 20 μm. The standards are Smithsonian Smith calcite (USNM 136321) for Ca; Smithsonian Smith siderite (USNM R2460) for Fe; Smithsonian Smith dolomite (USNM 10057) for Mg; C.M. Taylor spessartine for Mn; C.M.T. Amelia albite for Na; C.M. Taylor $BaSO_4$ for S; and Smithsonian Smith strontianite (NMNH R10065) for Sr. Counting times for each background element and peak are 20 s (Ca), 70 s (Fe), 120 s (Mg), 70 s (Mn), 60 s (Na), 120 s (S), and 60 s (Sr). Lower limits of detection for these elements in ppm are 220 for Ca, 50 for Mg, 190 for Fe and Mn, 70 for Na, 80 for S, and 310 for Sr. The instrument is standardized daily before analysis. Background counting, peak counting, and peak position are designated per element. To validate standardization, the dolomite and calcite standards are considered as an unknown to test proper calibration. Sample points are chosen based upon transmitted light and cathodoluminescence photomicrographs. Two parallel 9-point transects spaced a few hundred microns apart are taken from shell exterior to the interior. Points already sampled for $\delta^{13}C$ and $\delta^{18}O$ are chosen to investigate the trace element composition. Matrix and cement are also sampled.

4. RESULTS

4.1 Sample Characterization

Based on a Mn concentration of 250 ppm or less for NL to NL/SL areas in shells, 98 samples were considered unaltered (Figure 5). Twenty-three brachiopod samples are altered based on cathodoluminescence and Mn. Of the Virgilian time slice, the Ames samples have the lowest percentage of unaltered material, 54% as defined by cathodoluminescence and Mn. The Plattsmouth and Shumway brachiopods are all unaltered. For the Chesterian, 93% of the processed Grove Church shells proved to be unaltered, whereas all of the Bird Spring shells were judged unaltered. For both time slices, prismatic shell layers were more likely to be unaltered than fibrous layers, which showed signs of cathodoluminescence and higher Mn concentrations. Consequently, *Anthracospirifer* and *Neospirifer* shells were the more likely to be preserved whereas some *Composita*, *Crurithyris*, *Inflatia*, and *Kutorginella* shells showed alteration.

4.2 Stable Isotopes

Stable isotope data are summarized in Table 1, and Figures 6, 7, and 8. Carbon isotopic compositions of well-preserved Chesterian brachiopod shells from the Grove Church Formation range from 0.0 to 2.5‰, lower than those from the Bird Spring Formation (2.6 and 5.3‰). Virgilian brachiopod $\delta^{13}C$ from the Ames ranged from 0.30 to 3.2‰, while Shumway ranged from 2.9 to 3.5‰, and Plattsmouth from 3.4 to 5.4‰. Brachiopod $\delta^{18}O$ from the Grove Church varied from -4.1 to -2.2‰ while the Bird Spring was more enriched in ^{18}O with values from -2.4 to 0.1‰. Samples are lowest in

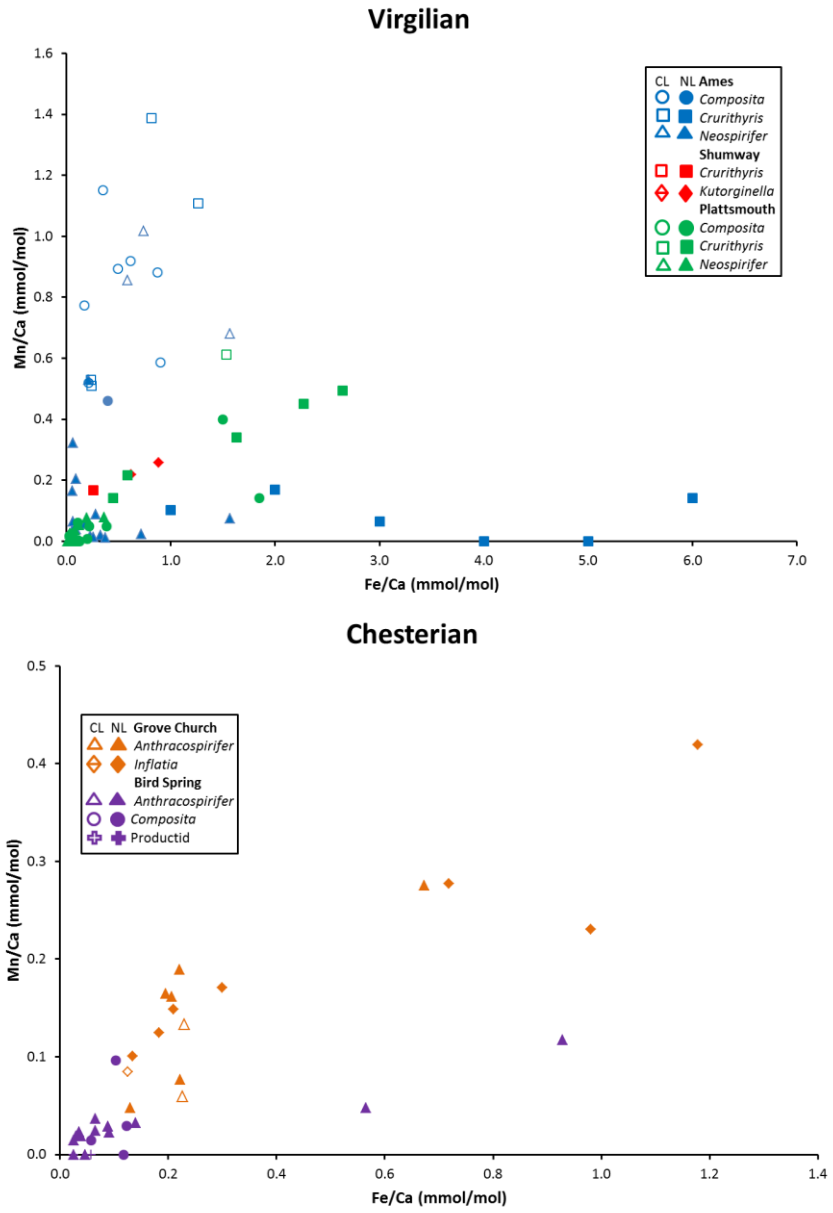

Figure 5. Scatter diagram of Mn/Ca versus Fe/Ca for brachiopod shells. A: Virgilian Ames, Shumway, and Plattsmouth Members. B: Chesterian Bird Spring and Grove Church Formations. Filled symbols indicate nonluminescent and unfilled indicate cathodoluminescent shell material.

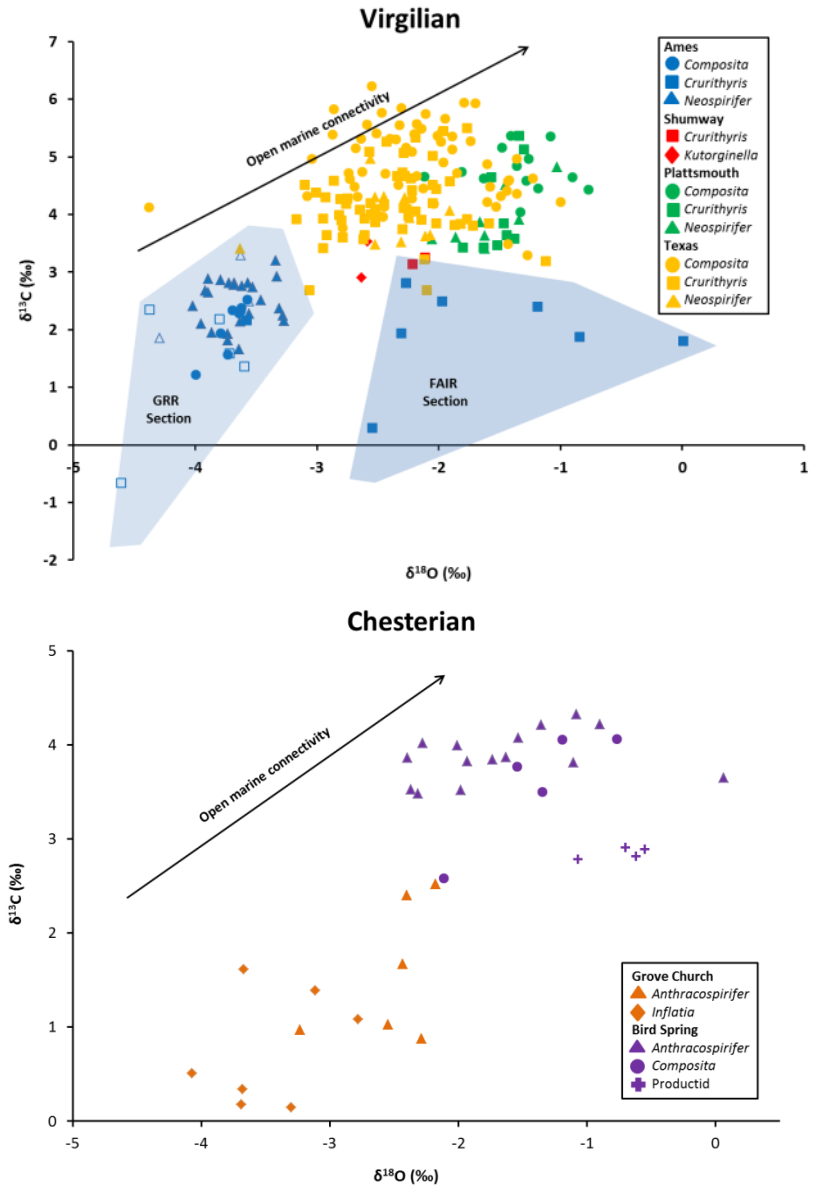

Figure 6. Scatter diagram of $\delta^{13}C$ versus $\delta^{18}O$ for brachiopod shells. A: Virgilian Ames(GRR and FAIR sections), Shumway Limestone Member, Plattsmouth Member, and data from similar intervals in Texas (Grossman et al., 1993). B: Chesterian Bird Spring and Grove Church Formations. Filled symbols indicate nonluminescent and unfilled indicate cathodoluminescent shell material.

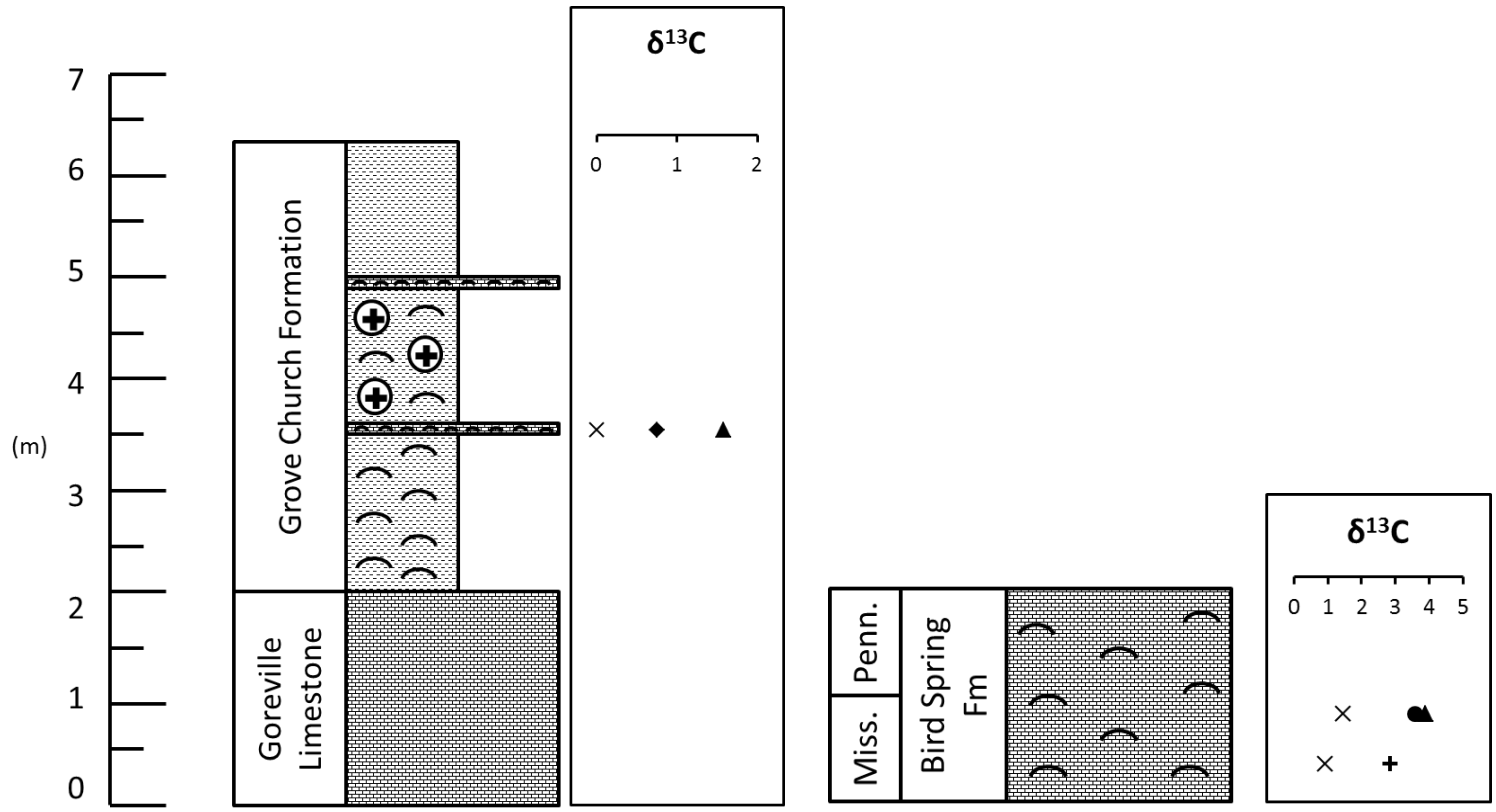

Figure 7. Stratigraphic columns and mean $\delta^{13}C$ data from Chesterian measured sections. Bird Spring Formation data from Jones et al. (2003).

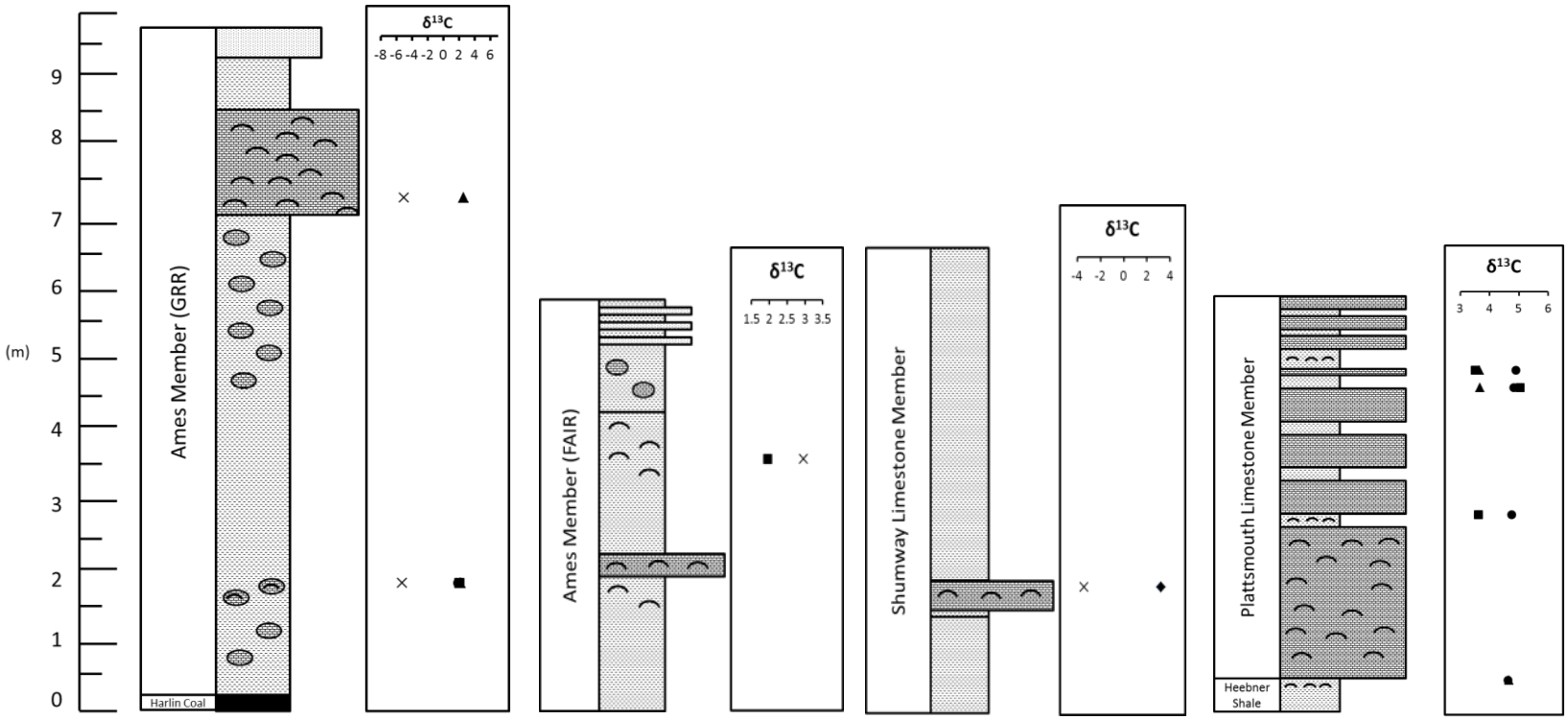

Figure 8. Stratigraphic columns and mean $\delta^{13}C$ data from Virgilian measured sections. Plattsmouth Limestone Member data are from Grossman et al. (1991).

TABLE 1. BRACHIOPOD $\delta^{13}C$ AND $\delta^{18}O$ FOR CHESTERIAN AND VIRGILIAN TIME SLICES.

Time slice	Formation	Genus	Count	Mean $\delta^{13}C$ (‰)	2x standard error	Mean $\delta^{18}O$ (‰)	2x standard error
Chesterian	Grove Church	Total	13	1.13	0.4	-3.03	1.3
		Anthracospirifer	6	1.58	0.6	-2.51	0.3
		Inflatia	7	0.75	0.5	-3.47	0.3
Chesterian	Bird Spring	Total	24	3.65	0.2	-1.44	0.3
		Anthracospirifer	15	3.88	0.1	-1.64	0.2
		Composita	5	3.59	0.5	-1.39	0.4
		Productid	4	2.85	0.1	-0.73	0.2
Virgilian	Glenshaw (Ames)	Total	35	2.33	0.2	-3.23	0.3
		Composita	3	2.39	0.1	-3.61	0.0
		Crurithyris	10	1.98	0.4	-2.18	0.8
		Neospirifer	22	2.47	0.2	-3.65	0.1
Virgilian	Mattoon (Shumway)	Total	4	3.20	0.3	-2.39	0.3
		Crurithyris	2	3.19	0.1	-2.16	0.1
		Kutorginella	2	3.21	0.6	-2.61	0.0
Virgilian	Oread (Plattsmouth)	Total	30	4.32	0.2	-1.46	0.1
		Composita	13	4.76	0.2	-1.36	0.2
		Crurithyris	9	4.06	0.5	-1.49	0.1
		Neospirifer	8	3.91	0.4	-1.58	0.2

$\delta^{18}O$ within the offshore Ames (-4.0 to 0.1‰), higher in the Shumway (-2.6 to -2.1‰), and highest in the Plattsmouth (-2.1 to -0.77‰).

4.3 Trace Elements

Trace element data are summarized in Table 2 and Figures 5 and 9. In both Chesterian and Virgilian specimens, Mn/Ca and Fe/Ca ratios for nonluminescent shell are more likely to be lower than those for cathodoluminescent shell (Figure 5). For the Chesterian shells, both Mg/Ca and Sr/Ca were lower in Bird Spring specimens relative to Grove Church specimens. The productids yielded the highest Mg/Ca and Sr/Ca values and *Composita* the lowest, with *Anthracospirifer* intermediate. For the Virgilian, Plattsmouth shells were lowest in Mg/Ca and Sr/Ca while Ames shells were intermediate and Shumway shells highest. Trace element differences between Virgilian taxa are systematic. *Neospirifer*, *Composita*, and *Crurithyris* mirror the same pattern in that they are lowest in the Plattsmouth, moderate in the Ames, and highest in Shumway. Sr/Ca within *Composita* and *Crurithyris* follow a similar pattern as before whereas Sr/Ca in *Neospirifer* is higher in the Plattsmouth than Ames.

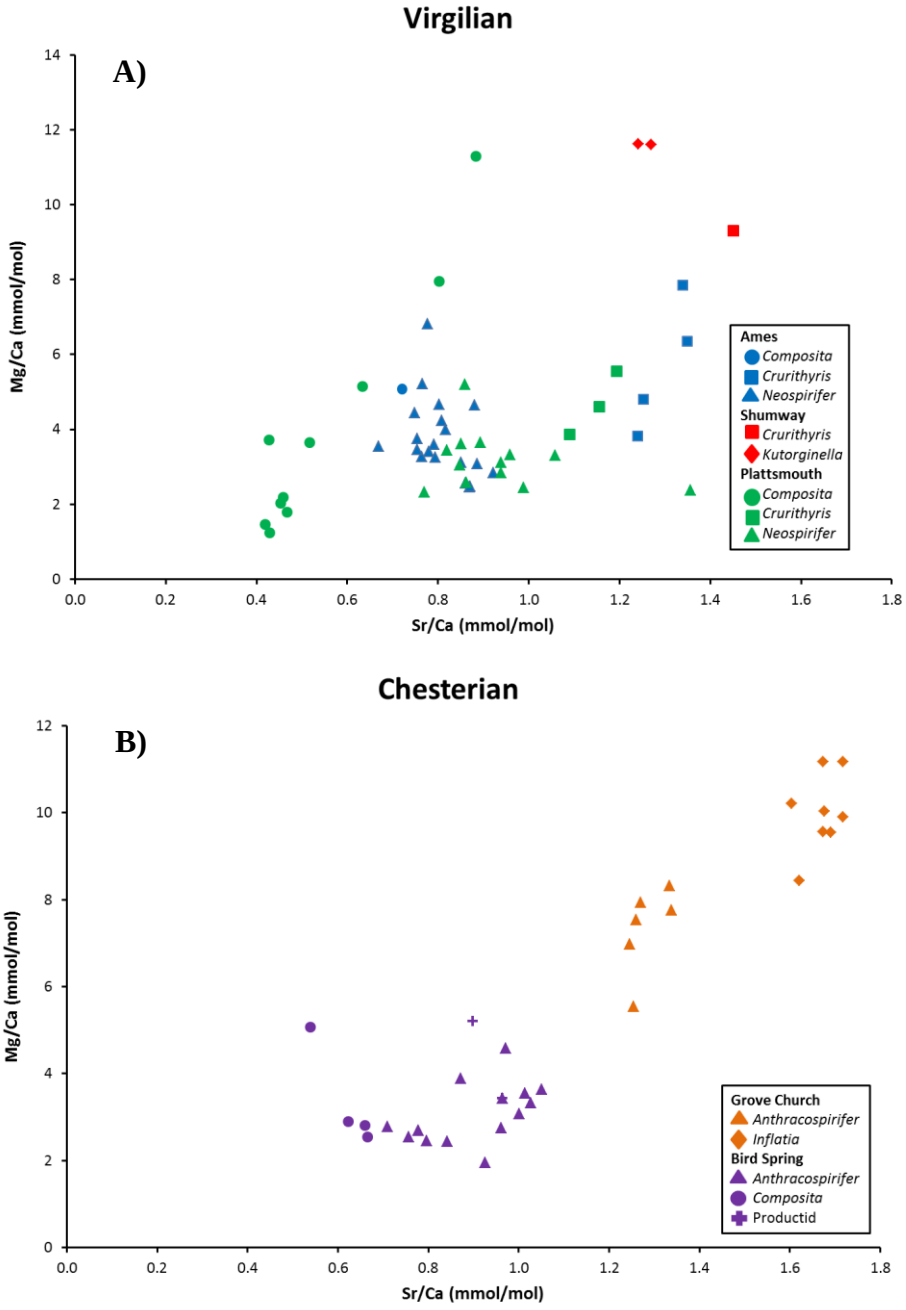

Figure 9. Scatter diagram of Mg/Ca versus Sr/Ca for brachiopod shells. A: Virgilian Ames, Shumway, and Plattsmouth Members. B: Chesterian Bird Spring and Grove Church Formations. Symbols indicate nonluminescent shell material.

TABLE 2. BRACHIOPOD TRACE ELEMENT DATA FOR CHESTERIAN AND VIRGILIAN TIME SLICES.

Time slice	Formation	Genus	Count	Mean Mg/Ca	2x Standard Error	Mean Sr/Ca	2x Standard Error	Mean Mn/Ca	2x Standard Error	Mean Fe/Ca	2x Standard Error
Chesterian	Grove Church	Total	13	8.69	0.86	1.49	0.11	0.18	0.05	0.41	0.20
		Anthracospirifer	6	7.34	0.81	1.28	0.03	0.15	0.07	0.27	0.16
		Inflatia	7	9.84	0.62	1.67	0.03	0.21	0.08	0.53	0.32
Chesterian	Bird Spring	Total	21	3.22	0.38	0.85	0.06	0.03	0.02	0.14	1.30
		Anthracospirifer	15	3.05	0.35	0.90	0.06	0.04	0.02	0.16	0.14
		Composita	4	3.33	1.17	0.62	0.06	0.04	0.04	0.10	0.03
		Productid	2	4.32	1.78	0.93	0.07	0.00	0.00	0.04	0.03
Virgilian	Glenshaw (Ames)	Total	27	4.25	0.65	0.89	0.08	0.14	0.07	0.19	0.07
		Composita	1	5.15	N/A	0.72	N/A	0.46	N/A	0.39	N/A
		Crurithyris	5	6.45	2.02	1.28	0.05	0.16	0.04	0.12	0.04
		Neospirifer	20	3.66	0.46	0.81	0.03	0.12	0.08	0.19	0.08
Virgilian	Mattoon (Shumway)	Total	3	10.85	1.55	1.32	0.13	0.21	0.05	0.59	0.36
		Crurithyris	1	9.30	N/A	1.45	N/A	0.17	N/A	0.26	N/A
		Kutorginella	2	11.62	0.01	1.26	0.03	0.24	0.04	0.75	0.26
Virgilian	Oread (Plattsmouth)	Total	30	3.67	0.70	0.78	0.10	0.09	0.05	0.45	0.27
		Composita	12	4.06	1.71	0.62	0.16	0.06	0.07	0.39	0.35
		Crurithyris	5	4.01	0.44	0.79	0.29	0.33	0.13	1.52	0.88
		Neospirifer	13	3.17	0.42	0.93	0.08	0.03	0.02	0.09	0.05

5. DISCUSSION

5.1 Stable Isotopes

5.1.1 Chesterian

The two Chesterian localities are separated by 2,300 kilometers and will be influenced by different environmental factors. First, lower sea levels during the Late Mississippian caused isolated basins to form (Smith and Read, 2001). The Illinois Basin was semi-restricted which would have limited exchange with waters to the west of the Panthalassa Ocean. The Grove Church Formation was deposited in a nearshore, shallow environment as indicated by the presence of brachiopods, bryozoans, corals, trilobites, and ostracods, and was located adjacent to a delta (Weibel and Norby, 1992). These conditions produced brachiopod shells with $\delta^{13}C$ and $\delta^{18}O$ values averaging 1.2‰ and -3.1‰ respectively (Figure 6). These factors combined with restriction likely enhanced the influence of freshwaters containing oxidized terrestrial carbon (Panchuk et al., 2006). The potential for organic matter oxidation is similar to modern analogues such as the Bahaman Banks and Florida Bay, which can show a ^{13}C depletion in dissolved inorganic carbon (DIC) up to 4‰ or more relative to the surrounding ocean (Patterson and Walter, 1994). In Arrow Canyon to the west, the Bird Spring brachiopods are more enriched in ^{13}C and ^{18}O, 3.7‰ and -1.5‰ respectively, compared with those from the Grove Church Formation. This is likely the result of freer exchange with the Panthalassa Ocean. Because the sample location is found at the western edge of Pangea, the $\delta^{13}C$ values should be more reflective of the global ocean.

Brand and Brenckle (2001) also analyzed brachiopods from the Bird Spring formation. Their $\delta^{13}C$ values ranged from 0.9 to 3.5‰ and average 1.5‰ lower than the values obtained in this study. This may be due to methodology. Our study thin-sectioned every shell and used cathodoluminescence to target suitable shell areas to micro-sample, whereas Brand and Brenckle (2001) collected data from brachiopod crystal fragments and used SEM imaging and trace elements for every sample to check for preservation. For the interval of interest, the brachiopod taxa were not identified, which can influence $\delta^{13}C$. Saltzman (2003) produced a $\delta^{13}C$ stratigraphy based on micritic limestone through the Bird Spring at Arrow Canyon. His values were on average 2.8‰ lower than those for pristine brachiopod shell from Jones et al. (2003). Latest Chesterian brachiopods from the foreland Antler Basin to the north of Arrow Canyon in present-day Idaho and Montana ranged in $\delta^{13}C$ from 2.1 to 2.9‰ (Figure 10a; Batt et al., 2007). These values were thought to be lower compared with those from open marine locations due to restriction in the basin and localized carbon inputs.

The oxygen isotopic compositions of the brachiopod shells ($\delta^{18}O_{cl}$ vs. VPDB) have been used to estimate paleotemperatures based on the equation from O'Neil et al. (1969) as reformulated by Hays and Grossman (1991):

$$T^oC = 15.7 - 4.36\,(\delta^{18}O_{cl} - \delta^{18}O_w) + 0.12\,(\delta^{18}O_{cl} - \delta^{18}O_w)^2 \qquad (1)$$

Assuming modern seawater values for $\delta^{18}O$ ($\delta^{18}O_w$ = 0‰ vs. VSMOW), brachiopods from the Grove Church and Bird Spring formations yield paleotemperatures of 26 to 35°C and 15 to 27°C respectively (Table 3). General circulation models (GCM) for the Carboniferous have estimated equatorial paleotemperatures were 20-30°C (Kutzbach and

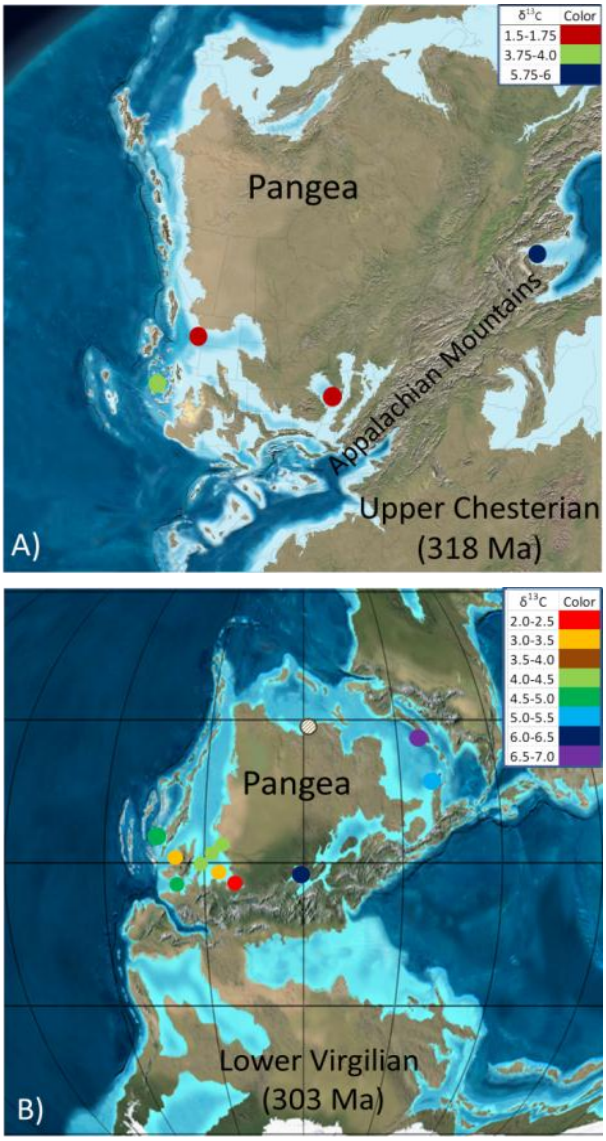

Figure 10. A. Upper Chesterian $\delta^{13}C$ data from this study, Batt et al. (2007), Popp et al. (1986a) and Jones et al. (2003). B. Lower Virgilian data from this study, Beauchamp et al. (1987), Grossman et al. (1991), Saltzman (2003), Mii et al. (1999,2001). Diagonal lines through symbols represent $\delta^{13}C$ from bulk carbonate. Arrow Canyon $\delta^{13}C$ has been adjusted by 2‰ to compensate for difference between bulk carbonate and brachiopod $\delta^{13}C$.

TABLE 3. BRACHIOPOD Mg/Ca AND OXYGEN PALEOTHERMOMETRY.

Time slice	Formation	Genus	Count	Mean Mg/Ca Temp (°C)	Min	Max	Mean Mg/Ca 2x Temp (°C)	Min	Max	Mean $\delta^{18}O$ Temp (°C)	Min	Max
Chesterian	Grove Church	Total	13	13	8	16	27	18	35	30	26	35
		Anthracospirifer	6	11	8	12	24	18	26	27	26	31
		Inflatia	7	15	13	16	31	27	35	32	29	35
Chesterian	Bird Spring	Total	24	6	4	9	12	8	18	23	15	27
		Anthracospirifer	15	6	4	8	11	8	16	23	15	27
		Composita	5	6	5	9	12	10	17	22	19	25
		Productid	4	7	6	9	15	12	18	19	18	20
Virgilian	Glenshaw (Ames)	Total	35	7	5	15	15	10	30	31	16	35
		Composita	3	9	9	9	17	17	17	33	33	33
		Crurithyris	10	11	7	15	21	14	30	21	13	25
		Neospirifer	22	7	5	11	13	10	22	33	31	35
Virgilian	Mattoon (Shumway)	Total	4	17	15	18	34	29	36	27	25	28
		Crurithyris	1	15	x	x	29	x	x	26	25	26
		Kutorginella	2	18	18	18	36	36	36	28	28	28
Virgilian	Oread (Plattsmouth)	Total	30	7	3	17	14	6	36	22	19	25
		Composita	13	7	3	17	15	6	36	22	19	25
		Crurithyris	9	7	6	8	15	13	16	22	22	23
		Neospirifer	8	6	5	9	12	10	18	23	20	25

Gallimore, 1989; Peyser and Poulsen, 2008) with increasing temperatures toward the eastern side of the epeiric sea. Some Bird Spring samples fall outside the lower temperature range because of slightly higher $\delta^{18}O$. However, models are not always representative of local conditions due to uncertainty in parameters such as global pCO_2. Also, models provide sea surface temperatures whereas brachiopods may live below the surface ocean. Grove Church samples are likely outside the modeled temperature boundary due to freshwater input (which would lower $\delta^{18}O_w$, consequently lowering brachiopod calcite $\delta^{18}O$), not diagenesis, because the Grove Church brachiopods contain unaltered shell material.

5.1.2 Virgilian

For the Virgilian time slice, the $\delta^{13}C$ values increase from east (Ames) to west (Shumway then Plattsmouth) (2.1 to 3.2 to 4.3‰) (Figure 6). The same east to west increase occurs for $\delta^{18}O$ (-3.3 to -2.4 to -1.5‰). The Ames Member in the Appalachian Basin records a nearshore environment that is shallow, and is farthest from the open-ocean and closest to Appalachian freshwater discharge (Figure 11) (Algeo and Heckel, 2008). The freshwater influx for the entire Late Pennsylvanian Midcontinent Sea is estimated to be 800–1500 $km^3\ yr^{-1}$, which is similar to the modern Hudson Bay (~975 $km^3\ yr^{-1}$) (Algeo et al., 2008). Of that influx, half flowed from the Appalachian Mountains and into the Appalachian Basin (Gibling et al., 1992). This is believed to have created a surface layer of brackish water that extended far into the US midcontinent. Water beneath this layer is believed to have been of normal marine salinity (Figure 11) (Algeo and Heckel, 2008). Stenohaline fauna such as brachiopods,

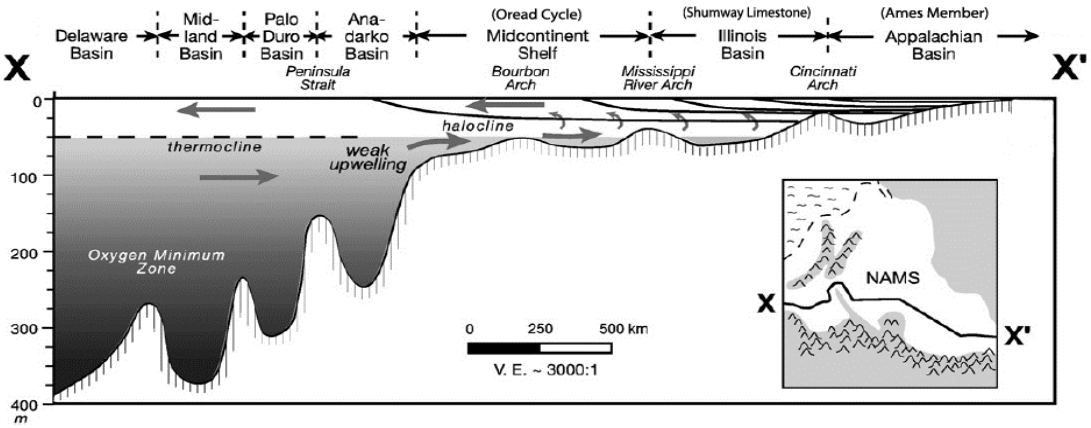

Figure 11. East to west transect of Late Pennsylvanian Midcontinent Sea showing the locations of the Ames Member, Shumway Limestone, and Oread Cycle. Adapted from Algeo and Heckel (2008).

conodonts, echinoderms, bryozoans, corals and sponges have been found in the Appalachian Basin, despite the high freshwater input (Bennington, 1996; Lebold and Kammer, 2006), implying normal marine salinities beneath the hypothetical brackish layer. In cores from the Hushpuckney and Stark shales (US Midcontinent), 80-100% of the organic material (vitrinite and inertinite) is from coals (Algeo et al., 2004), further indicating substantial terrestrial input. In the Midcontinent Sea there is variation in benthic redox proxies and sediments from the northeast to southwest (Algeo and Maynard, 2004). Within black shales, vanadium, uranium, and molybdenum have higher concentrations in the eastern side of the epeiric sea and decrease westward. This is indicative of a strong pycnocline in the east as a result of freshwater influx that tapers off in the west (Figure 12C). Similarly, organics and coarse clays were deposited in the Appalachian Basin closer to the source in the east, while finer clays are found in greater proportion in the west (Algeo et al., 1997). Sediment $\Sigma Nd_{(t)}$ values ($^{143}Nd/^{144}Nd$, corrected for age) from the Appalachians are similar ($\Sigma Nd_{(t)} = -9$) to those from Ouachita Basin and increase farther westward ($\Sigma Nd_{(t)} = -6$) due to higher influence from the eastern Panthalassa Ocean (Figure 12A) (Gleason et al., 1994; Patchett et al., 1999; Algeo and Heckel, 2008). The fresher water could have spread farther west in part because of gyral (counterclockwise) circulation (Figure 12B) (Heckel, 1980). In the Hushpuckney and Stark shales, illite increases relative to smectite which points to a eastern source as coarser clays are found in that direction (Algeo and Heckel, 2008) Because of the estuarine circulation spanning the Late Pennsylvanian Midcontinent Sea and the unrestricted movement of bottom water, it is considered to have superestuarine

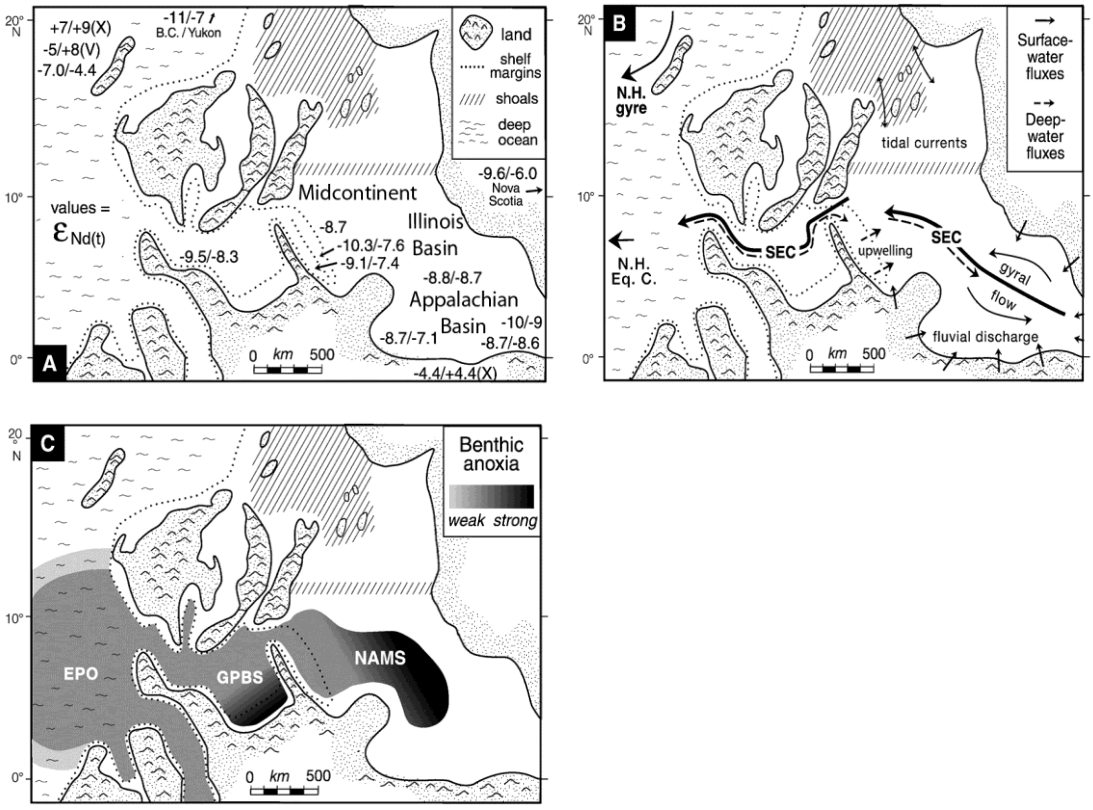

Figure 12. A. Nd isotopes across North America during the Pennsylvanian. Samples with no label are sedimentary, "X" is crystalline, and "V" is volcanic in origin. Appalachian data is provided by (Samson et al., 1995; Coler et al., 1997). The continental margin data is from Smith and Lambert (1995), Blein et al. (1996), Childe and Thompson (1997), Patchett and Gehrels (1998), Simard et al. (2003), and Schwartz et al. (2005). B. Flow of water circulation. "SEC" is supereustuarine and "N.H. Eq. C" is Northern Hemisphere Equatorial Current. C. Benthic anoxia patterns based on redox properties. "LPMS" is Late Pennsylvanian Midcontinent Sea, "GPBS" is Greater Permian Basin Seaway, and "EPO" Eastern Panthalassa Ocean. Data is from Coveney and Shaffer (1988), Cruse and Lyons (2004), and Algeo and Heckel (2008). Figure is adapted from Algeo and Heckel (2008).

circulation (Algeo and Heckel, 2008). Between the Appalachian and Illinois Basins is the Cincinnati Arch, which could slow the exchange of well mixed waters in the west with more restricted waters in the east (Algeo and Heckel, 2008). The Shumway is the mid-point in the east-west transect. The Illinois Basin is less restricted than the Appalachian Basin so the potential for a local-regional $\delta^{13}C$ influence is not as likely but still present. Plattsmouth brachiopods in the midcontinent are the most $\delta^{13}C$ enriched of the transect (4.3‰). To the west of the US midcontinent is deeper water that is well mixed with normal salinities (Algeo et al., 2008). These waters could exchange more readily than the other two basins. The $\delta^{18}O$ values for coeval brachiopods from Texas (Grossman et al., 1993) are lower than those from the US midcontinent. This effect was attributed to evaporation in the interior of the epeiric sea (Grossman et al., 1993).

Assuming $\delta^{18}O_w$ equals 0‰, Virgilian isotopic temperatures range from 16 – 35^{o}C (Table 3). The $\delta^{18}O$ values from the Ames appear low and typically would be interpreted as diagenetically altered but the *Neospirifer* shells are non-luminescent and have low Mn concentrations. Meteoric runoff combined with differing depositional environments is the likely cause of this large range in temperature. Ames *Neospirifer* samples (GRR section) span from 31 – 35^{o} C while *Crurithyris* shells in the FAIR section encompass 16 – 28^{o} C. The freshwater influx is corroborated by previously mentioned low $\Sigma Nd_{(t)}$ in the eastern half of the epeiric sea compared with higher values in the west. The *Crurithyris* $\delta^{18}O$ values and estimated paleotemperatures are interpreted to be the result of evaporative enrichment of $\delta^{18}O_w$. Thus, while the superestuarine circulation model proposed by Algeo and Heckel (2008) may explain the LPMS on a

larger scale, the high *Crurithyris* $\delta^{18}O$ values for the FAIR section suggest that restricted circulation and excess evaporation of waters occurred at least locally in the eastern Appalachian Basin. Shumway and Plattsmouth samples give paleotemperatures of 25 – 28^{o} C and 19 – 25^{o}C respectively. In comparison to the atmospheric general circulation model (GCM) predictions of 20-30^{o}C (Kutzbach and Gallimore, 1989; Peyser and Poulsen 2008), the Shumway results are within this model but the Plattsmouth are not. Except for two slightly enriched $\delta^{18}O$ shell values, Plattsmouth isotopic paleotemperatures and modeled temperatures are similar. Of this Virgilian time slice, the Plattsmouth (US midcontinent) temperatures are interpreted to be the most representative of the epeiric sea due to limited freshwater incursion. Based upon similar fossil assemblages throughout each transect, brachiopod paleodepth is expected to vary only slightly (Madi et al., 1996), ruling out the possibility of temperature dependence on water depth.

Unaltered Ames *Crurithyris* shells are enriched in ^{18}O relative to *Composita* and *Neospirifer*. An explanation for this could be the depositional environment. The Ames was sampled at two different locations. In the first, *Composita* and *Neospirifer* occurred in a light packstone whereas *Crurithyris* were found in a dark shaley mudrock. Lebold and Kammer (2006) interpreted these stratigraphic intervals as different depositional environments and classified them into two distinct biofacies. However, without a sediment gradient analysis or interpreted shoreline, the classification of depositional environments is tenuous. *Neospirifer* and *Composita* were stenohaline and found in a section (GRR) that was farther westward in the basin leading to the interpretation that

they were deposited in a more offshore environment that was well oxygenated with low turbidity (Biofacies 3). The other stratigraphic interval (FAIR), in which *Crurithyris* is the dominant brachiopod, is thought to be clastically dominated and more likely to have had variable salinities because of its location on the eastern edge of the basin and its faunal assemblage. In the section, infaunal bivalves and gastropods comprise 72% of the organisms while *Crurithyris* account for 22%. *Crurithyris* thrived in this environment because it could tolerate euryhaline conditions, higher turbidity, and lowered oxygen levels (Fursich and Hurst, 1980; Brezinski, 1983; Thayer, 1986). Furthermore, *Crurithyris* was opportunistic and could take advantage of stressful environments (Malinky and Heckel, 1998). Pennsylvanian mollusks in the Midcontinent have also been shown to favor low salinity conditions caused by freshwater runoff (Boardman et al., 1987). This lends support to the hypothesis that these *Crurithyris* lived in a restrictive location which could have allowed for evaporative enrichment of seawater $\delta^{18}O$.

An environment analogous to that hypothesized for the Ames FAIR section could be an evaporative zone in Florida Bay. Lloyd (1964) and Halley and Roulier (1999) showed that restriction combined with higher freshwater $\delta^{18}O$ values due to evaporation can increase $\delta^{18}O_w$ to 4.5‰. This could account for the roughly 2‰ $\delta^{18}O$ enrichment of *Crurithyris* relative to other Ames brachiopods (Figure 6). The Illinois Basin is more mixed relative to the Appalachian Basin due to better connectivity to the US midcontinent and declining influence of freshwater. Plattsmouth samples in the

midcontinent were deeper (but still shallower than 100 m) and the most mixed marine of the east-west transect.

Based on the brachiopod $\delta^{18}O$ data and estimates for the $\delta^{18}O$ of seawater and freshwater discharge from the Appalachian Mountains, the salinities at the different localities can be calculated using the following mass balance equation

$$S_m = S_{sw} + \Delta S = S_{sw} + (\delta^{18}O_{br,\,m} - \delta^{18}O_{br,\,sw}) \frac{(S_{fw} - S_{sw})}{(\delta^{18}O_{fw} - \delta^{18}O_{sw})} \quad (2)$$

br = brachiopod, m = measured, fw = freshwater, and sw = open ocean seawater. Salinity of seawater (S_{sw}) is assumed to be near modern levels, 34.5 psu. Note, however, that modeling results suggest that average salinity may have been as high as 46 psu in the Carboniferous (Hay et al., 2006). Salinity of freshwater is assumed to be zero. Measured $\delta^{18}O$ has been taken from the averages of brachiopod data for the Ames, Shumway, and Plattsmouth. Seawater $\delta^{18}O$ is assumed to be 0‰, reflecting modern seawater conditions. Papua New Guinea is a potential analog to the Appalachian Mountains due to its tropical location combined with mountainous terrain. Rainfall $\delta^{18}O$ in this area is -8‰ (Rozanski et al., 1993), which provides the freshwater end member to the equation. If the Plattsmouth Member $\delta^{18}O$ (-1.5‰) is assumed to represent precipitation in waters of normal marine salinity and assume no east-west gradient in temperature, then the Ames brachiopod $\delta^{18}O$ of -3.8‰ equates to a salinity of 25 psu. Farther west in the Shumway Formation (-2.4‰), salinity is estimated to have been 31 psu. Though brachiopods are generally considered to be stenohaline (Boardman et al., 1987), certain modern species have been shown to be euryhaline and tolerate salinities as low as 17.8 psu (Hammen and Lum, 1977).

5.1.3 Carbon Isotopic Evidence for Circulation Patterns

The impact of circulation patterns on the isotopic record of Permo-Carboniferous marginal and epicontinental seas was first observed by Beauchamp et al. (1987), who noted a decreasing $\delta^{13}C$ trend in limestones from Sverdrup Basin (4-7‰) through the Yukon Territory (3-5‰) to British Columbia (1-4‰). The high $\delta^{13}C$ values of the Sverdrup Basin were attributed to ocean stagnation and increased organic carbon burial, whereas the lower $\delta^{13}C$ values of the British Columbia limestones were explained by greater mixing with Panthalassa. In reinterpreting the mid-Carboniferous $\delta^{13}C$ shift of 3‰ observed by Popp et al. (1986a), Mii et al. (1999) proposed that 1.5‰ of the $\delta^{13}C$ increase reflected circulation changes with the closing of the equatorial seaway which resulted in upwelling in the eastern Panthalassa and downwelling in western Paleo-Tethys Oceans.

With restriction, local to regional influences are more likely to influence the character of waters contained in an epeiric sea (Holmden et al., 1998). Residence times of the epeiric seas during the Late Pennsylvanian are estimated to have been 70-130 years (Algeo et al., 2008). Brachiopod shells from Texas provide an example of isotopic records from more open ocean conditions (Grossman et al., 1991). These shells yielded the highest $\delta^{13}C$ values of the Virgilian in the eastern Panthalassa at 4.4‰ (Figure 10b). Farther west, samples from Arrow Canyon, Nevada show similar results (Table 1).

To compare carbon isotope studies of limestones and of brachiopod shells, one must correct for the $\delta^{13}C$ differences between sediment and shells. This correction is required because micritic limestone, unlike pristine brachiopod shell, contains some

diagenetic calcite cements (Grossman et al., 1999). For the Bird Spring Formation, Brand and Brenckle (2001) showed a difference of 1.7‰ between unaltered brachiopods and the surrounding matrix. Jones et al. (2003) also found that Bird Spring brachiopod shells average roughly 2‰ higher in $\delta^{13}C$ than bulk carbonates. Adding 2‰ to the $\delta^{13}C$ of fine-grained carbonate from the Virgilian section of the Bird Spring (Saltzman, 2003) results in "brachiopod-equivalent" $\delta^{13}C$ values averaging 4.5‰, which is very similar to that of Texas brachiopods (Grossman et al., 1991). Farther north, the bulk carbonate analyses from the Sverdrup Basin range between 3-5‰ (Beauchamp et al., 1987), equivalent to a brachiopod $\delta^{13}C$ of 5-7‰ when adjusted. These data suggest higher $\delta^{13}C$ values in the northern margins of Laurussia are due to the connection through the Uralian seaway to Paleo-Tethys. Nonluminescent brachiopods from Spain, representing the western end of Paleo-Tethys, have an average $\delta^{13}C$ of 6.3‰ (Popp et al., 1986a), which is approximately 2‰ higher than US midcontinent samples. Moreover, brachiopods from the Urals and Moscow Basin average 6.6‰ and 5.3‰ respectively (Mii et al., 2001), further indicating the $\delta^{13}C$ differences between eastern Panthalassa and Paleo-Tethys.

In summary, carbonates are higher in $\delta^{13}C$ and $\delta^{18}O$ westward from the Appalachian Basin to the eastern edges of Panthalassa in the Bird Spring and Texas sections. $\delta^{13}C$ continues to increase northward along the western margin of North America to the Sverdrup Basin. Localities eastward of the Sverdrup Basin and within western Paleo-Tethys record the highest $\delta^{13}C$ values of the Pennsylvanian. The

dichotomy between Panthalassa and Paleo-Tethys during the Carboniferous first described by Grossman et al. (1991) is further substantiated and more complex.

5.2 Trace Elements

Mg/Ca ratios in brachiopod shells vary in response to a variety of factors. These include temperature, physiology, precipitation rate, water chemistry, and vital effects. Mg/Ca ratios may vary within brachiopod shells in response to seasonal temperature change (Mii and Grossman, 1994). Primary Mg/Ca ratios can increase or decrease when subjected to meteoric diagenesis depending on the original concentrations and the Mg/Ca of the diagenetic fluids (Grossman et al., 1996). However, as discussed earlier, such diagenetic effects are obviated by cathodoluminescence and trace element screening.

Trace element differences between taxa (vital effects) can confound efforts to use trace elements as environmental proxies. Such vital effects are seen in the brachiopods analyzed in this study. For example, Chesterian Grove Church *Inflatia* (a productid) average 3 mmol/mol higher in Mg/Ca compared with *Anthracospirifer* (Figure 9*)*. A similar taxonomic effect was seen in Popp et al. (1986a), with the productid *Gigantoproductus* having higher Mg/Ca values than spiriferids *Choristites* and *Martinia.* In the Bird Spring, *Anthracospirifer* and *Composita* exhibit no difference in Mg/Ca (2 – 5 mmol/mol range). For a given temperature and brachiopod taxon, Mg/Ca values from well-mixed, open marine settings should not vary spatially. However, this may not be the case in more restrictive basins where waters have less exchange with the open ocean. For Chesterian samples, Mg/Ca values are higher in the Illinois Basin (Grove Church)

than in the Bird Spring Basin. Opposite to the relationship, $\delta^{18}O$ values are higher in the Bird Spring Basin and decrease eastward to the Illinois Basin (Grove Church; Fig. 11). One possible reason for why samples in the Illinois Basin have such a distinct enrichment in Mg/Ca compared with those of the Bird Spring Formation could be localized inputs. For example, weathering of silicates has been shown to increase the Mg/Ca of river waters, though the waters typically have a lower Mg/Ca than sea water except for watersheds with peridotite exposures (Meybeck et al., 1987). During the Chesterian, freshwater runoff from the Schreiber-Hemlo greenstone belt rocks of the eastern Canadian Shield by way of the Michigan River (Treworgy, 1991) likely brought waters of higher Mg/Ca derived from silicate weathering into the Illinois Basin. This belt, located in the Superior Province of the Canadian Shield contains a diverse lithology composed mainly of mafic to ultramafic volcanics (which would have higher Mg/Ca) and lesser amounts of felsic volcanics (Card, 1990). Mg/Ca values of Bird Spring brachiopods are 2 – 4 mmol/mol, lower than those in Grove Church specimens (5.5 to 12 mmol/mol). The likely causes are a combination of vital effect and restriction of the Illinois Basin. In a separate study by Brand and Brenckle (2001), brachiopod Mg/Ca from the same Chesterian time interval in Arrow Canyon averaged much higher, 10.2 mmol/mol. This may be due to differences in vital effect; unfortunately, the authors did not identify taxa in this interval, hindering comparison.

During the Virgilian, the Illinois Basin again is higher in Mg/Ca relative to the other locations. Virgilian *Neospirifer* from the Ames and Plattsmouth give similar Mg/Ca averages (3.7±1.1 and 3.2 ±0.8 mmol/mol) while the Shumway average is

10.9±1.3 mmol/mol (Figure 13). Within the Ames Member, *Crurithyris* shells have Mg/Ca values similar to those of *Neospirifer* and *Composita. Composita* in the Plattsmouth vary from 1.3 to 11.3 mmol/mol but they average 4.1 mmol/mol. Large Mg/Ca ranges such as this have been known to occur in a single shell (Grossman et al., 1996). During the time interval, Ames and Plattsmouth are similar on average while Shumway samples have much higher Mg/Ca ratios. This could indicate that the Appalachian Basin and US midcontinent are receiving a similar Mg/Ca water signal and the Illinois Basin has an additional influence. However, caution should be used in interpreting the data because of limited Shumway sample recovery. Again, perhaps restricted circulation and drainage from the Canadian Shield were causal factors, though the evidence is equivocal.

Sr/Ca ratios in brachiopod shells are influenced by similar factors as Mg/Ca ratios. Salinity also is influential on Sr/Ca ratios but only at levels of <10 psu (Dodd and Crisp, 1982). Ideally, metals that follow the thermodynamic distribution law for calcite precipitation will not vary in an evaporative zone because water will be removed but the overall metal-Ca ratio will be the same (Grossman et al., 1996). Within the Grove Church, *Anthracospirifer* has a higher Sr/Ca relative to *Composita* and in the Bird Spring *Inflatia* is enriched relative to *Anthracospirifer*. These same relationships between spiriferids and *Composita* and between productids and spiriferids have been seen in Popp et al. (1986a) and Grossman et al. (1996) and could be the result of vital effects related to precipitation rate. As with Mg/Ca ratios, another potential influence on Sr/Ca values is local hydrography. Sr/Ca in modern oceans varies globally by 2-3% (de

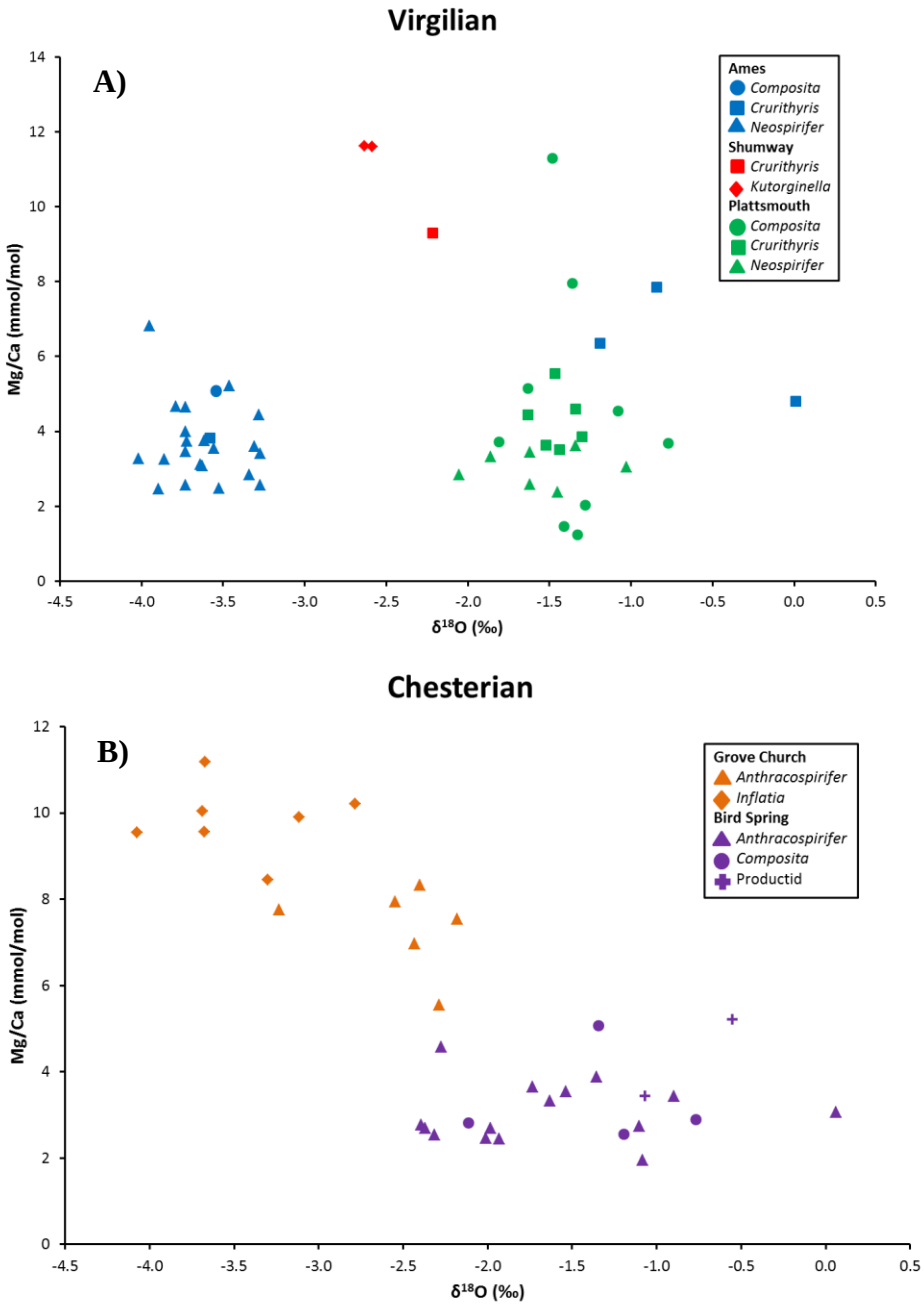

Figure 13. Scatter diagram of Mg/Ca versus $\delta^{18}O$ for brachiopod shells. A: Virgilian Ames, Shumway, and Plattsmouth Members. B: Chesterian Grove Church Formation and Bird Spring Formations.

Villiers, 1999), but within the Carboniferous transects there appears to be larger differences. These differences cannot be attributed to vital effects, as similar brachiopod taxa are compared. Thus, Sr/Ca differences between localities may be due to differences in local water chemistry.

Average seawater Sr/Ca for the Carboniferous has been estimated to be ~5 mmol/mol by Stueber and Veizer (2002) based on the compilation of brachiopod data in Veizer et al. (1999). This compilation does not differentiate between brachiopod taxa. Because the distribution coefficient for Sr in biogenic calcite is dependent on precipitation rate (Lorens, 1981; Mucci, 1986) and because brachiopods exhibit varied growth rates, the resulting Sr/Ca ratio will change depending on taxa. However, using modern brachiopod D_{Sr}, Paleozoic $Sr/Ca_{seawater}$ can be approximated. Using a D_{Sr} of 0.13 as in Steuber and Veizer (2002), Chesterian *Anthracospirifer* yield 8.5 and 6.0 mmol/mol for the Illinois Basin (Grove Church) and Bird Spring Basin (Bird Spring) waters respectively. Because the Bird Spring Basin is proximal to the Panthalassa Ocean, the Sr/Ca values will be closer to that of the global average. Perhaps water sources outside the Illinois Basin brought Sr-rich freshwater and, combined with restriction in the Illinois Basin, caused high Sr/Ca in the Shumway brachiopods.

For the Virgilian, Sr/Ca ratios for most Ames and Plattsmouth *Neospirifer* fall near the global Sr/Ca brachiopod curve of Stueber and Veizer (2002), while Shumway brachiopods values are higher. Using the same modern $D_{Sr} = 0.13$ for brachiopods, *Neospirifer* from the Ames and Plattsmouth average 5.4 mmol/mol and Plattsmouth 6.2 mmol/mol in seawater Sr/Ca respectively. Taxonomic differences complicate

interpretation as Sr/Ca values are highest in *Crurithyris* followed by *Neospirifer* and *Composita*, similar to the results of Grossman et al. (1996). There are neither *Neospirifer* nor *Composita* specimens from the Shumway and few unaltered *Composita* in the Ames, so defining regional variations in Sr/Ca is difficult. *Neospirifer* values from the Plattsmouth and Ames are not significantly different. *Crurithyris* values, albeit with limited data, do show some variation. Sr/Ca is lowest in the US midcontinent, intermediate in the Appalachian Basin, and highest in the Illinois Basin. Because a single species is used to avoid the vital effect, the differences may reflect regional influences enhanced by basinal water restriction.

5.3 Evaluation of Mg/Ca Paleothermometry

Mg/Ca ratios in mollusks have been shown to vary as a function of temperature (Klein et al., 1996; Vander Putten et al., 2000). Working with brachiopod shells, Grossman et al. (1994) showed that Mg/Ca correlated negatively with $\delta^{18}O$ suggesting that seasonal temperature changes could modulate Mg/Ca uptake. Subsequent studies of Mg/Ca thermometry in brachiopods (Perez-Huerta et al., 2008; Powell et al., 2009) have applied the equation from Vander Putten et al. (2000).

$$T\,^{\circ}C = \frac{\left(\frac{Mg}{Ca} * 1000\right) + 0.63(\pm.29)}{0.70(\pm 0.02)} \quad (3)$$

This equation is based on the mollusk *Mytilus edulis,* which like other mollusks, is subject to vital effects (Tanaka et al, 1986). The first problem with the general application of Mg/Ca thermometry is that brachiopods are composed of low magnesium calcite and mollusks precipitate aragonite, leading to possible differences Mg/Ca because of vital effects. (Popp et al., 1986a; Grossman et al., 1996). Secondly, the

equation does not consider the vital effects of different brachiopod taxa. Finally, there is no systematic relationship between Mg/Ca and $\delta^{18}O$ that would imply a temperature dependence on Mg/Ca ratio though, admittedly, $\delta^{18}O$ can also covary with $\delta^{18}O_w$ and is thus not a definitive measure of temperature.

Applying equation 2 to the brachiopod Mg/Ca data appears to underestimate every temperature calculated by $\delta^{18}O$. In the Klein (1996) study, Mg/Ca and $\delta^{18}O$ for the mollusks in question covaried significantly. The two most marine formations in this study, the Bird Spring and Plattsmouth, give Mg/Ca-derived temperatures less than 10°C, which are unreasonable for the tropics. Grove Church samples, even with very large average Mg/Ca values, 8.7 mmol/mol, still only yield a maximum estimated temperature of 16°C. The vital effect amongst brachiopods combined with local variations in seawater Mg/Ca likely distorts the temperature estimate. A Mg/Ca thermometry equation calibrated with brachiopod shells may allow for more accurate Mg/Ca paleotemperature determinations. Powell et al. (2009) attempted to rectify the low Mg/Ca temperature estimates by correcting for differences between modern and Carboniferous seawater Mg/Ca using the curve of Hardie (1996). Modern seawater Mg/Ca is 5.2 mol/mol (Hardie, 1996) while values for Chesterian and Virgilian seawater were estimated to be 2.5 mol/mol. After adjustment, the resulting minimum and maximum temperature are more extreme. For the Plattsmouth, the minimum temperature is 6°C and the maximum is 36°C with a mean of 14°C. In the location where Mg/Ca thermometry would be most useful, the Appalachian Basin, the temperatures are consistent with the rest of the findings. *Neospirifer* varies from 10 to 22°C, a value

unlikely in an equatorial environment. The only unit to approach reasonable tropical temperatures is the Chesterian Grove Church with a mean of 27^{o}C. Application of Mg/Ca thermometry to brachiopod shells may prove useful in the future, but until a suitable equation is found, the use of this as a paleothermometer is untenable.

6. CONCLUSIONS

Nonluminescent brachiopod shells from the Chesterian show an east-west increase in $\delta^{13}C$ and $\delta^{18}O$ from the Illinois Basin to the Bird Spring Shelf. This is interpreted as greater freshwater influx on more restricted basins in the east and more open ocean circulation in the west near the Panthalassa Ocean. The Virgilian transect shows a similar pattern of increasing in $\delta^{13}C$ and $\delta^{18}O$ from east to west and can be interpreted similarly. Assuming modern salinities (34.5 psu) for the U.S. midcontinent (Plattsmouth Member), estimated salinity is 25 psu in the Appalachian Basin (Ames Member) and increases to 31 psu in the Illinois Basin (Shumway Member). This is interpretation is supported by published neodymium isotope data and sedimentological and paleobiological evidence for depositional environment. $\Sigma Nd_{(t)}$ values increase from $\Sigma Nd_{(t)} = -9$ in the eastern part of the epeiric sea to $\Sigma Nd_{(t)} = -6$ indicating open marine conditions in the west. The freshwater influx, estimated by others to be 400–750 km^3 yr^{-1}, drained off of the Appalachian Mountains and into the eastern edge of the Appalachian Basin, entraining clastics and depositing preferentially larger grain sizes in the east.

There is no consistent relationship between Mg/Ca and $\delta^{18}O$ that would support a temperature dependence of Mg/Ca ratios in brachiopod shells. Application of the Mg/Ca paleothermometer based on mollusk shells vastly underestimates tropical temperatures even after correcting for the Mg/Ca of Carboniferous seawater. Mg/Ca and Sr/Ca ratios

are unusually high in Illinois Basin samples, suggesting restricted circulation in the basin.

REFERENCES CITED

Algeo, T.J., Hoffman, D.L., Maynard, J.B., Joachimski, M.M., Hower, J.C., Watney, W.L., 1997, Environmental reconstruction of anoxic marine systems: core black shales of Upper Pennsylvanian Midcontinent cyclothems, *in* Algeo, T.J., and Maynard, J.B. eds., Cyclic Sedimentation of Appalachian Devonian and Midcontinent Pennsylvanian Black Shales: Analysis of Ancient Anoxic Marine Systems – A Combined Core and Field Workshop. Joint Meeting of Eastern Section AAPG and The Society for Organic Petrography (TSOP), Lexington, Kentucky, Sept. 27-28, 1997, p. 103-147.

Algeo, T.J., and Maynard, J.B., 2004, Trace-element behavior and redox facies in core shales of Upper Pennsylvanian Kansas-type cyclothems: Chemical Geology, v. 206, p. 289-318.

Algeo, T.J., Schwark, L., and Hower, J.C., 2004, High-resolution geochemistry and sequence stratigraphy of the Hushpuckney Shale (Swope Formation, eastern Kansas): implications for climato-environmental dynamics of the Late Pennsylvanian Midcontinent Seaway: Chemical Geology, v. 206, p. 259-288.

Algeo, T. J. and Heckel, P. H., 2008, The Late Pennsylvanian Midcontinent Sea of North America: A review: Palaeogeography Palaeoclimatology Palaeoecology, v. 268, p. 205-221.

Algeo, T.J., Heckel, P.H., Maynard, J.B., Blakey, R., Rowe, H., 2008, Modern and ancient epicratonic seas and the superestuarine circulation model of marine

anoxia. *in* Holmden, C., and Pratt, B.R. eds., Dynamics of Epeiric Seas: Sedimentological, Paleontological and Geochemical Perspectives: Location, Geological Association of Canada Special Publication, vol. 48, p. 7–38.

Allan, J. R. and Matthews R.K., 1977, Carbon and oxygen isotopes and stratigraphic tools – surface and subsurface data, Barbados – West Indies: Geology, v. 5 p. 16-20.

Batt, L.S., Montanez, I.P., Isaacson, P., Pope, M.C., Butts, S.H., and Abplanalp, J., 2007, Multi-carbonate component reconstruction of mid-carboniferous (Chesterian) seawater $\delta^{13}C$: Palaeogeography, Palaeoclimatology, Palaeoecology, v. 256, p. 298-318.

Beauchamp, B., Oldershaw, A.E., and Krouse, H.R., 1987, Upper Carboniferous to Upper Permian C-13-enriched primary carbonates in the Sverdrup Basin, Canadian Arctic – Comparisons to coeval western North-American ocean margins: Chemical Geology, v. 65, p. 391-413.

Bennington, J.B., 1996, Stratigraphic and biofacies patterns in the Middle Pennsylvanian Magoffin Marine Unit in the Appalachian Basin, USA: International Journal of Coal Geology, v. 31, p. 169-193.

Berner, R. A., 1997, Paleoclimate: The rise of plants and their effect on weathering and atmospheric CO_2, Science, v. 276 p. 544-546.

Blakey, R.C., 2005, Paleogeography and tectonic evolution of late Paleozoic sedimentary basins, southwestern North America, Geological Society of America, Abstracts with Program, 2005 Salt Lake City Annual Meeting (October

16-19, 2005), v. 37, no. 7, p. 442. (images downloaded from: http://jan.ucc.nau.edu/~rcb7/nam.html; last accessed 9/8/2010).

Blein, O., Lapierre, H., Schweicker, R.A., Monie, P., Maluski, H., and Pecher, A., 1996, Remnants of the northern Sierra Nevada Paleozoic island arc in western Nevada: Journal of Geology, v. 104, p. 485-492.

Boardman, R.S., Cheetham, A.H., and Rowell, A.J., 1987, Fossil invertebrates: Palo Alto, California, Blackwell Scientific Publications.

Brand, U. and Veizer, J., 1980, Chemical diagenesis of a multicomponent carbonate system, trace-elements: Journal of Sedimentary Petrology, v. 50, p. 1219-1236.

Brand, U., and Brenckle, P., 2001, Chemostratigraphy of the Mid-Carboniferous boundary global stratotype section and point (GSSP), Bird Spring Formation, Arrow Canyon, Nevada, USA: Palaeogeography, Palaeoclimatology, Palaeoecology, v. 165, p. 321-347.

Brezinski, D.K., 1983, Developmental model for an Appalachian marine incursion: Northeastern Geology v.5, p.92–99.

Broecker, W.S., and Peng, T.-H., 1982, Tracers in the Sea: Palisades, New York, Eldigio Press.

Bruckschen, P., Oesmann, S., Veizer, J., 1999, Isotope stratigraphy of the European Carboniferous: Proxy signals for ocean chemistry, climate and tectonics: Chemical Geology, v. 161, p. 127-163.

Bruckschen, P., Veizer, J., Schwark, L., Leythaeuser, D., 2001, Isotope stratigraphy for the transition from the late Palaeozoic greenhouse in the Permo-Carboniferous icehouse—new results: Terra Nostra, v.4, p.7–11.

Card, K.D., 1990, review of the Superior Province of the Canadian Shield, a product of Archean accretion: Precambrian Research, v. 48, p. 99-156.

Carpenter, S. J. and. Lohmann, K.C., 1995, $\delta^{18}O$ and $\delta^{13}C$ values of modern brachiopod shells: Geochimica et Cosmochimica Acta, v. 59, p. 3749-3764.

Childe, F.C., and Thompson, J.F.H., 1997, Geological setting, U-Pb geochronology, and radiogenic isotopic characteristics of the Permo-Triassic Kutcho Assemblage, north-central British Columbia: Canadian Journal of Earth Sciences, v. 34, p. 1310-1324.

Coler, D.G., Samson, S.D., and Speer, J.A., 1997, Nd and Sr isotopic constraints on the source of Alleghanian granites in the Raleigh metamorphic belt and Eastern slate belt, southern Appalachians, U.S.A: Chemical Geology, v. 134, p. 257-275.

Compston, W., 1960, The carbon isotopic compositions of certain marine invertebrates and coals from the Australian Permian: Geochimica et Cosmochimica Acta, v. 18, p. 1-22.

Coveney, R.M., Jr., and Shaffer, N.R., 1988, Sulfur-isotope variations in Pennsylvanian shales of the midwestern United States: Geology, v. 16, p. 18-21.

Cruse, A.M., and Lyons, T.W., 2004, Trace metal records of regional paleoenvironmental variability in Pennsylvanian (Upper Carboniferous) black shales: Chemical Geology, v. 206, p. 319-345.

de Villiers, S., 1999, Seawater strontium and Sr/Ca variability in the Atlantic and Pacific oceans: Earth and Planetary Science Letters, v. 171, p. 623-634.

Dodd, J.R., and Crisp, E.L., 1982, Non-linear variation with salinity of Sr/Ca and Mg/Ca ratios in water and aragonitic bivalve shells and implications for paleosalinity studies: Palaeogeography, Palaeoclimatology, Palaeoecology, v. 38, p. 45-56.

Elrick, M. and Scott, L.A., 2010, Carbon and oxygen isotope evidence for high-frequency (10^4-10^5 yr) and My-scale glacio-eustasy in Middle Pennsylvanian cyclic carbonates (Gray Mesa Formation), Central New Mexico: Palaeogeography, Palaeoclimatology, Palaeoecology, v. 285, p. 307-320.

Fielding, C.R., Frank, T.D., and Isbell, J.L., 2008, Resolving the late Paleozoic ice age in time and space: Boulder, Colorado, Geological Society of America Special Publication 441, p. 354.

Fursich, F. T. and Hurst, J.M., 1980, Euryhalinity of Paleozoic articulate brachiopods: Lethaia, v. 13, p. 303-312.

Gibling, M.R., Calder, J.H., Ryan, R., Vandepoll, H.W., and Yeo, G.M., 1992, Late Carboniferous and early Permian drainage patterns in Atlantic Canada: Canadian Journal of Earth Sciences, v. 29, p. 338-352.

Gies, H., 1976, Zur Beziehung zwishchen Photolumineszenz und Chemismus naturlicher Karbonate: Neues Jahrbuch fur Mineralogie Abhandlungen, v. 127, p. 1-46.

Gleason, J.D., Patchett, P.J., Dickinson, W.R., and Ruiz, J., 1994, Nd isotopes link Ouachita turbidites to Appalachian sources: Geology, v. 22, p. 347-350.

Gross, M. G., 1964, Variations in the $\delta^{18}O$ and $\delta^{13}C$ ratios of diagenetically altered limestones in the Bermuda Islands: Journal of Geology, v. 72, p. 170-194.

Grossman, E.L., Zhang, C.L., and Yancey, T.E., 1991, Stable-isotope stratigraphy of brachiopods from Pennsylvanian shales in Texas: Geological Society of America Bulletin, v. 103, p. 953-965.

Grossman, E. L., Mii, H. S., Yancey, T. E., 1993, Stable isotopes in Late Pennsylvanian brachiopods from the United States – Implications for Carboniferous paleoceanography: Geological Society of America Bulletin, v. 105, p. 1284-1296.

Grossman, E.L., Mii, H.S., Zhang, C., Yancey, T.E., 1996, Chemical variation in Pennsylvanian brachiopod shells - Diagenetic, taxonomic, microstructural, and seasonal effects: Journal of Sedimentary Research, v. 66, p. 1011-1022.

Grossman, E.L., Yancey, T.E., Jones, T.E., Bruckschen, P., Chuvashov, B., Mazzullo, S.J., and Mii, H.-s., 2008, Glaciation, aridification, and carbon sequestration in the Permo-Carboniferous: The isotopic record from low latitudes: Palaeogeography, Palaeoclimatology, Palaeoecology, v. 268, p. 222-233.

Halley, R.B., and Roulier, L.M., 1999, Reconstructing the history of eastern and central Florida Bay using mollusk-shell isotope records: Estuaries, v. 22, p. 358-368.

Hammen, C.S., and Lum, S.C., 1977, Salinity tolerance and pedicle regeneration of lingula: Journal of Paleontology, v. 51, p. 548-551.

Hardie, L.A., 1996, Secular variation in seawater chemistry: An explanation for the coupled secular variation in the mineralogies of marine limestones and potash evaporites over the past 600 m.y: Geology, v. 24, p. 279-283.

Hay, W.W., Migdisov, A., Balukhovsky, A.N., Wold, C.N., Flogel, S., and Soding, E., 2006, Evaporites and the salinity of the ocean during the Phanerozoic: Implications for climate, ocean circulation and life: Palaeogeography, Palaeoclimatology, Palaeoecology, v. 240, p. 3-46.

Hays, P.D., and Grossman, E.L., 1991, Oxygen isotopes in meteoric and calcite cements and indicators of continental paleoclimate: Geology, v. 19, p. 441-444.

Heckel, P.H., 1977, Origin of phosphatic black shale facies in Pennsylvanian cyclothems of mid-continent North America: AAPG Bulletin, v. 61, p. 1045-1068.

Heckel, P.H., 1980,. Paleogeography of eustatic model for deposition of Midcontinent Upper Pennsylvanian cyclothems. *in* Fouch, T.D. and Magathan, E.R. eds., Paleozoic Paleogeography of the West-Central United States: Denver, Colorado, SEPM-Rocky Mountain Section, p. 197–215.

Heckel, P.H., Gibling, M.R., King, N.R., 1998, Stratigraphic model for glacial-eustatic Pennsylvanian cyclothems in highstand nearshore detrital regimes: Journal of Geology, v. 106, p. 373-383.

Holmden, C., Creaser, R. A., Muehlenbachs, K., Leslie, S. A., Bergstrom, S. M., 1998, Isotopic evidence for geochemical decoupling between ancient epeiric seas and bordering oceans - Implications for secular curves: Geology, v. 26, p. 567-570.

Joachimski, M.M., Simon, L., van Geldern, R., Lécuyer, C., 2005, Boron isotope geochemistry of Paleozoic brachiopod calcite: Implications for a secular change in the boron isotope geochemistry of seawater over the Phanerozoic: Geochimica et Cosmochimica Acta, v. 69, p. 4035-4044.

Joachimski, M. M., von Bitter, P.H., Buggisch, W., 2006, Constraints on Pennsylvanian glacioeustatic sea-level changes using oxygen isotopes of conodont apatite: Geology, v. 34, p. 277-280.

Johnson, K.S., 1989, Evaporite deposits in Carboniferous rocks of the U.S.A. XI Congrès International de Stratigraphie et de Géologie du Carbonifere, Beiing 1987. Compte Rendu, 4, p.51–65.

Jones, T.E., Grossman, E.L., and Yancey, T.E., 2003, Exploring the stable isotope record of global change and paleoclimate: The mid-Carboniferous GSSP (Arrow Canyon, Nevada) and the Ural Mountains, Russia: Geological Society of America Abstracts with Programs, v. 35, p. 254.

Klein, R. T., Lohmann, K.C., Thayer, C.W., 1996, Bivalve skeletons record sea-surface temperature and $\delta^{18}O$ via Mg/Ca and ^{18}O /^{16}O ratios: Geology, v. 24, p. 415-418.

Korte, C., Jasper, T., Kozur, H.W., and Veizer, J., 2005, $\delta\ ^{18}O$ and $\delta\ ^{13}C$ of Permian brachiopods: A record of seawater evolution and continental glaciation: Palaeogeography, Palaeoclimatology, Palaeoecology, v. 224, p. 333-351.

Kutzbach, J.E., and Gallimore, R.G., 1989, Pangean climates – Megamonsoons of the megacontinent: Journal of Geophysical Research-Atmospheres, v. 94, p. 3341-3357.

Lane, H. R., Brenckle, P. L., Baesemann, J. F., Richards, B., 1999, The IUGS boundary in the middle of the Carboniferous, Arrow Canyon, Nevada, USA: Episodes, v. 22, p. 272-283.

Langenheim, R.L., Carss, B.W., Kennerly, J.B., McCutcheon, V. A., Waines, R.H., 1962, Paleozoic Section in Arrow Canyon Range, Clark County, Nevada: Bulletin of the American Association of Petroleum Geologists, v. 46, p. 592-609.

Lebold, J. G. and Kammer, T.W., 2006, Gradient analysis of faunal distributions associated with rapid transgression and low accommodation space in a Late Pennsylvanian marine embayment: Biofacies of the Ames Member (Glenshaw Formation, Conemaugh Group) in the northern Appalachian Basin, USA: Palaeogeography, Palaeoclimatology, Palaeoecology, v. 231, p. 291-314.

Lloyd, R. M., 1964, Variations in the oxygen and carbon isotope ratios of Florida Bay mollusks and their environmental significance: Journal of Geology, v. 72, p. 84-111.

Lorens, R.B., 1981, Sr, Cd, Mn and Co distribution coefficients in calcite as a function of calcite precipitation rate: Geochimica et Cosmochimica Acta, v. 45, p. 553-561.

Lowenstam, H. A., 1961, Mineralogy, O^{18} / O^{16} ratios, and strontium and magnesium contents of recent brachiopods and their bearing on the history of the oceans: Journal of Geology, v. 69, p. 241-260.

Lowenstein, T.K., Timofeeff, M.N., Brennan, S.T., Hardie, L.A., and Demicco, R.V., 2001, Oscillations in Phanerozoic seawater chemistry: Evidence from fluid inclusions: Science, v. 294, p. 1086-1088.

Machel, H. G., 1985, Cathodoluminescence in calcite and dolomite and its chemical interpretation: Geoscience Canada, v. 12, p. 139-147.

Madi, A., Bourque, P.A., and Marnet, B.L., 1996, Depth-related ecological zonation of a Carboniferous carbonate ramp: Upper Visean of Bechar basin, western Algeria: Facies, v. 35, p. 59-79.

Malinky, J.M., and Heckel, P.H., 1998, Paleoecology and taphonomy of faunal assemblages in gray "core" (offshore) shales in midcontinent Pennsylvanian cyclothems: Palaios, v. 13, p. 311-334.

Medlin, W. L., 1961, Thermoluminescence in aragonite and magnesite: Journal of Physical Chemistry, v. 65, p. 1172-1185.

Meybeck, M., 1987, Global chemical weathering of surficial rocks estimated from river dissolved loads: American Journal of Science, v. 287, p. 401-428.

Mii, H.S., and Grossman, E.L., 1994, Late Pennsylvanian seasonality reflected in the $\delta^{18}O$ and elemental composition of a brachiopod shell: Geology, v. 22, p. 661-664.

Mii, H. S., Grossman, E.L., Yancey, T.E., 1999, Carboniferous isotope stratigraphies of North America, Implications for Carboniferous paleoceanography and Mississippian glaciation: Geological Society of America Bulletin, v. 111, p. 960-973.

Mii, H. S., Grossman, E.L., Yancey, T.E., Chuvashov, B., Egorov, A., 2001, Isotopic records of brachiopod shells from the Russian Platform - evidence for the onset of mid-Carboniferous glaciation: Chemical Geology, v. 175, p. 133-147.

Mucci, A., 1986, Growth kinetics and composition of magnesian calcite overgrowths precipitated from seawater: Quantitative influence of orthophosphate ions: Geochimica et Cosmochimica Acta, v. 50, p. 2255-2265.

O'Neil, J.R., Clayton, R.N., and Mayeda, T.K., 1969, Oxygen isotope fractionation in divalent metal carbonates: Journal of Chemical Physics, v. 51, p. 5547-5558.

Panchuk, K.M., Holmden, C., Kump, L. R., 2005, Sensitivity of the epeiric sea carbon isotope record to local-scale carbon cycle processes: Tales from the Mohawkian Sea: Palaeogeography, Palaeoclimatology, Palaeoecology, v. 228, p. 320-337.

Panchuk, K.M., Holmden, C. E., Leslie, S. A., 2006, Local controls on carbon cycling in the Ordovician midcontinent region of North America, with implications for carbon isotope secular curves: Journal of Sedimentary Research, v. 76, p. 200-211.

Patchett, P.J., and Gehrels, G.E., 1998, Continental influence on Canadian Cordilleran terranes from Nd isotope study, and significance for crustal growth processes: The Journal of Geology, v. 106, p. 269-280.

Patchett, P.J., Ross, G.M., and Gleason, J.D., 1999, Continental drainage in North America during the Phanerozoic from Nd isotopes: Science, v. 283, p. 671-673.

Patterson, W. P. and Walter, L.M., 1994, Depletion of $\delta^{13}C$ in seawater ΣCO_2 on modern carbonate platforms – Significance for the carbon isotopic record of carbonates: Geology, v. 22, p. 885-888.

Pérez-Huerta, A., Cusack, M., Jeffries, T.E., and Williams, C.T., 2008, High resolution distribution of magnesium and strontium and the evaluation of Mg/Ca thermometry in recent brachiopod shells: Chemical Geology, v. 247, p. 229-241.

Peyser, C.E., and Poulsen, C.J., 2008, Controls on Permo-Carboniferous precipitation over tropical Pangaea: A GCM sensitivity study: Palaeogeography, Palaeoclimatology, Palaeoecology, v. 268, p. 181-192.

Popp, B.N., Anderson, T.F., Sandberg, P.A., 1986a, Brachiopods as indicators of original isotopic compositions in some Paleozoic limestones: Geological Society of America Bulletin, v. 97, p. 1262-1269.

Popp, B.N., Anderson, T.F., Sandberg, P.A. 1986b, Textural, elemental, and isotopic variations among constituents in Middle Devonian limestones, North America: Journal of Sedimentary Petrology, v. 56, p. 715-727.

Powell, M.G., Schone, B.R., and Jacob, D.E., 2009, Tropical marine climate during the late Paleozoic ice age using trace element analyses of brachiopods: Palaeogeography, Palaeoclimatology, Palaeoecology, v. 280, p. 143-149.

Pryor, W.A., 1961, Sand trends and paleoslope in Illinois Basin and Mississippi Embayment. *in* Peterson, J.A. and Osmond, J.C., eds. Geometry of sandstone bodies, Tulsa, Oklahoma, American Association of Petroleum Geologists., p. 119–133.

Rozanski, K., Araguds-Araguds L.and Gonfiantini, R., 1993, Isotopic patterns in modem global precipitation. *in* P.K. Swart, K.C. Lohman, J. McKenzie and S. Savin eds. Climate Change in Continental Isotopic Records - Geophysical Monograph 78: Washington, D.C American Geophysical Union, p. 1-36.

Rygel, M.C., Fielding, C.R., Frank, T.D., and Birgenheier, L.P., 2008, The magnitude of late Paleozoic glacioeustatic fluctuations: A synthesis: Journal of Sedimentary Research, v. 78, p. 500-511.

Saltzman, M. R., 2003, Late Paleozoic ice age: Oceanic gateway or pCO_2?: Geology, v. 31, p. 151-154.

Samson, S.D., Coler, D.G., and Speer, J.A., 1995, Geochemical and Nd-Sr-Pb isotopic composition of Alleghanian granites of the southern Appalachians: Origin, tectonic setting, and source characterization: Earth and Planetary Science Letters, v. 134, p. 359-376.

Scheihing, M. H. and Langenheim, R.L., 1980, Brachiopods of the suborder Strophomenidina from the Shumway Cyclothem, Mattoon Formation, Virgilian of Illinois: Journal of Paleontology, v. 54, p. 1017-1034.

Schwartz, J.J., Frost, C.D., Snoke, A.W., 2005, Contrasting Nd isotopic characteristics from the Baker Terrane of northeastern Oregon; implications for tectonic evolution. Geological Society of America Abstracts with Programs, v.37, p. 19.

Simard, R.L., Dostal, J., and Roots, C.F., 2003, Development of late Paleozoic volcanic arcs in the Canadian Cordillera: An example from the Klinkit Group, northern

British Columbia and southern Yukon: Canadian Journal of Earth Sciences, v. 40, p. 907-924.

Smith, A.D., and Lambert, R.S., 1995, Nd, Sr, and Pb isotopic evidence for contrasting origins of late Paleozoic volcanic-rocks from the Slide Mountain and Cache Creek terranes, south-central British-Columbia: Canadian Journal of Earth Sciences, v. 32, p. 447-459.

Smith, L. B. and Read, J.F., 2000, Rapid onset of late Paleozoic glaciation on Gondwana: Evidence from Upper Mississippian strata of the Midcontinent, United States: Geology, v. 28, p. 279-282.

Smith, L.B., and Read, J.F., 2001, Discrimination of local and global effects on Upper Mississippian stratigraphy, Illinois Basin, USA: Journal of Sedimentary Research, v. 71, p. 985-1002.

Soreghan, G. S. and Giles, K.A., 1999, Amplitudes of Late Pennsylvanian glacioeustasy: Geology, v. 27, p. 255-258.

Steuber, T., and Veizer, J., 2002, Phanerozoic record of plate tectonic control of seawater chemistry and carbonate sedimentation: Geology, v. 30, p. 1123-1126.

Sutherland, P. K. and Henry, T.W., 1977, Carbonate platform facies and new stratigraphic nomenclature of Morrowan series (Lower and Middle Pennsylvanian), Northeastern Oklahoma: Geological Society of America Bulletin, v. 88, p. 425-440.

Swann, D.H., 1968, A summary geologic history of the Illinois Basin, *in* Illinois Geological Society and Indiana-Kentucky Geological Society eds., Geology and

Petroleum Production of the Illinois Basin: Evansville, Indiana, Illinois Geologic Society, p.3-21.

Tanaka, N., Monaghan, M.C., and Rye, D.M., 1986, Contribution of metabolic carbon to mollusc and barnacle shell carbonate: Nature, v. 320, p. 520-523.

Thayer, C.W., 1986, Are brachiopods better than bivalves? Mechanisms of turbidity tolerance and their interaction with feeding in articulates: Paleobiology, v. 12, p. 161-174.

Treworgy, J.D., 1990, Kaskaskia Sequence: Mississippian Valmeyeran and Chesterian Series, *in* Leighton, M.W. ed., Interior Cratonic Basins, Tulsa, Oklahoma, American Association of Petroleum Geologists, 1991, p. 125-142.

Tucker, J.K., 1976, Paleoecological notes on the fauna of the Shumway Limestone (Mattoon Formation, Upper Pennsylvania) of Illinois: Illinois State Academy of Sciences, v. 69, p. 327-335.

Vander Putten, E., Dehairs, F., Keppens, E., Baeyens, W., 2000, High resolution distribution of trace elements in the calcite shell layer of modern *Mytilus edulis:* Environmental and biological controls: Geochimica et Cosmochimica Acta, v. 64, p. 997-1011.

Veizer, J., 1983a, Trace elements and isotopes in sedimentary carbonates. *in* R.J. Reeder ed., Carbonates: Mineralogy and Chemistry: Washington, D.C, Mineralogical Society of America., Rev. Mineral., v. 11, p. 265-300.

Veizer, J., 1983b, Chemical diagenesis of carbonates: Theory and application of trace element technique. Society for Economic Paleontology and Mineralogy, Short Course, 10,: 3-1 to 3-100.

Weibel, C. P. and Norby, R.D., 1992, Paleopedology and conodont biostratigraphy of the Mississippian-Pennsylvanian boundary interval, type Grove Church Shale area, southern Illinois: Recent advances in Middle Carboniferous biostratigraphy; a symposium, Norman, Oklahoma, p. 94.

Woodard, S.C., Thomas, D.J., Grossman, E.L., Olszewski, T.D., Yancey, T.E., Raymond, A., and Miller, B.V., 2010, Nd isotopes as indicator of glacio-eustasy, mid-Carboniferous boundary Arrow Canyon, NV, Goldschmidt.Conference, Knoxville.

Wu, J. F. and Boyle, E.A., 1998, Determination of iron in seawater by high-resolution isotope dilution inductively coupled plasma mass spectrometry after $Mg(OH)_2$ coprecipitation: Analytica Chimica Acta, v. 367, p. 183-191.

APPENDIX

Stable isotope and trace element analyses of brachiopod shells from the Carboniferous. All stable isotope data are from this study except those for the Bird Spring Formation (Jones et al., 2003 and Oread formation (Grossman et a., 1993)). All trace element data from this study.

Sample ID Explanation: WPxx = waypoints, Species type, Shell sample, Different points within shell, sample type; s = shell, m = matrix, c = cement

Species type: AS = Anthracospirifer, Co = *Composita,* Cr = *Crurithyrus,* Inf = *Inflatia,* Kl = *Kutorg*

Microstructure: p = prismatic, f = fibrous, c = cement, op = opaque

Luminescence character: NL = nonluminescent, SL = slightly luminescent, CL = cathodoluminescent

Sample ID	Location	County	Locality Comments	Latitude	Longtitude	Period	Stage	Age (Ma)	Formation	Member	Conodont Zone	Interval	Taxa	Material	Micro-structure	Sample L.C	Shell L.C.	$\delta^{13}C$ (‰)	$\delta^{18}O$ (‰)	Mg/Ca (mmol/mol)	Sr/Ca (mmol/mol)	Mn/Ca (mmol/mol)	Fe/Ca (mmol/mol)
WP50 Co-1-1s	West Virginia	Monongalia	Central Monongalia County, inside Morgantown	39.620	-79.933	Carboniferous	Virgilian	303.9	Glenshaw	Ames	Idiognathodus simulator	Offshore	*Composita*	Shell	f	SL/NL	SL/NL	-0.62	-4.58	5.53	0.70	0.52	0.21
WP50 Co-1-2s	West Virginia	Monongalia	Central Monongalia County, inside Morgantown	39.620	-79.933	Carboniferous	Virgilian	303.9	Glenshaw	Ames	Idiognathodus simulator	Offshore	*Composita*	Shell	f	SL/NL	SL/NL	-1.15	-5.62	4.20	0.66	1.16	0.97
WP50 Co-1-3s	West Virginia	Monongalia	Central Monongalia County, inside Morgantown	39.620	-79.933	Carboniferous	Virgilian	303.9	Glenshaw	Ames	Idiognathodus simulator	Offshore	*Composita*	Shell	f	SL/NL	SL/NL	1.61	-3.63	5.01	0.68	0.59	0.20
WP50 Co-2-1s	West Virginia	Monongalia	Central Monongalia County, inside Morgantown	39.620	-79.933	Carboniferous	Virgilian	303.9	Glenshaw	Ames	Idiognathodus simulator	Offshore	*Composita*	Shell	f	NL/SL	NL/SL	1.56	-3.73	x	x	x	x
WP50 Co-2-2s	West Virginia	Monongalia	Central Monongalia County, inside Morgantown	39.620	-79.933	Carboniferous	Virgilian	303.9	Glenshaw	Ames	Idiognathodus simulator	Offshore	*Composita*	Shell	f	NL/SL	NL/SL	1.22	-4.00	x	x	x	x
WP50 Co-2-3s	West Virginia	Monongalia	Central Monongalia County, inside Morgantown	39.620	-79.933	Carboniferous	Virgilian	303.9	Glenshaw	Ames	Idiognathodus simulator	Offshore	*Composita*	Shell	f	SL/NL	SL/NL	2.34	-3.69	x	x	x	x
WP50 Co-3-1s	West Virginia	Monongalia	Central Monongalia County, inside Morgantown	39.620	-79.933	Carboniferous	Virgilian	303.9	Glenshaw	Ames	Idiognathodus simulator	Offshore	*Composita*	Shell	f	NL/SL	NL/SL	1.94	-3.79	x	x	x	x
WP50 Co-3-2s	West Virginia	Monongalia	Central Monongalia County, inside Morgantown	39.620	-79.933	Carboniferous	Virgilian	303.9	Glenshaw	Ames	Idiognathodus simulator	Offshore	*Composita*	Shell	f	NL/SL	NL/SL	0.79	-3.74	2.60	0.64	0.92	0.90
WP50 Co-3-3s	West Virginia	Monongalia	Central Monongalia County, inside Morgantown	39.620	-79.933	Carboniferous	Virgilian	303.9	Glenshaw	Ames	Idiognathodus simulator	Offshore	*Composita*	Shell	f	NL/SL	NL/SL	2.32	-3.63	x	x	x	x
WP50B Co-2-1s	West Virginia	Monongalia	Central Monongalia County, inside Morgantown	39.493	-80.079	Carboniferous	Virgilian	303.9	Glenshaw	Ames	Idiognathodus simulator	Offshore	*Composita*	Shell	f	CL	CL	1.66	-4.07	5.72	0.77	0.88	0.61
WP50B Co-2-2s	West Virginia	Monongalia	Central Monongalia County, inside Morgantown	39.493	-80.079	Carboniferous	Virgilian	303.9	Glenshaw	Ames	Idiognathodus simulator	Offshore	*Composita*	Shell	f	CL	CL	1.24	-3.83	x	x	x	x
WP50B Co-2-3s	West Virginia	Monongalia	Central Monongalia County, inside Morgantown	39.493	-80.079	Carboniferous	Virgilian	303.9	Glenshaw	Ames	Idiognathodus simulator	Offshore	*Composita*	Shell	f	SL/CL	SL/CL	0.65	-4.16	4.36	0.44	0.89	0.87
WP51 Co-1-1s	West Virginia	Marion	Eastern Marion County, just outside Fairmont	39.230	-80.296	Carboniferous	Virgilian	303.9	Glenshaw	Ames	Idiognathodus simulator	Nearshore	*Composita*	Shell	f	NL/SL	NL/SL	2.28	-3.64	x	x	x	x
WP51 Co-1-2s	West Virginia	Marion	Eastern Marion County, just outside Fairmont	39.230	-80.296	Carboniferous	Virgilian	303.9	Glenshaw	Ames	Idiognathodus simulator	Nearshore	*Composita*	Shell	f	NL/SL	NL/SL	2.52	-3.57	x	x	x	x
WP51 Co-1-3s	West Virginia	Marion	Eastern Marion County, just outside Fairmont	39.230	-80.296	Carboniferous	Virgilian	303.9	Glenshaw	Ames	Idiognathodus simulator	Nearshore	*Composita*	Shell	f	SL/NL	NL/SL	2.38	-3.62	x	x	x	x
WP53 Co-1-1s	West Virginia	Monongalia	Central Monongalia County, east of Morgantown	37.305	-81.335	Carboniferous	Virgilian	303.9	Glenshaw	Ames	Idiognathodus simulator	Nearshore	*Composita*	Shell	f	SL/NL	SL/NL	-0.14	-4.20	4.93	0.81	1.15	0.49
WP53 Co-1-2s	West Virginia	Monongalia	Central Monongalia County, east of Morgantown	37.305	-81.335	Carboniferous	Virgilian	303.9	Glenshaw	Ames	Idiognathodus simulator	Offshore	*Composita*	Shell	f	SL/NL	SL/NL	-0.92	-4.31	5.57	0.69	6.01	4.87
WP53 Co-2-1s	West Virginia	Monongalia	Central Monongalia County, east of Morgantown	37.305	-81.335	Carboniferous	Virgilian	303.9	Glenshaw	Ames	Idiognathodus simulator	Offshore	*Composita*	Shell	f	SL/CL	SL/CL	1.83	-4.23	5.66	0.78	1.11	0.60
WP53 Co-2-2s	West Virginia	Monongalia	Central Monongalia County, east of Morgantown	37.305	-81.335	Carboniferous	Virgilian	303.9	Glenshaw	Ames	Idiognathodus simulator	Offshore	*Composita*	Shell	f	SL/CL	SL/CL	1.46	-3.34	5.30	0.72	0.77	0.35
WP53 Co-2-3s	West Virginia	Monongalia	Central Monongalia County, east of Morgantown	37.305	-81.335	Carboniferous	Virgilian	303.9	Glenshaw	Ames	Idiognathodus simulator	Offshore	*Composita*	Shell	f	SL/CL	SL/CL	1.81	-3.28	3.43	0.69	0.54	0.17
WP50c Cr-1-1s	West Virginia	Monongalia	Central Monongalia County, east of Morgantown	39.230	-80.296	Carboniferous	Virgilian	303.9	Glenshaw	Ames	Idiognathodus simulator	Offshore	*Crurithyrus*	Shell	f	NL/SL	NL/SL	2.35	-4.37	8.34	1.14	0.58	0.25
WP50c Cr-1-2s	West Virginia	Monongalia	Central Monongalia County, east of Morgantown	39.230	-80.296	Carboniferous	Virgilian	303.9	Glenshaw	Ames	Idiognathodus simulator	Offshore	*Crurithyrus*	Shell	f	NL/SL	NL/SL	2.18	-3.80	9.43	1.22	0.34	0.20
WP50c Cr-2-2s	West Virginia	Monongalia	Central Monongalia County, east of Morgantown	39.230	-80.296	Carboniferous	Virgilian	303.9	Glenshaw	Ames	Idiognathodus simulator	Offshore	*Crurithyrus*	Shell	f	NL/SL	NL/SL	-0.66	-4.61	9.72	1.30	0.30	0.24
WP50c Cr-3-1s	West Virginia	Monongalia	Central Monongalia County, east of Morgantown	39.230	-80.296	Carboniferous	Virgilian	303.9	Glenshaw	Ames	Idiognathodus simulator	Offshore	*Crurithyrus*	Shell	f	NL/SL	NL/SL	2.16	-3.58	3.83	1.24	0.10	0.07
WP50c Cr-3-2s	West Virginia	Monongalia	Central Monongalia County, east of Morgantown	39.230	-80.296	Carboniferous	Virgilian	303.9	Glenshaw	Ames	Idiognathodus simulator	Offshore	*Crurithyrus*	Shell	f	NL/SL	NL/SL	1.88	-3.35	x	x	x	x
WP51 Cr-1-1s	West Virginia	Marion	Eastern Marion County, just outside Fairmont	39.230	-80.296	Carboniferous	Virgilian	303.9	Glenshaw	Ames	Idiognathodus simulator	Nearshore	*Crurithyrus*	Shell	p	NL/SL	NL/SL	-7.16	-1.44	x	x	x	x
WP51 Cr-1-2s	West Virginia	Marion	Eastern Marion County, just outside Fairmont	39.230	-80.296	Carboniferous	Virgilian	303.9	Glenshaw	Ames	Idiognathodus simulator	Nearshore	*Crurithyrus*	Shell	p	NL/SL	NL/SL	-7.38	-1.59	x	x	x	x
WP51 Cr-1-3s	West Virginia	Marion	Eastern Marion County, just outside Fairmont	39.230	-80.296	Carboniferous	Virgilian	303.9	Glenshaw	Ames	Idiognathodus simulator	Nearshore	*Crurithyrus*	Shell	p	NL/SL	NL/SL	2.40	-0.84	7.85	1.34	0.17	0.11
WP51 Cr-2-1s	West Virginia	Marion	Eastern Marion County, just outside Fairmont	39.230	-80.296	Carboniferous	Virgilian	303.9	Glenshaw	Ames	Idiognathodus simulator	Nearshore	*Crurithyrus*	Shell	f	NL/SL	NL/SL	2.81	-1.19	6.35	1.35	0.06	0.12
WP51 Cr-2-2s	West Virginia	Marion	Eastern Marion County, just outside Fairmont	39.230	-80.296	Carboniferous	Virgilian	303.9	Glenshaw	Ames	Idiognathodus simulator	Nearshore	*Crurithyrus*	Shell	f	NL/SL	NL/SL	0.30	-2.27	x	x	x	x
WP51 Cr-2-3s	West Virginia	Marion	Eastern Marion County, just outside Fairmont	39.230	-80.296	Carboniferous	Virgilian	303.9	Glenshaw	Ames	Idiognathodus simulator	Nearshore	*Crurithyrus*	Shell	f	NL/SL	NL/SL	1.81	-2.54	x	x	x	x
WP51 Cr-3-1s	West Virginia	Marion	Eastern Marion County, just outside Fairmont	39.230	-80.296	Carboniferous	Virgilian	303.9	Glenshaw	Ames	Idiognathodus simulator	Nearshore	*Crurithyrus*	Shell	f	NL/SL	NL/SL	2.49	0.01	4.80	1.25	0.14	0.09
WP51 Cr-3-2s	West Virginia	Marion	Eastern Marion County, just outside Fairmont	39.230	-80.296	Carboniferous	Virgilian	303.9	Glenshaw	Ames	Idiognathodus simulator	Nearshore	*Crurithyrus*	Shell	f	NL/SL	SL/NL	1.94	-1.97	x	x	x	x
WP51 Cr-3-3s	West Virginia	Marion	Eastern Marion County, just outside Fairmont	39.230	-80.296	Carboniferous	Virgilian	303.9	Glenshaw	Ames	Idiognathodus simulator	Nearshore	*Crurithyrus*	Shell	f	NL/SL	SL/NL	1.88	-2.31	x	x	x	x
WP53 Cr-1-1s	West Virginia	Monongalia	Central Monongalia County, east of Morgantown	37.305	-81.335	Carboniferous	Virgilian	303.9	Glenshaw	Ames	Idiognathodus simulator	Offshore	*Crurithyrus*	Shell	op	CL/SL	L	2.00	-3.38	x	x	x	x
WP53 Cr-2-2s	West Virginia	Monongalia	Central Monongalia County, east of Morgantown	37.305	-81.335	Carboniferous	Virgilian	303.9	Glenshaw	Ames	Idiognathodus simulator	Offshore	*Crurithyrus*	Shell	op	CL/SL	L	1.59	-3.72	6.43	1.09	1.39	0.81
WP54 Cr-2-1s	West Virginia	Monongalia	Central Monongalia County, east of Morgantown	37.305	-81.336	Carboniferous	Virgilian	303.9	Glenshaw	Ames	Idiognathodus simulator	Offshore	*Crurithyrus*	Shell	op	CL/SL	SL/CL	3.26	-0.80	13.16	1.16	0.66	0.26
WP54 Cr-3-1s	West Virginia	Monongalia	Central Monongalia County, east of Morgantown	37.305	-81.336	Carboniferous	Virgilian	303.9	Glenshaw	Ames	Idiognathodus simulator	Offshore	*Crurithyrus*	Shell	f	NL/SL	NL/SL	1.36	-3.60	4.73	1.25	0.43	0.23
WP54 Cr-3-2s	West Virginia	Monongalia	Central Monongalia County, east of Morgantown	37.305	-81.336	Carboniferous	Virgilian	303.9	Glenshaw	Ames	Idiognathodus simulator	Offshore	*Crurithyrus*	Shell	f	NL/SL	SL/CL	0.44	-4.17	x	x	x	x
WP50 NS-1-1s	West Virginia	Monongalia	Central Monongalia County, inside Morgantown	39.620	-79.933	Carboniferous	Virgilian	303.9	Glenshaw	Ames	Idiognathodus simulator	Offshore	*Neosprifer*	Shell	p	NL/SL	NL/SL	2.10	-3.95	6.81	0.78	0.32	0.71
WP50 NS-1-2s	West Virginia	Monongalia	Central Monongalia County, inside Morgantown	39.620	-79.933	Carboniferous	Virgilian	303.9	Glenshaw	Ames	Idiognathodus simulator	Offshore	*Neosprifer*	Shell	p	NL	NL	2.41	-4.02	3.27	0.76	0.18	0.23
WP50 NS-1-3s	West Virginia	Monongalia	Central Monongalia County, inside Morgantown	39.620	-79.933	Carboniferous	Virgilian	303.9	Glenshaw	Ames	Idiognathodus simulator	Offshore	*Neosprifer*	Shell	p	NL	NL	2.76	-3.62	3.74	0.75	0.21	0.28
WP50 NS-2-1s	West Virginia	Monongalia	Central Monongalia County, inside Morgantown	39.620	-79.933	Carboniferous	Virgilian	303.9	Glenshaw	Ames	Idiognathodus simulator	Offshore	*Neosprifer*	Shell	p	NL	NL/SL	2.14	-3.63	3.09	0.89	0.00	0.06
WP50 NS-2-2s	West Virginia	Monongalia	Central Monongalia County, inside Morgantown	39.620	-79.933	Carboniferous	Virgilian	303.9	Glenshaw	Ames	Idiognathodus simulator	Offshore	*Neosprifer*	Shell	p	NL	NL/SL	1.66	-3.64	3.12	0.85	0.06	0.09
WP50 NS-2-3s	West Virginia	Monongalia	Central Monongalia County, inside Morgantown	39.620	-79.933	Carboniferous	Virgilian	303.9	Glenshaw	Ames	Idiognathodus simulator	Offshore	*Neosprifer*	Shell	p	NL/SL	NL/SL	2.37	-3.31	x	x	x	x
WP50 NS-3-1s	West Virginia	Monongalia	Central Monongalia County, inside Morgantown	39.620	-79.933	Carboniferous	Virgilian	303.9	Glenshaw	Ames	Idiognathodus simulator	Offshore	*Neosprifer*	Shell	p	NL	NL/SL	1.95	-3.86	3.60	0.79	0.02	0.06
WP50 NS-3-2s	West Virginia	Monongalia	Central Monongalia County, inside Morgantown	39.620	-79.933	Carboniferous	Virgilian	303.9	Glenshaw	Ames	Idiognathodus simulator	Offshore	*Neosprifer*	Shell	p	NL	NL/SL	2.27	-3.56	3.24	0.79	0.02	0.09
WP50 NS-3-3s	West Virginia	Monongalia	Central Monongalia County, inside Morgantown	39.620	-79.933	Carboniferous	Virgilian	303.9	Glenshaw	Ames	Idiognathodus simulator	Offshore	*Neosprifer*	Shell	p	NL	NL/SL	2.25	-3.28	3.54	0.67	0.09	0.18
WP50 NS-3-5s	West Virginia	Monongalia	Central Monongalia County, inside Morgantown	39.620	-79.933	Carboniferous	Virgilian	303.9	Glenshaw	Ames	Idiognathodus simulator	Offshore	*Neosprifer*	Shell	p	NL/SL	L	1.85	-3.24	x	x	x	x
WP50B NS-1-1s	West Virginia	Monongalia	Central Monongalia County, inside Morgantown	39.493	-80.079	Carboniferous	Virgilian	303.9	Glenshaw	Ames	Idiognathodus simulator	Offshore	*Neosprifer*	Shell	p	NL	NL/SL	2.86	-3.79	4.23	0.81	0.68	1.57
WP50B NS-1-2s	West Virginia	Monongalia	Central Monongalia County, inside Morgantown	39.493	-80.079	Carboniferous	Virgilian	303.9	Glenshaw	Ames	Idiognathodus simulator	Offshore	*Neosprifer*	Shell	p	NL	NL/SL	2.49	-3.56	3.57	0.79	0.86	0.58
WP50B NS-1-3s	West Virginia	Monongalia	Central Monongalia County, inside Morgantown	39.493	-80.079	Carboniferous	Virgilian	303.9	Glenshaw	Ames	Idiognathodus simulator	Offshore	*Neosprifer*	Shell	p	NL	NL/SL	2.51	-3.46	4.45	0.75	0.32	0.33

Sample ID	Location	County	Locality Comments	Latitude	Longtitude	Period	Stage	Age (Ma)	Formation	Member	Conodont Zone	Interval	Taxa	Material	Micro-structure	Sample L.C	Shell L.C.	$\delta^{13}C$ (‰)	$\delta^{18}O$ (‰)	Mg/Ca (mmol/mol)	Sr/Ca (mmol/mol)	Mn/Ca (mmol/mol)	Fe/Ca (mmol/mol)
WP50B-NS-2-1s	West Virginia	Monongalia	Central Monongalia County, inside Morgantown	39.493	-80.079	Carboniferous	Virgilian	303.9	Glenshaw	Ames	Idiognathodus simulator	Offshore	*Neosprifer*	Shell	p	NL	NL	3.29	-3.62	4.10	0.75	1.02	0.74
WP50B-NS-2-2s	West Virginia	Monongalia	Central Monongalia County, inside Morgantown	39.493	-80.079	Carboniferous	Virgilian	303.9	Glenshaw	Ames	Idiognathodus simulator	Offshore	*Neosprifer*	Shell	p	NL	NL	2.88	-3.89	4.67	0.80	0.20	0.21
WP50B-NS-2-3s	West Virginia	Monongalia	Central Monongalia County, inside Morgantown	39.493	-80.079	Carboniferous	Virgilian	303.9	Glenshaw	Ames	Idiognathodus simulator	Offshore	*Neosprifer*	Shell	p	NL	NL	2.80	-3.72	5.21	0.77	0.17	0.37
WP50B-NS-2-4s	West Virginia	Monongalia	Central Monongalia County, inside Morgantown	39.493	-80.079	Carboniferous	Virgilian	303.9	Glenshaw	Ames	Idiognathodus simulator	Offshore	*Neosprifer*	Shell	p	NL	NL	2.81	-3.68	x	x	x	x
WP50B NS-3-1s	West Virginia	Monongalia	Central Monongalia County, inside Morgantown	39.493	-80.079	Carboniferous	Virgilian	303.9	Glenshaw	Ames	Idiognathodus simulator	Offshore	*Neosprifer*	Shell	p	NL/SL	NL/SL	1.85	-4.29	12.43	1.17	0.00	1.88
WP50B NS-3-2s	West Virginia	Monongalia	Central Monongalia County, inside Morgantown	39.493	-80.079	Carboniferous	Virgilian	303.9	Glenshaw	Ames	Idiognathodus simulator	Offshore	*Neosprifer*	Shell	p	NL/SL	NL/SL	1.20	-4.99	3.60	0.89	0.23	0.39
WP50B NS-3-3s	West Virginia	Monongalia	Central Monongalia County, inside Morgantown	39.493	-80.079	Carboniferous	Virgilian	303.9	Glenshaw	Ames	Idiognathodus simulator	Offshore	*Neosprifer*	Shell	p	NL/SL	NL/SL	1.93	-3.73	2.45	0.87	0.04	0.25
WP50B NS-3-6s	West Virginia	Monongalia	Central Monongalia County, inside Morgantown	39.493	-80.079	Carboniferous	Virgilian	303.9	Glenshaw	Ames	Idiognathodus simulator	Offshore	*Neosprifer*	Shell	p	NL	NL	2.15	-3.27	3.74	0.72	0.07	0.11
WP53 NS-1-2s	West Virginia	Monongalia	Central Monongalia County, east of Morgantown	37.305	-81.335	Carboniferous	Virgilian	303.9	Glenshaw	Ames	Idiognathodus simulator	Offshore	*Neosprifer*	Shell	p	NL	NL/SL	3.19	-3.34	3.46	0.75	0.06	0.06
WP53 NS-1-3s	West Virginia	Monongalia	Central Monongalia County, east of Morgantown	37.305	-81.335	Carboniferous	Virgilian	303.9	Glenshaw	Ames	Idiognathodus simulator	Offshore	*Neosprifer*	Shell	p	NL/SL	NL/SL	1.81	-3.73	4.65	0.88	0.07	0.08
WP53 NS-2-1s	West Virginia	Monongalia	Central Monongalia County, east of Morgantown	37.305	-81.335	Carboniferous	Virgilian	303.9	Glenshaw	Ames	Idiognathodus simulator	Offshore	*Neosprifer*	Shell	p	NL	NL	2.74	-3.53	3.40	0.78	0.02	0.06
WP53 NS-2-2s	West Virginia	Monongalia	Central Monongalia County, east of Morgantown	37.305	-81.335	Carboniferous	Virgilian	303.9	Glenshaw	Ames	Idiognathodus simulator	Offshore	*Neosprifer*	Shell	p	NL	NL	2.92	-3.33	3.99	0.82	0.53	0.62
WP53 NS-2-3s	West Virginia	Monongalia	Central Monongalia County, east of Morgantown	37.305	-81.335	Carboniferous	Virgilian	303.9	Glenshaw	Ames	Idiognathodus simulator	Offshore	*Neosprifer*	Shell	p	NL	NL/SL	2.81	-3.57	x	x	x	x
WP53-NS-3-1s	West Virginia	Monongalia	Central Monongalia County, east of Morgantown	37.305	-81.335	Carboniferous	Virgilian	303.9	Glenshaw	Ames	Idiognathodus simulator	Offshore	*Neosprifer*	Shell	p	NL	NL	2.67	-3.92	2.84	0.92	0.01	0.11
WP53-NS-3-2s	West Virginia	Monongalia	Central Monongalia County, east of Morgantown	37.305	-81.335	Carboniferous	Virgilian	303.9	Glenshaw	Ames	Idiognathodus simulator	Offshore	*Neosprifer*	Shell	p	NL	NL/SL	2.64	-3.89	2.56	0.86	0.01	0.03
WP53-NS-3-3s	West Virginia	Monongalia	Central Monongalia County, east of Morgantown	37.305	-81.335	Carboniferous	Virgilian	303.9	Glenshaw	Ames	Idiognathodus simulator	Offshore	*Neosprifer*	Shell	p	NL	NL/SL	2.78	-3.69	2.47	0.87	0.05	0.09
WP50 Co-1-4c	West Virginia	Monongalia	Central Monongalia County, inside Morgantown	39.620	-79.933	Carboniferous	Virgilian	303.9	Glenshaw	Ames	Idiognathodus simulator	Offshore	n/a	Cement	n/a	n/a	n/a	-7.17	-8.94	x	x	x	x
WP50 Co-1-5m	West Virginia	Monongalia	Central Monongalia County, inside Morgantown	39.620	-79.933	Carboniferous	Virgilian	303.9	Glenshaw	Ames	Idiognathodus simulator	Offshore	n/a	Matrix	n/a	n/a	n/a	-5.61	-5.83	x	x	x	x
WP50 Co-2-4c	West Virginia	Monongalia	Central Monongalia County, inside Morgantown	39.620	-79.933	Carboniferous	Virgilian	303.9	Glenshaw	Ames	Idiognathodus simulator	Offshore	n/a	Cement	n/a	n/a	n/a	-6.80	-9.24	x	x	x	x
WP50 Co-2-5m	West Virginia	Monongalia	Central Monongalia County, inside Morgantown	39.620	-79.933	Carboniferous	Virgilian	303.9	Glenshaw	Ames	Idiognathodus simulator	Offshore	n/a	Matrix	n/a	n/a	n/a	-5.36	-6.57	x	x	x	x
WP50 Co-3-4m	West Virginia	Monongalia	Central Monongalia County, inside Morgantown	39.620	-79.933	Carboniferous	Virgilian	303.9	Glenshaw	Ames	Idiognathodus simulator	Offshore	n/a	Matrix	n/a	n/a	n/a	-5.16	-4.23	x	x	x	x
WP50 Co-3-5m	West Virginia	Monongalia	Central Monongalia County, inside Morgantown	39.620	-79.933	Carboniferous	Virgilian	303.9	Glenshaw	Ames	Idiognathodus simulator	Offshore	n/a	Matrix	n/a	n/a	n/a	-5.38	-3.48	x	x	x	x
WP50B Co-2-4m	West Virginia	Monongalia	Central Monongalia County, inside Morgantown	39.493	-80.079	Carboniferous	Virgilian	303.9	Glenshaw	Ames	Idiognathodus simulator	Offshore	n/a	Matrix	n/a	n/a	n/a	-7.29	-5.26	x	x	x	x
WP50B Co-2-5m	West Virginia	Monongalia	Central Monongalia County, inside Morgantown	39.493	-80.079	Carboniferous	Virgilian	303.9	Glenshaw	Ames	Idiognathodus simulator	Offshore	n/a	Matrix	n/a	n/a	n/a	-5.66	-4.89	x	x	x	x
WP51 Co-1-4m	West Virginia	Marion	Eastern Marion County, just outside Fairmont	39.230	-80.296	Carboniferous	Virgilian	303.9	Glenshaw	Ames	Idiognathodus simulator	Nearshore	n/a	Matrix	n/a	n/a	n/a	1.48	-3.73	x	x	x	x
WP51 Co-1-5m	West Virginia	Marion	Eastern Marion County, just outside Fairmont	39.230	-80.296	Carboniferous	Virgilian	303.9	Glenshaw	Ames	Idiognathodus simulator	Nearshore	n/a	Matrix	n/a	n/a	n/a	-1.77	-5.71	x	x	x	x
WP53 Co-1-4m	West Virginia	Monongalia	Central Monongalia County, east of Morgantown	37.305	-81.335	Carboniferous	Virgilian	303.9	Glenshaw	Ames	Idiognathodus simulator	Offshore	n/a	Matrix	n/a	n/a	n/a	-5.08	-6.01	x	x	x	x
WP53 Co-2-4m	West Virginia	Monongalia	Central Monongalia County, east of Morgantown	37.305	-81.335	Carboniferous	Virgilian	303.9	Glenshaw	Ames	Idiognathodus simulator	Offshore	n/a	Matrix	n/a	n/a	n/a	-4.65	-4.24	x	x	x	x
WP53 Co-2-5m	West Virginia	Monongalia	Central Monongalia County, east of Morgantown	37.305	-81.335	Carboniferous	Virgilian	303.9	Glenshaw	Ames	Idiognathodus simulator	Offshore	n/a	Matrix	n/a	n/a	n/a	-2.54	-3.40	x	x	x	x
WP50c Cr-1-4m	West Virginia	Monongalia	Central Monongalia County, inside Morgantown	39.230	-80.296	Carboniferous	Virgilian	303.9	Glenshaw	Ames	Idiognathodus simulator	Offshore	n/a	Matrix	n/a	n/a	n/a	-4.75	-5.01	x	x	x	x
WP50c Cr-1-5m	West Virginia	Monongalia	Central Monongalia County, inside Morgantown	39.230	-80.296	Carboniferous	Virgilian	303.9	Glenshaw	Ames	Idiognathodus simulator	Offshore	n/a	Matrix	n/a	n/a	n/a	-5.82	-6.79	x	x	x	x
WP50c Cr-2-4m	West Virginia	Monongalia	Central Monongalia County, inside Morgantown	39.230	-80.296	Carboniferous	Virgilian	303.9	Glenshaw	Ames	Idiognathodus simulator	Offshore	n/a	Matrix	n/a	n/a	n/a	-8.50	-8.81	x	x	x	x
WP50c Cr-2-5m	West Virginia	Monongalia	Central Monongalia County, inside Morgantown	39.230	-80.296	Carboniferous	Virgilian	303.9	Glenshaw	Ames	Idiognathodus simulator	Offshore	n/a	Matrix	n/a	n/a	n/a	1.57	-4.20	x	x	x	x
WP50c Cr-3-4m	West Virginia	Monongalia	Central Monongalia County, inside Morgantown	39.230	-80.296	Carboniferous	Virgilian	303.9	Glenshaw	Ames	Idiognathodus simulator	Offshore	n/a	Matrix	n/a	n/a	n/a	-3.77	-5.61	x	x	x	x
WP50c Cr-3-5m	West Virginia	Monongalia	Central Monongalia County, inside Morgantown	39.230	-80.296	Carboniferous	Virgilian	303.9	Glenshaw	Ames	Idiognathodus simulator	Offshore	n/a	Matrix	n/a	n/a	n/a	-3.65	-3.54	x	x	x	x
WP51 Cr-1-4m	West Virginia	Marion	Eastern Marion County, just outside Fairmont	39.230	-80.296	Carboniferous	Virgilian	303.9	Glenshaw	Ames	Idiognathodus simulator	Nearshore	n/a	Matrix	n/a	n/a	n/a	2.30	-1.09	x	x	x	x
WP51 Cr-1-5m	West Virginia	Marion	Eastern Marion County, just outside Fairmont	39.230	-80.296	Carboniferous	Virgilian	303.9	Glenshaw	Ames	Idiognathodus simulator	Nearshore	n/a	Matrix	n/a	n/a	n/a	4.42	-1.69	x	x	x	x
WP51 Cr-2-4m	West Virginia	Marion	Eastern Marion County, just outside Fairmont	39.230	-80.296	Carboniferous	Virgilian	303.9	Glenshaw	Ames	Idiognathodus simulator	Nearshore	n/a	Matrix	n/a	n/a	n/a	2.75	0.68	x	x	x	x
WP51 Cr-2-5m	West Virginia	Marion	Eastern Marion County, just outside Fairmont	39.230	-80.296	Carboniferous	Virgilian	303.9	Glenshaw	Ames	Idiognathodus simulator	Nearshore	n/a	Matrix	n/a	n/a	n/a	2.44	-2.26	x	x	x	x
WP51 Cr-3-4m	West Virginia	Marion	Eastern Marion County, just outside Fairmont	39.230	-80.296	Carboniferous	Virgilian	303.9	Glenshaw	Ames	Idiognathodus simulator	Nearshore	n/a	Matrix	n/a	n/a	n/a	2.73	-4.49	x	x	x	x
WP51 Cr-3-5m	West Virginia	Marion	Eastern Marion County, just outside Fairmont	39.230	-80.296	Carboniferous	Virgilian	303.9	Glenshaw	Ames	Idiognathodus simulator	Nearshore	n/a	Matrix	n/a	n/a	n/a	3.15	-3.19	x	x	x	x
WP53 Cr-1-3m	West Virginia	Monongalia	Central Monongalia County, east of Morgantown	37.305	-81.335	Carboniferous	Virgilian	303.9	Glenshaw	Ames	Idiognathodus simulator	Offshore	n/a	Matrix	n/a	n/a	n/a	-4.62	-3.49	x	x	x	x
WP53 Cr-1-4m	West Virginia	Monongalia	Central Monongalia County, east of Morgantown	37.305	-81.335	Carboniferous	Virgilian	303.9	Glenshaw	Ames	Idiognathodus simulator	Offshore	n/a	Matrix	n/a	n/a	n/a	-5.24	-4.52	x	x	x	x
WP53 Cr-2-3m	West Virginia	Monongalia	Central Monongalia County, east of Morgantown	37.305	-81.335	Carboniferous	Virgilian	303.9	Glenshaw	Ames	Idiognathodus simulator	Offshore	n/a	Matrix	n/a	n/a	n/a	-4.45	-5.04	x	x	x	x
WP53 Cr-2-4m	West Virginia	Monongalia	Central Monongalia County, east of Morgantown	37.305	-81.335	Carboniferous	Virgilian	303.9	Glenshaw	Ames	Idiognathodus simulator	Offshore	n/a	Matrix	n/a	n/a	n/a	-4.10	-4.55	x	x	x	x
WP54 Cr-2-4m	West Virginia	Monongalia	Central Monongalia County, east of Morgantown	37.305	-81.336	Carboniferous	Virgilian	303.9	Glenshaw	Ames	Idiognathodus simulator	Offshore	n/a	Matrix	n/a	n/a	n/a	0.42	-4.43	x	x	x	x
WP54 Cr-2-5m	West Virginia	Monongalia	Central Monongalia County, east of Morgantown	37.305	-81.336	Carboniferous	Virgilian	303.9	Glenshaw	Ames	Idiognathodus simulator	Offshore	n/a	Matrix	n/a	n/a	n/a	-11.73	-5.82	x	x	x	x
WP54 Cr-3-4m	West Virginia	Monongalia	Central Monongalia County, east of Morgantown	37.305	-81.336	Carboniferous	Virgilian	303.9	Glenshaw	Ames	Idiognathodus simulator	Offshore	n/a	Matrix	n/a	n/a	n/a	1.45	-3.38	x	x	x	x
WP54 Cr-3-5m	West Virginia	Monongalia	Central Monongalia County, east of Morgantown	37.305	-81.336	Carboniferous	Virgilian	303.9	Glenshaw	Ames	Idiognathodus simulator	Offshore	n/a	Matrix	n/a	n/a	n/a	-10.01	-5.27	x	x	x	x
WP50 NS-1-4m	West Virginia	Monongalia	Central Monongalia County, inside Morgantown	39.620	-79.933	Carboniferous	Virgilian	303.9	Glenshaw	Ames	Idiognathodus simulator	Offshore	n/a	Matrix	n/a	n/a	n/a	-7.27	-5.99	x	x	x	x
WP50 NS-1-5m	West Virginia	Monongalia	Central Monongalia County, inside Morgantown	39.620	-79.933	Carboniferous	Virgilian	303.9	Glenshaw	Ames	Idiognathodus simulator	Offshore	n/a	Matrix	n/a	n/a	n/a	-7.12	-4.40	x	x	x	x
WP50 NS-2-4m	West Virginia	Monongalia	Central Monongalia County, inside Morgantown	39.620	-79.933	Carboniferous	Virgilian	303.9	Glenshaw	Ames	Idiognathodus simulator	Offshore	n/a	Matrix	n/a	n/a	n/a	-6.38	-5.83	x	x	x	x
WP50 NS-2-5m	West Virginia	Monongalia	Central Monongalia County, inside Morgantown	39.620	-79.933	Carboniferous	Virgilian	303.9	Glenshaw	Ames	Idiognathodus simulator	Offshore	n/a	Matrix	n/a	n/a	n/a	-6.38	-4.24	x	x	x	x
WP50 NS-3-4m	West Virginia	Monongalia	Central Monongalia County, inside Morgantown	39.620	-79.933	Carboniferous	Virgilian	303.9	Glenshaw	Ames	Idiognathodus simulator	Offshore	n/a	Matrix	n/a	n/a	n/a	2.12	-4.05	x	x	x	x
WP50 NS-3-6m	West Virginia	Monongalia	Central Monongalia County, inside Morgantown	39.620	-79.933	Carboniferous	Virgilian	303.9	Glenshaw	Ames	Idiognathodus simulator	Offshore	n/a	Matrix	n/a	n/a	n/a	-6.03	-5.26	x	x	x	x
WP50B NS-1-4m	West Virginia	Monongalia	Central Monongalia County, inside Morgantown	39.493	-80.079	Carboniferous	Virgilian	303.9	Glenshaw	Ames	Idiognathodus simulator	Offshore	n/a	Matrix	n/a	n/a	n/a	-5.47	-5.43	x	x	x	x
WP50B NS-1-5m	West Virginia	Monongalia	Central Monongalia County, inside Morgantown	39.493	-80.079	Carboniferous	Virgilian	303.9	Glenshaw	Ames	Idiognathodus simulator	Offshore	n/a	Matrix	n/a	n/a	n/a	-3.74	-5.25	x	x	x	x
WP50B NS-1-6c	West Virginia	Monongalia	Central Monongalia County, inside Morgantown	39.493	-80.079	Carboniferous	Virgilian	303.9	Glenshaw	Ames	Idiognathodus simulator	Offshore	n/a	Cement	n/a	n/a	n/a	-5.23	-6.16	x	x	x	x
WP50B-NS-2-5m	West Virginia	Monongalia	Central Monongalia County, inside Morgantown	39.493	-80.079	Carboniferous	Virgilian	303.9	Glenshaw	Ames	Idiognathodus simulator	Offshore	n/a	Matrix	n/a	n/a	n/a	-6.24	-6.97	x	x	x	x

Sample ID	Location	County	Locality Comments	Latitude	Longtitude	Period	Stage	Age (Ma)	Formation	Member	Conodont Zone	Interval	Taxa	Material	Micro-structure	Sample L.C	Shell L.C.	$\delta^{13}C$ (‰)	$\delta^{18}O$ (‰)	Mg/Ca (mmol/mol)	Sr/Ca (mmol/mol)	Mn/Ca (mmol/mol)	Fe/Ca (mmol/mol)
WP50B NS-3-4m	West Virginia	Monongalia	Central Monongalia County, inside Morgantown	39.493	-80.079	Carboniferous	Virgilian	303.9	Glenshaw	Ames	Idiognathodus simulator	Offshore	n/a	Matrix	n/a	n/a	n/a	-4.65	-5.19	x	x	x	x
WP50B NS-3-5m	West Virginia	Monongalia	Central Monongalia County, inside Morgantown	39.493	-80.079	Carboniferous	Virgilian	303.9	Glenshaw	Ames	Idiognathodus simulator	Offshore	n/a	Matrix	n/a	n/a	n/a	-5.87	-7.24	x	x	x	x
WP53 NS-1-4s	West Virginia	Monongalia	Central Monongalia County, east of Morgantown	37.305	-81.335	Carboniferous	Virgilian	303.9	Glenshaw	Ames	Idiognathodus simulator	Offshore	n/a	Matrix	n/a	n/a	n/a	0.69	-3.85	x	x	x	x
WP53 NS-1-5m	West Virginia	Monongalia	Central Monongalia County, east of Morgantown	37.305	-81.335	Carboniferous	Virgilian	303.9	Glenshaw	Ames	Idiognathodus simulator	Offshore	n/a	Matrix	n/a	n/a	n/a	-11.57	-4.44	x	x	x	x
WP53 NS-1-6m	West Virginia	Monongalia	Central Monongalia County, east of Morgantown	37.305	-81.335	Carboniferous	Virgilian	303.9	Glenshaw	Ames	Idiognathodus simulator	Offshore	n/a	Matrix	n/a	n/a	n/a	-10.80	-4.61	x	x	x	x
WP53 NS-2-4m	West Virginia	Monongalia	Central Monongalia County, east of Morgantown	37.305	-81.335	Carboniferous	Virgilian	303.9	Glenshaw	Ames	Idiognathodus simulator	Offshore	n/a	Matrix	n/a	n/a	n/a	-5.97	-7.08	x	x	x	x
WP53 NS-2-5m	West Virginia	Monongalia	Central Monongalia County, east of Morgantown	37.305	-81.335	Carboniferous	Virgilian	303.9	Glenshaw	Ames	Idiognathodus simulator	Offshore	n/a	Matrix	n/a	n/a	n/a	-6.22	-7.51	x	x	x	x
WP53-NS-3-4m	West Virginia	Monongalia	Central Monongalia County, east of Morgantown	37.305	-81.335	Carboniferous	Virgilian	303.9	Glenshaw	Ames	Idiognathodus simulator	Offshore	n/a	Matrix	n/a	n/a	n/a	-3.85	-3.97	x	x	x	x
WP53-NS-3-5m	West Virginia	Monongalia	Central Monongalia County, east of Morgantown	37.305	-81.335	Carboniferous	Virgilian	303.9	Glenshaw	Ames	Idiognathodus simulator	Offshore	n/a	Matrix	n/a	n/a	n/a	-4.73	-5.76	x	x	x	x
WP62 Cr-2-1s	Illinois	Effingham	Shoal Creek, N Effingham County	39.187	-88.611	Carboniferous	Virgilian	303.9	Mattoon	Shumway Limestone	Idiognathodus simulator	x	*Crurithyrus*	Shell	f	NL/SL	SL/NL	3.13	-2.21	9.30	1.45	0.17	0.26
WP62 Cr-2-2s	Illinois	Effingham	Shoal Creek, N Effingham County	39.187	-88.611	Carboniferous	Virgilian	303.9	Mattoon	Shumway Limestone	Idiognathodus simulator	x	*Crurithyrus*	Shell	f	NL/SL	SL/NL	3.25	-2.12	x	x	x	x
WP62A Kl-1-1s	Illinois	Effingham	Shoal Creek, N Effingham County	39.187	-88.611	Carboniferous	Virgilian	303.9	Mattoon	Shumway Limestone	Idiognathodus simulator	x	*Kutorginella*	Shell	f	SL/NL	SL/CL	3.53	-2.59	11.61	1.27	0.26	0.88
WP62A Kl-1-2s	Illinois	Effingham	Shoal Creek, N Effingham County	39.187	-88.611	Carboniferous	Virgilian	303.9	Mattoon	Shumway Limestone	Idiognathodus simulator	x	*Kutorginella*	Shell	f	SL/NL	SL/CL	2.90	-2.63	11.63	1.24	0.22	0.62
WP62 Cr-1-3m	Illinois	Effingham	Shoal Creek, N Effingham County	39.187	-88.611	Carboniferous	Virgilian	303.9	Mattoon	Shumway Limestone	Idiognathodus simulator	x	n/a	Matrix	n/a	n/a	n/a	-2.45	-5.79	x	x	x	x
WP62 Cr-1-4m	Illinois	Effingham	Shoal Creek, N Effingham County	39.187	-88.611	Carboniferous	Virgilian	303.9	Mattoon	Shumway Limestone	Idiognathodus simulator	x	n/a	Matrix	n/a	n/a	n/a	-2.61	-5.31	x	x	x	x
WP62 Cr-2-3m	Illinois	Effingham	Shoal Creek, N Effingham County	39.187	-88.611	Carboniferous	Virgilian	303.9	Mattoon	Shumway Limestone	Idiognathodus simulator	x	n/a	Matrix	n/a	n/a	n/a	-2.95	-4.34	x	x	x	x
WP62 Cr-2-4m	Illinois	Effingham	Shoal Creek, N Effingham County	39.187	-88.611	Carboniferous	Virgilian	303.9	Mattoon	Shumway Limestone	Idiognathodus simulator	x	n/a	Matrix	n/a	n/a	n/a	-2.60	-4.84	x	x	x	x
WP62 KL-1-4m	Illinois	Effingham	Shoal Creek, N Effingham County	39.187	-88.611	Carboniferous	Virgilian	303.9	Mattoon	Shumway Limestone	Idiognathodus simulator	x	n/a	Matrix	n/a	n/a	n/a	-6.85	-1.86	x	x	x	x
WP62 KL-1-5m	Illinois	Effingham	Shoal Creek, N Effingham County	39.187	-88.611	Carboniferous	Virgilian	303.9	Mattoon	Shumway Limestone	Idiognathodus simulator	x	n/a	Matrix	n/a	n/a	n/a	-8.10	-1.32	x	x	x	x
WP62 KL-2-4m	Illinois	Effingham	Shoal Creek, N Effingham County	39.187	-88.611	Carboniferous	Virgilian	303.9	Mattoon	Shumway Limestone	Idiognathodus simulator	x	n/a	Matrix	n/a	n/a	n/a	-1.90	-6.83	x	x	x	x
WP62 KL-2-5m	Illinois	Effingham	Shoal Creek, N Effingham County	39.187	-88.611	Carboniferous	Virgilian	303.9	Mattoon	Shumway Limestone	Idiognathodus simulator	x	n/a	Matrix	n/a	n/a	n/a	-10.11	-5.56	x	x	x	x
WP62 KL-3-4m	Illinois	Effingham	Shoal Creek, N Effingham County	39.187	-88.611	Carboniferous	Virgilian	303.9	Mattoon	Shumway Limestone	Idiognathodus simulator	x	n/a	Matrix	n/a	n/a	n/a	1.71	-3.98	x	x	x	x
WP62 KL-3-5m	Illinois	Effingham	Shoal Creek, N Effingham County	39.187	-88.611	Carboniferous	Virgilian	303.9	Mattoon	Shumway Limestone	Idiognathodus simulator	x	n/a	Matrix	n/a	n/a	n/a	1.94	-3.48	x	x	x	x
KOR01	Kansas	Coffey	NE Coffey County	38.423	-95.577	Carboniferous	Virgilian	303.9	Oread	Plattsmouth Limestone	Idiognathodus simulator	470 cm	*Composita subtilita*	Shell	p	NL	x	4.74	-1.81	3.72	0.43	0.05	0.22
KOR01-2	Kansas	Coffey	NE Coffey County	38.423	-95.577	Carboniferous	Virgilian	303.9	Oread	Plattsmouth Limestone	Idiognathodus simulator	470 cm	*Composita subtilita*	Shell	p	NL	x	x	x	3.65	0.52	0.06	0.11
KOR02	Kansas	Coffey	NE Coffey County	38.423	-95.577	Carboniferous	Virgilian	303.9	Oread	Plattsmouth Limestone	Idiognathodus simulator	470 cm	*Composita subtilita*	Shell	p	NL	x	4.58	-1.28	2.02	0.45	0.00	0.04
KOR02-2	Kansas	Coffey	NE Coffey County	38.423	-95.577	Carboniferous	Virgilian	303.9	Oread	Plattsmouth Limestone	Idiognathodus simulator	470 cm	*Composita subtilita*	Shell	p	NL	x	x	x	2.18	0.46	0.02	0.03
KOR03	Kansas	Coffey	NE Coffey County	38.423	-95.577	Carboniferous	Virgilian	303.9	Oread	Plattsmouth Limestone	Idiognathodus simulator	470 cm	*Composita subtilita*	Shell	p	NL	x	5.37	-1.41	1.46	0.42	0.00	0.03
KOR03-2	Kansas	Coffey	NE Coffey County	38.423	-95.577	Carboniferous	Virgilian	303.9	Oread	Plattsmouth Limestone	Idiognathodus simulator	470 cm	*Composita subtilita*	Shell	p	NL	x	x	x	1.79	0.47	0.03	0.05
KOR04	Kansas	Coffey	NE Coffey County	38.423	-95.577	Carboniferous	Virgilian	303.9	Oread	Plattsmouth Limestone	Idiognathodus simulator	470 cm	*Crurithyris planoconvexa*	Shell	f	SL/NL	x	3.47	-1.52	3.62	0.46	0.45	2.27
KOR05	Kansas	Coffey	NE Coffey County	38.423	-95.577	Carboniferous	Virgilian	303.9	Oread	Plattsmouth Limestone	Idiognathodus simulator	470 cm	*Crurithyris planoconvexa*	Shell	f	SL/NL	x	3.64	-1.44	3.52	0.71	0.34	1.63
KOR06	Kansas	Coffey	NE Coffey County	38.423	-95.577	Carboniferous	Virgilian	303.9	Oread	Plattsmouth Limestone	Idiognathodus simulator	470 cm	*Crurithyris planoconvexa*	Shell	f	SL/NL	x	3.42	-1.63	4.44	0.52	0.49	2.65
KOR07	Kansas	Coffey	NE Coffey County	38.423	-95.577	Carboniferous	Virgilian	303.9	Oread	Plattsmouth Limestone	Idiognathodus simulator	470 cm	*Neospirifer dunbari*	Shell	p	NL	x	3.40	-1.62	2.58	0.86	0.03	0.04
KOR07-2	Kansas	Coffey	NE Coffey County	38.423	-95.577	Carboniferous	Virgilian	303.9	Oread	Plattsmouth Limestone	Idiognathodus simulator	470 cm	*Neospirifer dunbari*	Shell	p	NL	x	x	x	2.45	0.99	0.02	0.04
KOR08	Kansas	Coffey	NE Coffey County	38.423	-95.577	Carboniferous	Virgilian	303.9	Oread	Plattsmouth Limestone	Idiognathodus simulator	470 cm	*Neospirifer dunbari*	Shell	p	NL	x	3.91	-1.34	3.62	0.85	0.00	0.08
KOR08-2	Kansas	Coffey	NE Coffey County	38.423	-95.577	Carboniferous	Virgilian	303.9	Oread	Plattsmouth Limestone	Idiognathodus simulator	470 cm	*Neospirifer dunbari*	Shell	p	NL	x	x	x	5.20	0.86	0.08	0.36
KOR09	Kansas	Coffey	NE Coffey County	38.423	-95.577	Carboniferous	Virgilian	303.9	Oread	Plattsmouth Limestone	Idiognathodus simulator	470 cm	*Neospirifer dunbari*	Shell	p	NL	x	3.63	-1.62	3.44	0.82	0.00	0.07
KOR10	Kansas	Coffey	NE Coffey County	38.423	-95.577	Carboniferous	Virgilian	303.9	Oread	Plattsmouth Limestone	Idiognathodus simulator	460 cm	*Crurithyris planoconvexa*	Shell	f	NL/SL	x	5.37	-1.34	4.60	1.16	0.14	0.45
KOR11	Kansas	Coffey	NE Coffey County	38.423	-95.577	Carboniferous	Virgilian	303.9	Oread	Plattsmouth Limestone	Idiognathodus simulator	460 cm	*Crurithyris planoconvexa*	Shell	f	SL/NL	x	5.13	-1.30	3.85	1.09	0.22	0.59
KOR12	Kansas	Coffey	NE Coffey County	38.423	-95.577	Carboniferous	Virgilian	303.9	Oread	Plattsmouth Limestone	Idiognathodus simulator	460 cm	*Crurithyris planoconvexa*	Shell	f	SL/NL	x	4.65	-1.57	x	x	x	x
KOR13	Kansas	Coffey	NE Coffey County	38.423	-95.577	Carboniferous	Virgilian	303.9	Oread	Plattsmouth Limestone	Idiognathodus simulator	460 cm	*Composita subtilita*	Shell	p	NL/SL	x	5.16	-1.48	11.30	0.88	0.40	1.50
KOR14	Kansas	Coffey	NE Coffey County	38.423	-95.577	Carboniferous	Virgilian	303.9	Oread	Plattsmouth Limestone	Idiognathodus simulator	460 cm	*Composita subtilita*	Shell	p	NL	x	4.63	-1.63	5.14	0.63	0.05	0.38
KOR15	Kansas	Coffey	NE Coffey County	38.423	-95.577	Carboniferous	Virgilian	303.9	Oread	Plattsmouth Limestone	Idiognathodus simulator	460 cm	*Composita subtilita*	Shell	p	NL	x	4.66	-2.12	x	x	x	x
KOR16	Kansas	Coffey	NE Coffey County	38.423	-95.577	Carboniferous	Virgilian	303.9	Oread	Plattsmouth Limestone	Idiognathodus simulator	460 cm	*Neospirifer dunbari*	Shell	p	NL	x	3.60	-1.86	3.31	0.96	0.08	0.19
KOR16-2	Kansas	Coffey	NE Coffey County	38.423	-95.577	Carboniferous	Virgilian	303.9	Oread	Plattsmouth Limestone	Idiognathodus simulator	460 cm	*Neospirifer dunbari*	Shell	p	NL	x	x	x	3.65	0.89	0.04	0.08
KOR16-3	Kansas	Coffey	NE Coffey County	38.423	-95.577	Carboniferous	Virgilian	303.9	Oread	Plattsmouth Limestone	Idiognathodus simulator	460 cm	*Neospirifer dunbari*	Shell	p	NL	x	x	x	2.33	0.77	0.05	0.12
KOR17	Kansas	Coffey	NE Coffey County	38.423	-95.577	Carboniferous	Virgilian	303.9	Oread	Plattsmouth Limestone	Idiognathodus simulator	460 cm	*Neospirifer dunbari*	Shell	p	NL	x	3.87	-1.66	x	x	x	x
KOR18	Kansas	Coffey	NE Coffey County	38.423	-95.577	Carboniferous	Virgilian	303.9	Oread	Plattsmouth Limestone	Idiognathodus simulator	460 cm	*Neospirifer dunbari*	Shell	p	NL	x	3.57	-2.06	2.84	0.94	0.00	0.08
KOR18-2	Kansas	Coffey	NE Coffey County	38.423	-95.577	Carboniferous	Virgilian	303.9	Oread	Plattsmouth Limestone	Idiognathodus simulator	460 cm	*Neospirifer dunbari*	Shell	p	NL	x	x	x	3.12	0.94	0.02	0.05
KOR18-3	Kansas	Coffey	NE Coffey County	38.423	-95.577	Carboniferous	Virgilian	303.9	Oread	Plattsmouth Limestone	Idiognathodus simulator	460 cm	*Neospirifer dunbari*	Shell	p	NL	x	x	x	3.31	1.06	0.03	0.07
KOR20	Kansas	Coffey	NE Coffey County	38.423	-95.577	Carboniferous	Virgilian	303.9	Oread	Plattsmouth Limestone	Idiognathodus simulator	250 cm	*Composita subtilita*	Shell	p	NL	x	4.04	-1.33	1.24	0.59	0.00	0.11
KOR21	Kansas	Coffey	NE Coffey County	38.423	-95.577	Carboniferous	Virgilian	303.9	Oread	Plattsmouth Limestone	Idiognathodus simulator	250 cm	*Composita subtilita*	Shell	p	NL	x	4.84	-1.36	7.95	1.39	0.14	1.85
KOR22	Kansas	Coffey	NE Coffey County	38.423	-95.577	Carboniferous	Virgilian	303.9	Oread	Plattsmouth Limestone	Idiognathodus simulator	250 cm	*Composita subtilita*	Shell	p	NL	x	5.36	-1.08	4.54	0.43	0.00	0.13
KOR23	Kansas	Coffey	NE Coffey County	38.423	-95.577	Carboniferous	Virgilian	303.9	Oread	Plattsmouth Limestone	Idiognathodus simulator	250 cm	*Crurithyris planoconvexa*	Shell	f	SL/NL	x	3.85	-1.47	5.54	1.19	0.61	1.53
KOR24	Kansas	Coffey	NE Coffey County	38.423	-95.577	Carboniferous	Virgilian	303.9	Oread	Plattsmouth Limestone	Idiognathodus simulator	250 cm	*Crurithyris planoconvexa*	Shell	f	SL/NL	x	3.43	-1.80	x	x	x	x
KOR25	Kansas	Coffey	NE Coffey County	38.423	-95.577	Carboniferous	Virgilian	303.9	Oread	Plattsmouth Limestone	Idiognathodus simulator	250 cm	*Crurithyris planoconvexa*	Shell	f	NL/SL	x	3.58	-1.38	x	x	x	x
KOR26	Kansas	Coffey	NE Coffey County	38.423	-95.577	Carboniferous	Virgilian	303.9	Oread	Plattsmouth Limestone	Idiognathodus simulator	-5 cm	*Composita subtilita*	Shell	p	NL	x	4.43	-0.77	3.68	0.80	0.01	0.20

Sample ID	Location	County	Locality Comments	Latitude	Longtitude	Period	Stage	Age (Ma)	Formation	Member	Conodont Zone	Interval	Taxa	Material	Micro-structure	Sample L.C	Shell L.C.	$\delta^{13}C$ (‰)	$\delta^{18}O$ (‰)	Mg/Ca (mmol/mol)	Sr/Ca (mmol/mol)	Mn/Ca (mmol/mol)	Fe/Ca (mmol/mol)
KOR27	Kansas	Coffey	NE Coffey County	38.423	-95.577	Carboniferous	Virgilian	303.9	Oread	Plattsmouth Limestone	Idiognathodus simulator	-5 cm	*Neospirifer dunbari*	Shell	p	NL	x	4.82	-1.03	3.05	0.85	0.00	0.03
KOR28	Kansas	Coffey	NE Coffey County	38.423	-95.577	Carboniferous	Virgilian	303.9	Oread	Plattsmouth Limestone	Idiognathodus simulator	-5 cm	*Neospirifer dunbari*	Shell	p	NL	x	4.51	-1.45	2.38	1.36	0.00	0.01
KOR29	Kansas	Coffey	NE Coffey County	38.423	-95.577	Carboniferous	Virgilian	303.9	Oread	Plattsmouth Limestone	Idiognathodus simulator	-5 cm	*Composita subtilita*	Shell	p	NL	x	4.96	-1.26	x	x	x	x
KOR30	Kansas	Coffey	NE Coffey County	38.423	-95.577	Carboniferous	Virgilian	303.9	Oread	Plattsmouth Limestone	Idiognathodus simulator	-5 cm	*Composita subtilita*	Shell	p	NL/SL	x	4.45	-1.19	x	x	x	x
KOR31	Kansas	Coffey	NE Coffey County	38.423	-95.577	Carboniferous	Virgilian	303.9	Oread	Plattsmouth Limestone	Idiognathodus simulator	-5 cm	*Composita subtilita*	Shell	p	NL/SL	x	4.65	-0.90	x	x	x	x
WP58A AS-1-1s	Illinois	Johnson	NW Johnson County	37.483	-84.688	Carboniferous	Chesterian	318.5	Kincaid	Grove Church	Adetognathus unicornis	x	*Anthracospirifer*	Shell	p	NL/SL		1.67	-2.43	6.97	1.25	0.16	0.21
WP58A AS-1-2s	Illinois	Johnson	NW Johnson County	37.483	-84.688	Carboniferous	Chesterian	318.5	Kincaid	Grove Church	Adetognathus unicornis	x	*Anthracospirifer*	Shell	p	NL/SL		2.52	-2.18	7.54	1.26	0.16	0.20
WP58A AS-1-3s	Illinois	Johnson	NW Johnson County	37.483	-84.688	Carboniferous	Chesterian	318.5	Kincaid	Grove Church	Adetognathus unicornis	x	*Anthracospirifer*	Shell	p	NL/SL		2.40	-2.40	8.32	1.33	0.19	0.22
WP58A AS-2-2s	Illinois	Johnson	NW Johnson County	37.483	-84.688	Carboniferous	Chesterian	318.5	Kincaid	Grove Church	Adetognathus unicornis	x	*Anthracospirifer*	Shell	op	SL/CL		1.77	-4.70	x	x	x	x
WP58 AS-1-1s	Illinois	Johnson	NW Johnson County	37.483	-84.688	Carboniferous	Chesterian	318.5	Kincaid	Grove Church	Adetognathus unicornis	x	*Anthracospirifer*	Shell	p	CL/SL		-0.40	-3.66	10.74	1.50	0.13	0.23
WP58 AS-1-2s	Illinois	Johnson	NW Johnson County	37.483	-84.688	Carboniferous	Chesterian	318.5	Kincaid	Grove Church	Adetognathus unicornis	x	*Anthracospirifer*	Shell	p	SL/NL		0.97	-3.23	7.75	1.34	0.28	0.67
WP58 AS-2-1s	Illinois	Johnson	NW Johnson County	37.483	-84.688	Carboniferous	Chesterian	318.5	Kincaid	Grove Church	Adetognathus unicornis	x	*Anthracospirifer*	Shell	p	NL/SL		0.88	-2.29	5.55	1.25	0.05	0.13
WP58 AS-2-2s	Illinois	Johnson	NW Johnson County	37.483	-84.688	Carboniferous	Chesterian	318.5	Kincaid	Grove Church	Adetognathus unicornis	x	*Anthracospirifer*	Shell	p	NL/SL		1.02	-2.55	7.93	1.27	0.08	0.22
WP58 AS-2-3s	Illinois	Johnson	NW Johnson County	37.483	-84.688	Carboniferous	Chesterian	318.5	Kincaid	Grove Church	Adetognathus unicornis	x	*Anthracospirifer*	Shell	p	NL/SL			-3.44	4.12	1.12	0.06	0.23
WP58 Inf-1-1s	Illinois	Johnson	NW Johnson County	37.483	-84.688	Carboniferous	Chesterian	318.5	Kincaid	Grove Church	Adetognathus unicornis	x	*Inflatia*	Shell	f	NL/SL		1.39	-3.11	9.91	1.72	0.28	0.72
WP58 Inf-1-2s	Illinois	Johnson	NW Johnson County	37.483	-84.688	Carboniferous	Chesterian	318.5	Kincaid	Grove Church	Adetognathus unicornis	x	*Inflatia*	Shell	f	NL/SL		0.15	-3.30	8.45	1.62	0.12	0.18
WP58 Inf-1-3s	Illinois	Johnson	NW Johnson County	37.483	-84.688	Carboniferous	Chesterian	318.5	Kincaid	Grove Church	Adetognathus unicornis	x	*Inflatia*	Shell	f	NL/SL		0.18	-3.69	10.03	1.68	0.10	0.13
WP58 Inf-2-1s	Illinois	Johnson	NW Johnson County	37.483	-84.688	Carboniferous	Chesterian	318.5	Kincaid	Grove Church	Adetognathus unicornis	x	*Inflatia*	Shell	f	SL/NL		0.51	-4.07	9.55	1.69	0.15	0.21
WP58 Inf-2-2s	Illinois	Johnson	NW Johnson County	37.483	-84.688	Carboniferous	Chesterian	318.5	Kincaid	Grove Church	Adetognathus unicornis	x	*Inflatia*	Shell	f	SL/NL		0.34	-3.68	9.57	1.67	0.23	0.98
WP58 Inf-2-3s	Illinois	Johnson	NW Johnson County	37.483	-84.688	Carboniferous	Chesterian	318.5	Kincaid	Grove Church	Adetognathus unicornis	x	*Inflatia*	Shell	f	SL/NL		1.61	-3.67	11.17	1.72	0.42	1.18
WP58 Inf-3-1s	Illinois	Johnson	NW Johnson County	37.483	-84.688	Carboniferous	Chesterian	318.5	Kincaid	Grove Church	Adetognathus unicornis	x	*Inflatia*	Shell	f	SL/NL		1.08	-2.78	10.21	1.60	0.17	0.30
WP58 Inf-3-2s	Illinois	Johnson	NW Johnson County	37.483	-84.688	Carboniferous	Chesterian	318.5	Kincaid	Grove Church	Adetognathus unicornis	x	*Inflatia*	Shell	f	SL/NL		-0.01	-4.00	11.17	1.67	0.08	0.13
WP58 Inf-3-3s	Illinois	Johnson	NW Johnson County	37.483	-84.688	Carboniferous	Chesterian	318.5	Kincaid	Grove Church	Adetognathus unicornis	x	*Inflatia*	Shell	f	SL/NL		1.93	-3.69	x	x	x	x
WP58A AS-1-4m	Illinois	Johnson	NW Johnson County	37.483	-84.688	Carboniferous	Chesterian	318.5	Kincaid	Grove Church	Adetognathus unicornis	x	n/a	Matrix	n/a	n/a	n/a	1.57	-3.38	x	x	x	x
WP58A AS-2-4m	Illinois	Johnson	NW Johnson County	37.483	-84.688	Carboniferous	Chesterian	318.5	Kincaid	Grove Church	Adetognathus unicornis	x	n/a	Matrix	n/a	n/a	n/a	0.31	-6.72	x	x	x	x
WP58 AS-1-3m	Illinois	Johnson	NW Johnson County	37.483	-84.688	Carboniferous	Chesterian	318.5	Kincaid	Grove Church	Adetognathus unicornis	x	n/a	Matix	n/a	n/a	n/a	0.34	-5.87	x	x	x	x
WP58 AS-1-4m	Illinois	Johnson	NW Johnson County	37.483	-84.688	Carboniferous	Chesterian	318.5	Kincaid	Grove Church	Adetognathus unicornis	x	n/a	Matrix	n/a	n/a	n/a	-0.10	-6.22	x	x	x	x
WP58 AS-2-4m	Illinois	Johnson	NW Johnson County	37.483	-84.688	Carboniferous	Chesterian	318.5	Kincaid	Grove Church	Adetognathus unicornis	x	n/a	Matrix	n/a	n/a	n/a	-0.03	-6.09	x	x	x	x
WP58 AS-2-5m	Illinois	Johnson	NW Johnson County	37.483	-84.688	Carboniferous	Chesterian	318.5	Kincaid	Grove Church	Adetognathus unicornis	x	n/a	Matrix	n/a	n/a	n/a	-0.07	-6.02	x	x	x	x
WP58 Inf-1-4m	Illinois	Johnson	NW Johnson County	37.483	-84.688	Carboniferous	Chesterian	318.5	Kincaid	Grove Church	Adetognathus unicornis	x	n/a	Matrix	n/a	n/a	n/a	0.35	-4.47	x	x	x	x
WP58 Inf-1-5m	Illinois	Johnson	NW Johnson County	37.483	-84.688	Carboniferous	Chesterian	318.5	Kincaid	Grove Church	Adetognathus unicornis	x	n/a	Matrix	n/a	n/a	n/a	-0.68	-5.78	x	x	x	x
WP58 Inf-2-4m	Illinois	Johnson	NW Johnson County	37.483	-84.688	Carboniferous	Chesterian	318.5	Kincaid	Grove Church	Adetognathus unicornis	x	n/a	Matrix	n/a	n/a	n/a	-0.42	-6.33	x	x	x	x
WP58 Inf-2-5m	Illinois	Johnson	NW Johnson County	37.483	-84.688	Carboniferous	Chesterian	318.5	Kincaid	Grove Church	Adetognathus unicornis	x	n/a	Matrix	n/a	n/a	n/a	-0.49	-6.59	x	x	x	x
WP58 Inf-3-4m	Illinois	Johnson	NW Johnson County	37.483	-84.688	Carboniferous	Chesterian	318.5	Kincaid	Grove Church	Adetognathus unicornis	x	n/a	Matrix	n/a	n/a	n/a	-0.35	-4.72	x	x	x	x
WP58 Inf-3-5m	Illinois	Johnson	NW Johnson County	37.483	-84.688	Carboniferous	Chesterian	318.5	Kincaid	Grove Church	Adetognathus unicornis	x	n/a	Matrix	n/a	n/a	n/a	-0.52	-4.48	x	x	x	x
WP58 Inf-3-6c	Illinois	Johnson	NW Johnson County	37.483	-84.688	Carboniferous	Chesterian	318.5	Kincaid	Grove Church	Adetognathus unicornis	x	n/a	Cement	n/a	n/a	n/a	-2.22	-8.64	x	x	x	x
NV002-POV2-D	Nevada	Clark	Arrow Canyon	36.736	-114.778	Carboniferous	Chesterian	318.5	Bird Spring	BSb	Adetognathus unicornis	A55	*Anthracospirifer*	Shell	p	NL	x	4.07	-1.54	3.54	1.01	0.02	0.04
NV003-POV2-A	Nevada	Clark	Arrow Canyon	36.736	-114.778	Carboniferous	Chesterian	318.5	Bird Spring	BSb	Adetognathus unicornis	A55	*Anthracospirifer*	Shell	p	NL	x	3.53	-2.37	2.69	0.78	0.03	0.09
NVOO2-POV1-A	Nevada	Clark	Arrow Canyon	36.736	-114.778	Carboniferous	Chesterian	318.5	Bird Spring	BSb	Adetognathus unicornis	A55	*Anthracospirifer*	Shell	p	NL	x	4.22	-0.90	3.42	0.96	0.00	0.03
NVOO2-POV1-B	Nevada	Clark	Arrow Canyon	36.736	-114.778	Carboniferous	Chesterian	318.5	Bird Spring	BSb	Adetognathus unicornis	A55	*Anthracospirifer*	Shell	p	NL	x	4.33	-1.08	1.95	0.93	0.00	0.05
NVOO2-POV1-C	Nevada	Clark	Arrow Canyon	36.736	-114.778	Carboniferous	Chesterian	318.5	Bird Spring	BSb	Adetognathus unicornis	A55	*Anthracospirifer*	Shell	p	NL	x	4.21	-1.35	3.88	0.87	0.12	0.93
NVOO2-POV1-D	Nevada	Clark	Arrow Canyon	36.736	-114.778	Carboniferous	Chesterian	318.5	Bird Spring	BSb	Adetognathus unicornis	A55	*Anthracospirifer*	Shell	p	NL	x	3.81	-1.10	2.74	0.96	0.01	0.02
NVOO2-POV2-A	Nevada	Clark	Arrow Canyon	36.736	-114.778	Carboniferous	Chesterian	318.5	Bird Spring	BSb	Adetognathus unicornis	A55	*Anthracospirifer*	Shell	p	NL	x	3.84	-1.73	3.64	1.05	0.05	0.56
NVOO2-POV2-B	Nevada	Clark	Arrow Canyon	36.736	-114.778	Carboniferous	Chesterian	318.5	Bird Spring	BSb	Adetognathus unicornis	A55	*Anthracospirifer*	Shell	p	NL	x	3.87	-1.63	3.32	1.03	0.04	0.07
NVOO2-POV2-C	Nevada	Clark	Arrow Canyon	36.736	-114.778	Carboniferous	Chesterian	318.5	Bird Spring	BSb	Adetognathus unicornis	A55	*Anthracospirifer*	Shell	p	NL	x	3.65	0.06	3.07	1.00	0.02	0.07
NVOO3-POV1-A	Nevada	Clark	Arrow Canyon	36.736	-114.778	Carboniferous	Chesterian	318.5	Bird Spring	BSb	Adetognathus unicornis	A55	*Anthracospirifer*	Shell	p	NL	x	3.52	-1.98	2.69	0.78	0.03	0.09
NVOO3-POV1-B	Nevada	Clark	Arrow Canyon	36.736	-114.778	Carboniferous	Chesterian	318.5	Bird Spring	BSb	Adetognathus unicornis	A55	*Anthracospirifer*	Shell	p	NL	x	4.02	-2.28	4.57	0.97	0.03	0.14
NVOO3-POV1-C	Nevada	Clark	Arrow Canyon	36.736	-114.778	Carboniferous	Chesterian	318.5	Bird Spring	BSb	Adetognathus unicornis	A55	*Anthracospirifer*	Shell	p	NL	x	3.82	-1.93	2.44	0.84	0.02	0.03
NVOO3-POV2-B	Nevada	Clark	Arrow Canyon	36.736	-114.778	Carboniferous	Chesterian	318.5	Bird Spring	BSb	Adetognathus unicornis	A55	*Anthracospirifer*	Shell	p	NL	x	3.48	-2.32	2.54	0.76	0.02	0.04
NVOO3-POV2-C	Nevada	Clark	Arrow Canyon	36.736	-114.778	Carboniferous	Chesterian	318.5	Bird Spring	BSb	Adetognathus unicornis	A55	*Anthracospirifer*	Shell	p	NL	x	3.86	-2.39	2.77	0.71	0.14	14.14
NVOO3-POV2-D	Nevada	Clark	Arrow Canyon	36.736	-114.778	Carboniferous	Chesterian	318.5	Bird Spring	BSb	Adetognathus unicornis	A55	*Anthracospirifer*	Shell	p	NL	x	3.99	-2.01	2.46	0.80	0.02	0.09
NVOO1-POV1-C	Nevada	Clark	Arrow Canyon	36.736	-114.778	Carboniferous	Chesterian	318.5	Bird Spring	BSb	Adetognathus unicornis	A55	*Composita*	Shell	p	NL	x	2.58	-2.11	2.81	0.66	0.01	0.06
NVOO1-POV2-A	Nevada	Clark	Arrow Canyon	36.736	-114.778	Carboniferous	Chesterian	318.5	Bird Spring	BSb	Adetognathus unicornis	A55	*Composita*	Shell	p	NL	x	4.06	-0.77	2.89	0.62	0.00	0.12
NVOO1-POV2-B	Nevada	Clark	Arrow Canyon	36.736	-114.778	Carboniferous	Chesterian	318.5	Bird Spring	BSb	Adetognathus unicornis	A55	*Composita*	Shell	p	NL	x	4.05	-1.19	2.54	0.67	0.10	0.10
NVOO1-POV2-C	Nevada	Clark	Arrow Canyon	36.736	-114.778	Carboniferous	Chesterian	318.5	Bird Spring	BSb	Adetognathus unicornis	A55	*Composita*	Shell	p	NL	x	3.50	-1.35	5.07	0.54	0.03	0.12
NVOO1-POV2-D	Nevada	Clark	Arrow Canyon	36.736	-114.778	Carboniferous	Chesterian	318.5	Bird Spring	BSb	Adetognathus unicornis	A55	*Composita*	Shell	p	NL	x	3.77	-1.54	x	x	x	x
NVOO7-POV1-A	Nevada	Clark	Arrow Canyon	36.736	-114.778	Carboniferous	Chesterian	318.5	Bird Spring	BSb	Adetognathus unicornis	A55	Productid	Shell	f	NL	x	2.78	-1.07	3.42	0.96	0.00	0.03
NVOO7-POV1-B	Nevada	Clark	Arrow Canyon	36.736	-114.778	Carboniferous	Chesterian	318.5	Bird Spring	BSb	Adetognathus unicornis	A55	Productid	Shell	f	NL	x	2.89	-0.55	5.21	0.90	0.00	0.06
NVOO7-POV1-C	Nevada	Clark	Arrow Canyon	36.736	-114.778	Carboniferous	Chesterian	318.5	Bird Spring	BSb	Adetognathus unicornis	A55	Productid	Shell	f	NL	x	2.91	-0.70	x	x	x	x
NVOO7-POV1-D	Nevada	Clark	Arrow Canyon	36.736	-114.778	Carboniferous	Chesterian	318.5	Bird Spring	BSb	Adetognathus unicornis	A55	Productid	Shell	f	NL	x	2.81	-0.62	x	x	x	x

VITA

Name:	Ryan Christopher Flake
Address:	Department of Geology and Geophysics, MS 3115 Texas A&M University, College Station, Texas 77843-3115
Email Address:	Ryan.Flake@Gmail.com
Education:	B.S., Geology, Washington State University, 2008
Employment:	Exxon Mobil Corporation, 2011